1 MAY 2003 BİNGÖL EARTHQUAKE ENGINEERING REPORT

TECHNICAL EDITORS

GÜNEY ÖZCEBE

JULIO RAMIREZ

S. TANVIR WASTI

AHMET YAKUT

This report was prepared jointly by two teams of engineers, one assembled by the Middle East Technical University (METU) with support from the Scientific and Technical Research Council of Turkey (TÜBİTAK) and the other by Purdue University with support by the U.S. National Science Foundation (NSF). Opinions, findings, conclusions, and recommendations included in the report are those of the authors listed and do not reflect the views of TÜBİTAK, NSF, METU and Purdue.

Unless otherwise identified in the figure caption, all illustrations were provided by the contributors whose names are listed in the section on "Chapter Contributors and their Affiliations."

Copies of this publication may be downloaded with acknowledgment from the following web addresses: This report will be published in February 2004.

http://www.seru.metu.edu.tr/archives.html

http://www.anatolianquake.org

ISBN 975-403-320-X

CONTENTS

PREFACE

According to a Turkish proverb, one disaster is worth more than a thousand pieces of advice. In the last 10 years, seven major earthquakes in Turkey, the 1992 Erzincan, 1995 Dinar, 1998 Ceyhan, 1999 Marmara, 1999 Düzce, 2002 Afyon–Sultandağı and the 2003 Bingöl earthquakes, have resulted in the deaths of thousands of people and brought about great devastation. In spite of the resoluteness, forbearance and inner strength reserves of the population, the resulting burdens to Turkey have been immense. Huge economic losses have occurred due to the collapse of thousands of buildings, along with the disruption of industry and business. Furthermore, damaged structures in need of rehabilitation have also been a large component of the overall problem.

It is a primary responsibility of engineers to learn from disasters, first by studying in detail the disaster itself, and then by applying available technology to ensure that the each recurrence of disaster will result in less damage than its predecessor. Given the relatively short history of earthquake engineering, the process of seismic amelioration is, of necessity, an iterative exercise. Old habits of ignorance and slipshod nonengineered construction die hard.

After the Bingöl Earthquake of May 1, 2003, teams from Turkey and the U.S.A. were dispatched to investigate the structural, geological, geotechnical and seismological aspects of the earthquake. The teams, formed by 7 faculty members and 4 graduate students of the department of civil engineering of Middle East Technical University, 4 faculty members and 3 graduate students of Purdue University, 1 faculty member from the University of Kansas, two practicing engineers from Wiss Janney Elstner, one faculty from department of geological engineering of Hacettepe University and a volunteer, collected extensive data, conducted field damage assessment surveys and made geological and geotechnical observations. As also mentioned in the Acknowledgments page, the U.S. and Turkish teams were jointly sponsored by the National Science Foundation [NSF] and the Scientific and Technical Research Council of Turkey [TÜBİTAK].

The present report comprises a detailed evaluation of the ground motion recorded in Bingöl, a summary of the geological and geotechnical characteristics of the region, observed soil related damage and a comprehensive account of school, governmental and residential building performance. The draft reports produced by the NSF-TÜBİTAK team have been merged together by the technical editors. In the process, in order to avoid large-scale excision of material, a certain amount of overlap has been inevitable. Names of authors and contributors with their affiliations have been included on a chapter by chapter basis. To optimize publishing costs, photographs in color are reproduced and made available in the CD which accompanies each copy of the report.

It is the hope of all who have participated in the writing and production of this report that it will serve as a positive contribution to the goal of minimizing losses to life and property due to earthquakes, in Turkey and elsewhere.

Güney Özcebe
Julio A. Ramirez
S. Tanvir Wasti
Ahmet Yakut

Technical Editors

November 30, 2003

ACKNOWLEDGMENTS

This report on the Bingöl earthquake of May 1, 2003 is the result of a joint investigative effort by research teams from Turkey and the United States in the Bingöl earthquake region along with several sessions of discussion both face to face and subsequently by e-mail. It was sponsored on the U.S. side by the National Science Foundation [NSF] and on the Turkish side by the Turkish Scientific and Technical Research Council [TÜBİTAK]. The NSF team comprised researchers from Purdue and Kansas universities and engineers from Wiss, Janney, Elstner Associates, Inc. [WJE]. The TÜBİTAK team comprised faculty and research assistants from Middle East Technical University [METU] and also from Hacettepe University. The support provided by NSF and TÜBİTAK is gratefully acknowledged. In particular, acknowledgment should be made on the NSF side to Dr Steven McCabe, Program Officer, Division of Civil and Mechanical Systems, Structural Systems and Hazards Mitigation of Structures. Joan Sozen collaborated in many aspects of the investigation conducted by the NSF team in Bingöl, and deserves thanks for her efforts.

Support from the Earthquake Engineering Research Institute [EERI – Oakland, California] enabled the participation of Professors Sadık Bakır, Kemal Ö. Çetin and Reşat Ulusay as part of the group investigating Geotechnical Events connected with the earthquake. Sincere thanks are due to EERI for extending this support. The financial support given by Middle East Technical University to the investigations conducted by a team of researchers under the leadership of Professor Polat Gülkan immediately after the earthquake is gratefully acknowledged.

The contributions of graduate students Ufuk Yazgan and Sezgin Küçükçoban are also acknowledged. We would like to extend our thanks to the municipality of Bingöl which provided city maps and guidance during the field surveys.

The logistical support provided by the Presidents of Fırat University and İnönü University are appreciated. On the ground, the help and assistance provided by the Governor of Bingöl, the Mayor of Bingöl and the local Directorate of Public Works greatly facilitated our task. Furthermore, we are thankful to Mr. Mümtaz Turfan [then General Director, State Hydraulics Works] for his arrangement of accommodation in Elazığ for the survey team and for making available information relating to earlier geotechnical investigations in the area. The architectural and structural drawings related to school buildings in Bingöl were kindly provided by the relevant department of the Ministry of Education.

The accelerograms utilized in the analyses for this report were made available by the Earthquake Research Division of the General Directorate of Disaster Affairs in Ankara. We would like to offer our thanks to them for this generosity. Dr. David M. Boore from the U.S. Geological Survey gave invaluable suggestions and opinions with relation to some of the analyses of the NSF team and deserves sincere commendations for his assistance.

The investigation reported in the present volume was spread altogether over two weeks and involved many other persons who took part and helped in the assembly of data, photographs and in work on site. It is fair to state that they bore a substantial part of the workload that went into the preparation of the report. These include (in alphabetical order):

L. Akin, Graduate Research Assistant, School of Civil Engineering, Purdue University
V. Aydoğan, Research Assistant, Civil Engineering Department, METU
S. Bayılı, Research Assistant, Civil Engineering Department, METU
A. Cihan Pay, Graduate Research Assistant, School of Civil Engineering, Purdue University
İ. Erdem, Research Assistant, Civil Engineering Department, METU
S. Pujol, WJE Assoc., Inc.
B. Yalım, Research Assistant, Civil Engineering Department, METU

We would like to express our sincere thanks to all of the above.

LIST OF ABBREVIATIONS

In general all abbreviations are explained in full in the text where they first occur.

EAF	East Anatolian Fault
EERI	Earthquake Engineering Research Institute, Oakland, California, USA
ERD	Earthquake Research Department, General Directorate of Disaster Affairs, Ankara Turkey
HU	Hacettepe University, Ankara, Turkey
KOERI	Kandilli Observatory and Earthquake Research Institute, Istanbul, Turkey
METU	Middle East Technical University, Ankara, Turkey
NAF	North Anatolian Fault
NSF	National Science Foundation, Washington DC, USA
TÜBİTAK	Turkish acronym for the Scientific and Technical Research Council of Turkey, Ankara, Turkey
USGS	United States Geological Survey, VA, USA
WJE	Wiss, Janney, Elstner Associates, Inc., USA

CHAPTER CONTRIBUTORS AND AFFILIATIONS

TÜBİTAK Contributors

D. S. Akkar, Assistant Professor, Civil Engineering Department, METU
U. Akyüz, Assistant Professor, Civil Engineering Department, METU
S. Bakır, Civil Engineering Department, METU
K. Ö. Çetin, Assistant Professor, Civil Engineering Department, METU
P. Gülkan, Professor of Civil Engineering, METU
G. Özcebe, Professor of Civil Engineering, METU
R. Ulusay, Professor of Geology, Hacettepe University
A. Türer, Assistant Professor, Civil Engineering Department, METU
S. T. Wasti, Professor of Civil Engineering, METU
A. Yakut, Assistant Professor, Civil Engineering Department, METU

NSF Contributors

A. Bobet, Associate Professor of Civil Engineering, Purdue University
T. Gür, Graduate Research Assistant, School of Civil Engineering, Purdue University
A. Irfanoglu, WJE Assoc., Inc.
A. Johnson, Professor of Geology, School of Earth and Atmospheric Sciences, Purdue University
A. Matamoros, Assistant Professor of Civil Engineering, University of Kansas
J. A. Ramirez, Professor of Civil Engineering Purdue University
M. A. Sozen, Kettelhut Distinguished Professor of Structural Engineering, Purdue University

1

INTRODUCTION

1.1 THE EVENT

The earthquake of moment magnitude 6.4 (USGS and KOERI) occurred at 10 km north of Bingöl at 03:27 am (local time) on 1 May 2003. The epicenter of the earthquake was at 38.94N- 40.51E (ERD-Ankara) (Figure 1.1). The depth of the quake was estimated to be at 6 km. As of 1:32 pm local time on 2 May 2003 aftershocks between magnitudes 2.8 and 4.3 had been recorded. The magnitudes of the possible aftershocks can be expected to be as high as 5.1 within one week after the main event. The strongest record of the earthquake was registered at Bingöl. The peak ground accelerations (PGA) of the three components of this record are 0.55g (NS), 0.28g (EW) and 0.47g (UP). The duration of the strong motion was 17 s. High vertical acceleration indicates that the station at Bingöl was very close to the source of the quake. The official number of fatalities is 168. The city of Bingöl is located almost at the intersection of the North Anatolian Fault (NAF) and the East Anatolian Fault (EAF) (Figure 1.2). A map of the various residential and commercial districts within and surrounding the municipal boundaries of the city is given in Figure 1.3 so as to facilitate the identification and pinpoint the location of public and private buildings investigated in the Bingöl area after the earthquake.

Figure 1.1 Bingöl region

The previous earthquake disaster of magnitude 6.8 in the city occurred in 1971. The earthquake was associated with a 38-km long left-lateral surface rupture. The horizontal slip was observed to be 0.6 m along the surface rupture. The total number of fatalities was 875. Almost 9 000 residential units had medium to severe damage.

1.2 THE TASK

Immediately following the 1 May 2003 earthquake in Turkey, a US reconnaissance team composed of researchers and practicing engineers under sponsorship of the US National Science Foundation (NSF) set out to join a Turkish team sponsored by the Scientific and Technical Research Council of Turkey (TÜBİTAK) so as to study the impact of the event. The NSF team was led by researchers from Purdue University, working closely with researchers from the University of Kansas, engineers from WJE and Associates in California. The TÜBİTAK team was led by researchers from the Middle East Technical University (METU) in Ankara. This team consisted of faculty and graduate students in structural engineering, geotechnical engineering, and geological science. From this point on reference shall be made to the combined teams as the NSF-TÜBİTAK team or group. The present joint report sponsored by the National Science Foundation (US) and TÜBİTAK (Turkey) summarizes the results of this collaboration. The main objectives were to document: (a) the damage to reinforced concrete buildings and (b) the geotechnical and geological aspects of the earthquake. The teams also paid some attention to mosques, masonry and nonengineered structures. The group concentrated its efforts in the vicinity of Bingöl.

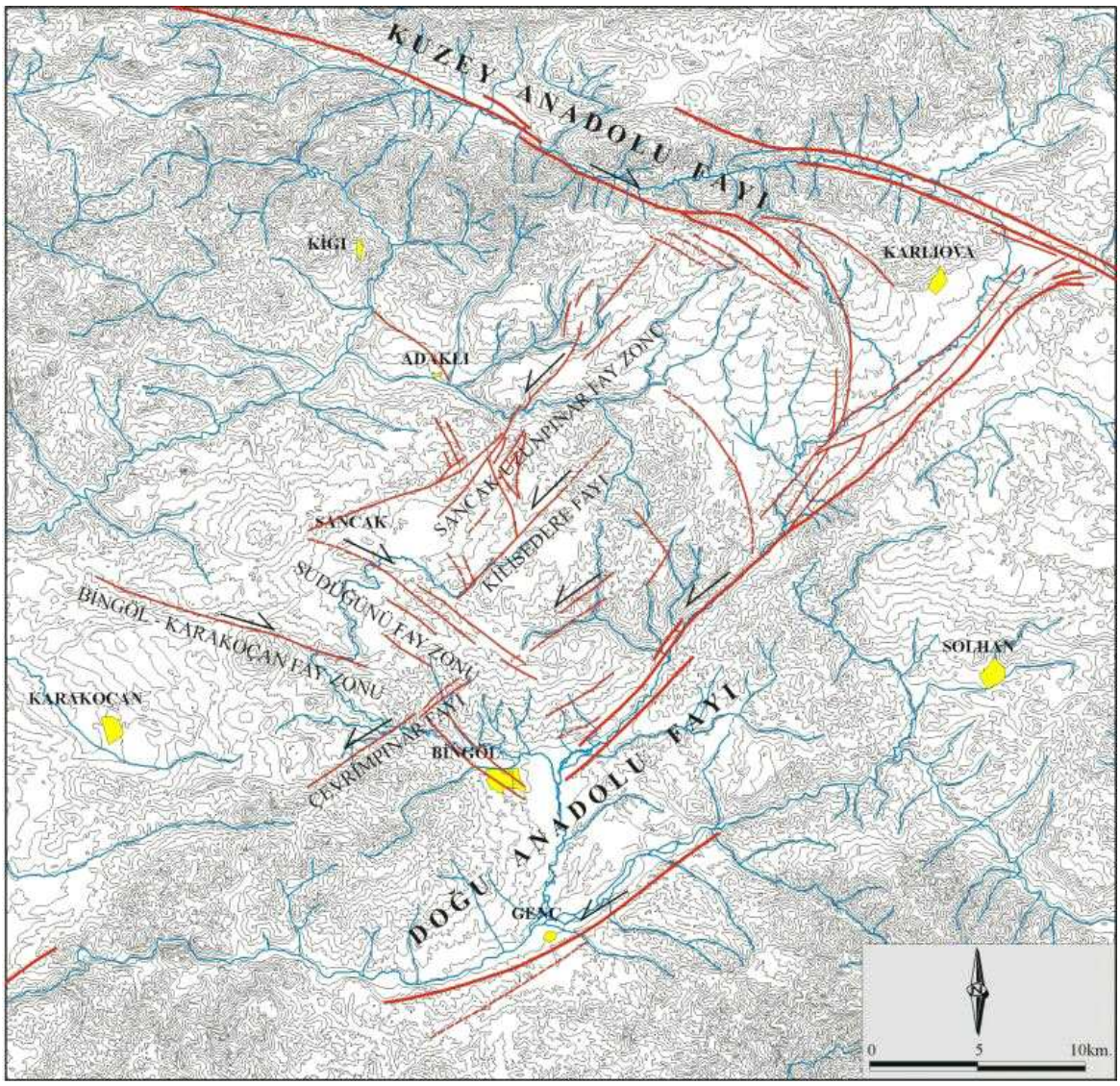

Figure 1.2 The active faults near Bingöl

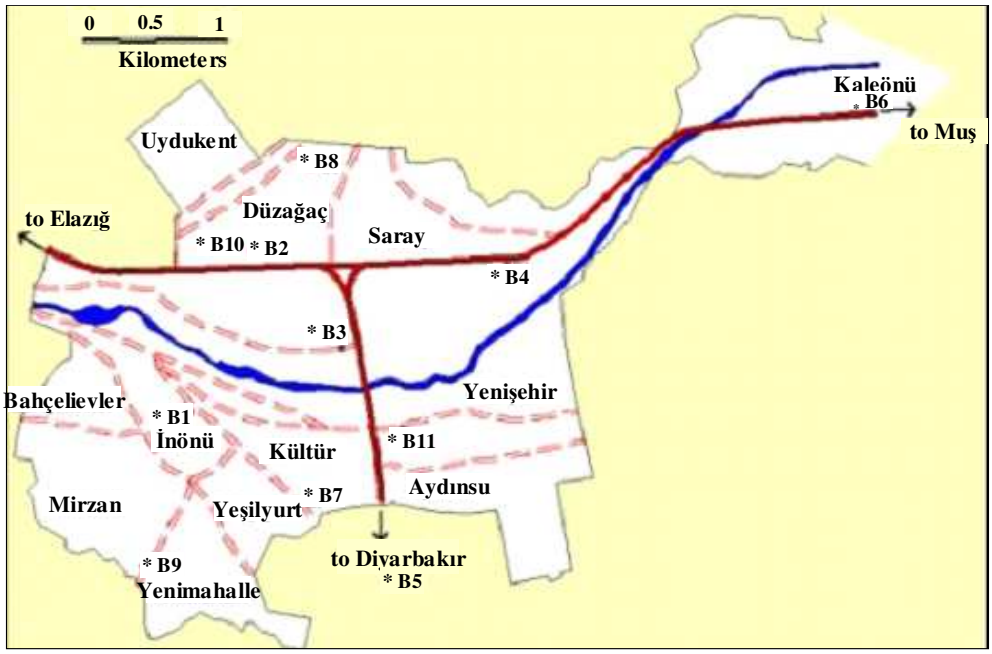

Figure 1.3 Districts of Bingöl (from KOERI)

1.3 SURVEY APPROACH

The TÜBİTAK group conducted its investigations on the spot in Bingöl between 5 and 9 May 2003. An earlier reconnaissance batch from TÜBİTAK was in Bingöl as early as May 2, 2003. Results of the TÜBİTAK survey were discussed in Ankara with the NSF group and joint strategy of coordination was established before the NSF team left for the earthquake zone.

The NSF reconnaissance team arrived at the city of Elazığ on 11 May 2003 and was in Bingöl the same afternoon surveying damage and working the appropriate logistics in the form of permits and assistance by the local authorities. The NSF team continued its investigations in the city of Bingöl and the surrounding area until May 17, 2003. The information obtained from the two surveys after being pooled together may be divided as follows:

The TÜBİTAK team studied a total of 96 reinforced concrete buildings of which 57 were residential, 21 were school buildings and 18 were governmental (public) buildings.

The NSF team studied a total of 62 reinforced concrete buildings of which 33 were residential and 29 were school buildings.

In general the investigated buildings were low- and medium-rise reinforced concrete frame buildings. The observed damage was documented for each case.

Between the two groups 14 buildings comprising 10 schools and 4 residential buildings were common, i.e. investigated by both NSF and TÜBİTAK teams. Thus, the grand total of buildings visited and studied is 144.

Furthermore, the NSF-TÜBİTAK team also documented damage to mosques and minarets by inspecting 7 mosques in the vicinity of Bingöl.

Members of both teams talked with practicing engineers and building officials in order to obtain information about local design and construction practices and evaluated the geotechnical and geological aspects of the earthquake.

1.4 FRAMEWORK OF REPORT

The report is a joint effort and, after inevitable discussions, substantial agreement obtains between the NSF and TÜBİTAK teams on the division of the contents into chapters with the headings given, as also on the material contained therein. Apart from providing information on the Bingöl earthquake, the damage assessment data gathered from the Bingöl area will be used to augment a planned common database. A start has been made on the database and further information is available at the following address:

http://www.seru.metu.edu.tr/archives.html

Agreement has also been reached on the possible future publication of the present report in abridged form in Turkish by the TÜBİTAK team, as well as in the form of another report in English to be submitted to the National Science Foundation by the NSF team for separate publication.

CHAPTER AUTHORS

Coordinators

J. A. Ramirez, Purdue University
S. T. Wasti, Middle East Technical University

Contributors

A. Irfanoglu, WJE Assoc., Inc.
A. Johnson, Purdue University
A. Matamoros, University of Kansas
G. Özcebe, Middle East Technical University
M. A. Sozen, Purdue University

2

EVALUATION OF THE STRONG GROUND MOTION

2.1 INTRODUCTION

The city of Bingöl was struck by an earthquake (M_w=6.4, ERD) on May 1, 2003 at 03:27 local time (01:27 GMT). The epicenter of the main shock was located to the north of the Bingöl, a city that is surrounded by a set of very complex and heterogeneous fault patterns. On the macroseismic scale, the earthquake occurred inside the Bingöl-Karlıova-Erzincan triangle that is confined by the Karlıova triple junction from the east, the right lateral strike-slip North Anatolian fault (NAF) from the north and left lateral strike-slip East Anatolian fault (EAF) from the south. The Bingöl-Karlıova-Erzincan triangle is confined and traversed by conjugate faults of the NAF and EAF that run in the NE-SW and NW-SE directions. The right lateral strike-slip conjugate faults extend from the NAF and follow a parallel pattern to the EAF (i.e. NE-SW direction). The left lateral strike-slip conjugate faults extend from the EAF and follow a pattern parallel to the NAF (i.e. the NW-SE direction). These faults do not follow a straight path but rather define an echelon form series. A representative sketch of the general seismotectonic descriptions is shown in Figure 2.1. The 1784 Yedisu and 1866 Göynük-Karlıova historic earthquakes were historically the most devastating ground motions experienced in the province of Bingöl (Ambraseys, 1985). The last damaging earthquake before this recent event was the May 22, 1971 Bingöl earthquake (M_s=6.8) that was located on the EAF, approximately 10 km to the south of the city (Ambraseys and Jackson, 1998). Considering the seismicity of the Bingöl-Karlıova-Erzincan triangle from different resources (Ambraseys, 1985; Ambraseys and Jackson, 1998; Seymen and Aydın, 1972; Gencoglu et al., 1992) the May 1 event can be considered as a medium size earthquake that could be expected to occur within the faulting system described above. Table 2.1 lists some of the important historical events observed within this region.

Figure 2.2 shows the distribution of the aftershock epicenters. The dense aftershock distribution is accumulated on the complex-strike slip conjugate faults that have lengths varying from several kilometers to approximately 40 km. No confirmed evidence indicating the occurrence of a surface rupture has been reported.

Four strong motion stations were triggered during the main shock of the Bingöl earthquake. Among these, the ground motions recorded by the Tercan, Erzincan and Elazığ stations have peak ground acceleration (PGA) values of less than 0.01 g since they were located at large distances from the epicenter.

This chapter presents the results of preliminary analyses conducted on the Bingöl record. After a detailed description of the recording station and strong motion instrument some engineering features of the record are discussed. The authors establish polarization of the waveforms, and show that the local site conditions may have influenced this polarization. Possible effects of observed pounding between adjacent blocks of the Bingöl station are examined to rationalize an uncommon spectral amplification in the acceleration spectrum. As the final part of this study, the influence of the pulse-signal on the nonlinear deformation demand of the nondegrading oscillators is also examined.

2.2 INFORMATION ON THE ACCELERATION SENSOR AND THE RECORDING STATION

The strong ground motion instrument deployed in the Bingöl station is a ±2 g-limit force-balanced, tri-axial accelerometer (SSA-320 by Terra Technology Corp.[1]) that has a natural frequency of 50 Hz and a critical damping ratio of 0.7 as default factory settings. The accelerometer response approximates a second order system that is fairly flat in amplitude for frequencies below and in the near vicinity of the natural frequency. Above the natural frequency the response is asymptotic to the –12dB octave. The data acquisition system is a 16-bit analog-to-digital recorder (GSR-16 GeoSys AG[2]) that was set to have a pre-event memory of 20 s and a sampling rate of 100 Hz at the time of the earthquake event.

The pictures in Figure 2.3 show the general view of the Bingöl recording station. This is a reinforced concrete office complex of the Bingöl Public Works and Settlement (Figure 2.3a and Figure 2.3b). The strong ground motion instrument is placed inside the one story auxiliary structure that is adjacent to the mid-rise office buildings (Figure 2.3c). Expansion joints separate each adjacent block in the complex. The buildings have been designed and constructed according to template designs developed by the parent Ministry. Identical provincial Public Works and Settlement building complexes exist in many cities of the country. The station is located in the north of the city, on an estimated 50 m high alluvial terrace between two streams. The terrace material is dense formations comprising predominantly uniform granular alluvial deposits. Further north from the building, there are slopes toward the bottom of the valley formed by the second stream. The authors do not have an upper 30 m shear wave velocity variation of the area of interest but the geological formation described above suggests that the soil profile in this area would be classified as USGS site class C or D (i.e., $360 \leq v_s < 750$m/s and $180 \leq v_s < 360$m/s, respectively).

Figure 2.4 shows a general view of the recording instrument that is placed on a reinforced concrete pedestal in one of the storage rooms of the one-story auxiliary building. The pedestal is inside a 0.5m deep, 1m by 1m excavation to minimize the interaction between the structure and the sensor. This figure also shows the directions of the principal axes of the tri-axial sensor[3]. While computing the directions of the sensor axes, the authors also considered the effect of sensor electric field on the compass polarity. Their derivations have a 10 degrees difference with respect to the directions reported by Earthquake Research Department (ERD) of the General Directorate of Disaster Affairs that owns the recording station and is responsible from the dissemination of the raw data.

2.3 RECORD PROCESSING

Figure 2.5 shows the integrated velocity and displacement traces of the unprocessed acceleration record. The integrated raw velocity time series shows a linearly increasing trend that translates to a higher order polynomial in the displacement traces. Thus, a baseline correction is required in order to obtain a more reliable view of the particle motion for the main event. Of the numerous baseline correction procedures, the results of only two alternative methods will be discussed here. The first trial (alternative 1) simply fits a straight line on the final portion of the raw velocity data where the ground motion is about to cease. The fitted straight line is then used to find the time (referred to as t_2) at which the ground velocity becomes zero. This procedure is a modified version of the data processing scheme proposed by Iwan et al. (1985) and described in detail by Boore (1999). The second correction process (alternative 2) is the filtering of raw acceleration data. The authors used the lowest order acausal Butterworth filter with a corner frequency (f_c) of 0.04 Hz. The

1 Terra Technology Corp. Redmond, Washington 98052 U.S.A.
2 GeoSys AG Kanalstrasse 11 8152 Glattbrugg Switzerland
3 These directions were derived by communicating with the NSF team which measured the polarity of the principal sensor axes during field trips to the station.

linear trend observed in the raw velocity time series suggest that the lowest order Butterworth filtering would be sufficient for all practical purposes of this study. Acausal filters do not have phase distortions that result in diminished sensitivity of the filter cut-off frequencies on the inelastic spectral displacement computations. Note that the leading and trailing zeros are required for acausal filters and this is achieved by using the procedure suggested by Converse and Brady (1979). The filtration and integration processes of the raw data were done by public software.[4] As part of these correction procedures, the pre-event mean is always removed from the raw data before any of the above steps are carried out. This is called the *zeroth* order correction.

Figure 2.6 presents the comparative results for the derived displacement traces. The difference between the processed acceleration and velocity waveforms is almost indistinguishable. The leading and trailing zeros for the filtered data are excluded from the corrected traces. This is done to facilitate observing the differences between the alternative correction procedures. In other words, Figure 2.6 presents the actual event duration for both cases, except that in the filtered data this duration is shifted (and extended) due to zero padding. The precursory motion of the displacements that are derived from filtering is due to the leading zeros required in acausal filtering. The filtered E10S displacements fluctuate about zero whereas alternative 1 computes a residual displacement of approximately 10 cm for this component. The peak amplitude of the pulse signal in the N10E component is calculated to be less by filtering. The merits of baseline correction procedures are out of the scope of this text. The authors made various trials with the data derived by these alternative correction procedures and did not see any significant difference for the computations that are of concern within this study. The precursory motions resulting from zero padding may lead to possible misinterpretation in the discussions on ground motion polarization. Thus, the ground motions corrected by alternative 1 will be used for the rest of this article.

2.4 SOME IMPORTANT ASPECTS OF THE GROUND MOTION DATA

Table 2.2 lists some of the important strong ground motion parameters of the Bingöl station data. The effective peak acceleration (EPA) values of the horizontal components are approximately 85 percent of their corresponding peak ground acceleration (PGA) values. The Arias intensity (AI) of the N10E component is almost 2.5 times larger than that of the E10S component. This indicates that the potential destructive power of the N10E component is significantly larger than that of the other horizontal component. Figure 2.7 shows the Husid plots of the horizontal components. The rapid built-up of significantly large AI values in N10E with respect to E10S also shows the considerable amount of energy that was imparted by N10E to the structures within a significantly short interval of time. This observation is supported by the effective duration (t_{eff}) computations shown in Table 2.2. The effective duration values computed according to the Trifunac and Brady (1975) definition suggest that the strong motion duration of the N10E component is approximately 4.5 seconds and almost all of the input energy is released within this short interval of time. This interval is approximately 7 seconds in the E10S component, and the energy imparted to the structures is almost 40 percent of the N10E. The authors believe that the high amount of energy in this component is mostly due to the 4-second period pulse signal. The pulse can be clearly observed in the displacement plots shown in Figure 2.6. The average of the Arias intensities of the horizontal components is 135.85 cm/s. A recent AI based attenuation relationship (Travasarou et al., 2003) suggests a median value between 65 cm/s and 25 cm/s for closest site-to-fault rupture distances, 10 km $\leq$ d $\leq$ 20 km and site conditions similar to the Bingöl station. These values are significantly smaller than the Arias intensities computed for the Bingöl station.

The PGV/PGA ratios listed in Table 2.2 show that the E10S component yields a larger value than the N10E component that contains a pulse in the signal. For comparative purposes, the PGV/PGA ratios of ground motions from $6.5 \leq M_w \leq 6.9$ events are compared with those computed in this study. For consistency, ground motion signals have been chosen only from the recording stations

[4] http://quake.usgs.gov/~boore

that are located on USGS site classes B and C. The distances to fault of these stations are between 5.1km and 17.5km. These restrictions are believed to be amply representative for a fair comparison for the values in hand and the general trend. The ground motions chosen are divided into two groups: records that contain pulses in the signals, and records without pulses. Table 2.3 describes the features of these ground motions. The scatter plots of PGV/PGA versus distance are shown in Figure 2.8. Limited to the data at hand, the ground motions with pulses show a drop in PGV/PGA as the distance to the station increases. The PGV/PGA ratio of the N10E component that exhibits a pulse signal remains below the observed PGV/PGA ratio range. For ground motions that do not possess a pulse in their signal, the PGA/PGV ratio seems to have less dependency on distance changes. The E10S component PGV/PGA ratio for the Bingöl station is within the limits observed in the general trend.

The existence of a pulse in the N10E component can be interpreted as a possible effect of forward rupture directivity. In order to see the polarization of waves, the authors plotted the hodograph diagrams of the horizontal components. These plots are drawn only for the strong motion part of the acceleration, velocity and displacement traces, and are presented in Figure 2.9. These plots also show the strike of the fault rupture reported by Koçyiğit and Kaymakçı (2003) and the theoretical strike computed by the USGS from the fault-plane solution. The authors must note that the fault plane solution of Harvard CMT is similar to that given by USGS. The hodographs are drawn for three consecutive time intervals of the strong ground motion duration in order to infer a possible change in the direction of polarization during the course of the event. The plots in Figure 2.9 shown for acceleration, velocity and displacement are consistent, and indicate that the dominant polarization is closely parallel to the strike of the fault rupture reported by Koçyiğit and Kaymakçı (2003). In theory, the dominant polarization of the ground motions with forward directivity effects should be observed perpendicular to the strike of the fault. A recent research that evaluated some ground motions recorded at the Coyote Lake Dam has noted similar unexpected differences in the polarization of motions recorded from different events and suggested that those might be attributed to the complex site response (Boore et al., 2003). Additional research is required to distinguish the local site interference from the polarization of waveforms.

2.5 SPECTRA COMPUTATIONS

The pseudo-spectral acceleration (PSA) and spectral displacement (SD) of the horizontal components are presented in Figure 2.10. The site-specific design spectra constructed by using the PSA values at 0.2 s and 1.0 s are also shown on these plots. The large PSA amplification of the N10E component at approximately 0.15s exhibits a very short plateau, and produces an inadequate envelope of the design spectrum between 0.3 s and 1.0 s. Concerned about this observation, the authors made a series of analyses to draw the reasons for this amplification.

Figure 2.11 shows evidence for the pounding between the two mid-rise office buildings observed immediately after the main shock. The pounding occurred mainly in the NS direction and the distance between the strong ground motion instrument and the office buildings is approximately 15 m. The authors conducted Fourier analysis on 59 sets of aftershock time series recorded by the same instrument. Aftershock motions have PGA values of less than 0.01 g. The purpose was to see any dominant site behavior at the recording station. These analyses focused on the N10E component because it is the direction of pounding observed in the adjacent blocks. Figure 2.12 is the normalized Fourier spectra for the main shock and geometric mean aftershock data arranged for comparison purposes. The authors considered the maximum amplitude of the geometric mean for the normalization of aftershock data. The Fourier components of the N10E curves are amplified in the near proximity of 0.15 s (i.e. 6.67 Hz). The mean aftershock Fourier components reach the maximum at 7.38 Hz (0.14 s), and the main shock Fourier components have a significant amplification at 6.39 Hz (0.16 s). The slight shift in the frequency between the main shock and aftershock data might be attributed to possible nonlinearity of the soil during the main shock. The geometric mean of the E10S aftershock data also reaches its maximum value at about 6.7 Hz. The comparison of the main shock

and aftershock data in the E10S direction reveals that both sets have similar frequency characteristics in the high end whereas the main shock data is richer in the frequency components toward the low end of the range. The amplification of aftershock data in the vicinity of 0.15 s may be an indication of strong amplification within that period range. The pounding of the adjacent blocks seems to have had no discernible effect on the main shock data. Otherwise the authors would normally not have seen the amplification of the aftershock at 0.15 s that might be attributed to contamination at high frequencies caused by pounding. It is perplexing that the collision between two building frames went unrecorded by a sensor nearby.

The authors also computed the Fourier amplitude spectral ratios of some of the aftershock data that were recorded both at the fourth level of the 5-story office building and the 1-story auxiliary structure. The normalized spectral ratios of three aftershocks are presented in Figure 2.13. The normalizations were done for the maximum amplitude ratio of each component. The plots in Figure 2.13 consistently show that the maximum amplification is between 1.6 Hz and 2.0 Hz indicating that the building fundamental period is in the range between 0.5 and 0.6 s. The spectral ratios in the E10S component also show amplification at about 9 and 10 Hz, a possible indication of another modal frequency of the main building system in that direction. The spectral ratios of the N10E direction diminish after the maximum amplification. The exception is the spectral ratios computed from the aftershock event presented in the middle row of Figure 2.13. The spectral ratios in the N10E direction are amplified at 6 Hz. This can be attributed to a possible interference of the main structure in the sensor record. In other words, it is also possible to interpret the PSA peak at 0.15 s as the combined effect of structural interference and site amplification that happened to coincide at that period. In the absence of data from sensors deployed nearby such meditations must be considered as qualitative.

Inelastic spectral displacements (S_{di}) are straightforward parameters for defining the deformation demand of ground motions on structural systems. Figure 2.14 shows the amplification of S_{di} with respect to elastic spectral displacement S_{de} for elasto-plastic systems whose lateral capacities are defined by strength reduction factors, R. The strength reduction factor is simply the elastic strength normalized by the yield strength of the oscillator. Inelastic displacement spectra computed for a given R show the calculated inelastic deformation demand of the ground motion for that lateral strength capacity. As expected from the fundamentals of nonlinear dynamic behavior of structures, the S_{di}/S_{de} ratio computed for the E10S component is very sensitive to the changes in R for T less than approximately 1 s. On average, the S_{di}/S_{de} ratios are equal to 1 or less than 1 for periods larger than 1.25 s which validates the equal displacement rule. The N10E component yields S_{di}/S_{de} values significantly larger than 1 even for periods of vibration longer than 3 s. This is the influence of the pulse signal that has a period of 4 s. In fact, if the same spectral curves were drawn for periods normalized with respect to the pulse period, the authors would have obtained a clearer picture for the effect of pulse signal on the calculated inelastic deformation demands. This is done in Figure 2.15. The curves in Figure 2.15 show that the equal displacement rule is valid for periods of vibration approximately 10 to 20 percent larger than the pulse period. This important seismological feature of pulse-like signals is sometimes overlooked in most building performance assessment methods. Figure 2.14 also shows that the N10E component has a very local S_{di}/S_{de} amplification at about of 1.25 s. The normalized Fourier spectrum of this component presented in Figure 2.12 also shows a significant amplification within this period range. This constitutes a good demonstration for the importance of excitation frequency content in nonlinear structural behavior.

2.6 SUMMARY AND CONCLUSIONS

This study has presented a detailed evaluation of the Bingöl station accelerogram recorded during the May 1, 2003 Bingöl earthquake. The earthquake occurred on a very complex faulting system that is inside one of the most seismically active zones in Turkey. The strong ground motion parameters discussed in this paper might be expected to serve as important tools for strong motion seismology research. The record the authors examine in this article is a lone item, so its interpretation is tentative and not unequivocal.

The results based on AI and Husid plots show that the N10E component that exhibits a pulse signal has significantly larger energy than the orthogonal E10S component. The mean AI of the horizontal Bingöl station components is considerable. In contrast to AI and Husid diagram results, the PGV/PGA ratio of the N10E component is below the general observations made from the similar ground motions that contain pulse signals in their waveforms. The pulse signal of the Bingöl record does not necessarily confirm that the record is affected by forward directivity. The polarization of the horizontal acceleration, velocity and displacement components shows the ground motion took place principally along the strike of the ruptured fault. This observation can be attributed to local site characteristics.

The unusual spectral acceleration peak at 0.15 s observed in the N10E component seems to be site amplification. We have not succeeded in isolating effects of possible building pounding in close proximity of the recording station.

The pulse in the signal of the N10E component (whether due to forward directivity or not) has a significant influence on the calculated inelastic deformation demands. The inelastic deformations of this component are significantly higher than the elastic deformations for periods of vibration less than the pulse period. This seismological feature should be incorporated in the maximum inelastic deformation estimations of performance-based seismic design guidelines.

CHAPTER AUTHORS

Coordinator

P. Gülkan, Middle East Technical University

Contributor

D. S. Akkar, Middle East Technical University

Table 2.1 Earthquakes within Bingöl and Vicinity

Date dd.mm.yy	Lat. (N)	Long. (E)	Depth (km)	Magnitude (Local)	Notes
--.03.01	39.92	41.30	-	5.7	
28.04.03	39.10	42.50	-	6.3	Bulanık-Muş
--.--.05	38.30	38.60	-	5.7	
04.12.05	39.00	39.00	-	6.8	Akçapınar
04.12.05	39.00	39.00	-	5.8	
04.12.05	39.00	39.00	-	5.6	
--.--.06	39.92	41.30	-	5.7	
27.01.07	39.10	42.50	-	6.3	Malazgirt
05.03.09	39.70	40.50	-	5.5	
14.02.15	38.80	42.50	-	5.6	
13.09.24	39.96	41.94	10	6.8	Pasinler
10.12.30	39.72	39.24	30	5.6	
12.11.34	38.54	41.00	50	5.9	Yenibaşak
27.11.34	37.90	40.20	-	6.2	Diyarbakır
15.12.34	38.90	40.50	-	5.8	
21.11.39	39.82	39.71	80	5.9	Tercan
26.12.39	39.80	39.51	20	7.9	Erzincan
18.10.40	39.60	42.20	15	5.6	
08.11.41	39.70	39.70	-	5.5	
12.11.41	39.74	39.43	70	5.9	Erzincan
31.05.46	39.29	41.21	60	5.9	Varto-Hınış
14.12.47	39.90	42.50	-	5.5	
17.08.49	39.57	40.62	40	6.7	Karlıova
03.01.52	39.95	41.67	40	5.8	
25.10.59	39.47	41.70	-	5.8	
02.03.60	37.90	41.10	-	5.5	
01.03.61	38.40	39.30	-	5.5	
12.02.62	39.00	41.60	-	5.5	
17.02.62	38.70	41.50	-	5.5	
31.08.65	39.36	40.79	11	5.6	
07.03.66	39.20	41.60	26	5.6	
19.08.66	39.17	41.56	26	6.9	Varto
20.08.66	39.42	40.98	14	6.2	Varto
20.08.66	39.16	40.70	33	6.1	Varto
26.07.67	39.54	40.38	30	5.9	Pülümür
22.05.71	38.85	40.52	3	6.8	Bingöl*
06.09.75	38.51	40.77	32	6.6	Lice
13.03.92	39.71	39.61	27	6.8	Erzincan
15.03.92	39.60	39.60	17	6.1	Pülümür
27.01.03	39.52	39.78	10	5.8	Pülümür

* This earthquake caused 900 deaths

Table 2.2 Important strong ground motion parameters of the Bingöl station record

Component	PGA (cm/s2)	PGV (cm/s)	PGD (cm)	EPA (cm/s2)	AI (cm/s)	teff (s)	PGV/PGA (s)
N10E	535.3	36.1	26.6	441.2	192.2	4.58	0.067
E10S	271.5	22.1	10.1	253.1	79.5	6.90	0.081
UP	463.3	13.6	8.5				0.029

Table 2.3 Summary of ground motions used in observing the variation of PGV/PGA ratio with distance for records that have pulse signals and that do not have pulse signals.

Earthquake	Station	PGA (cm/s2)	PGV (cm/s)	PGA/ PGV	Fault	Site (USGS)	D (km)	M_w
Imp. Val., 10/15/79	EC DIFF ARRAY, 270 (USGS Stat 5165)	345	71.2	0.206	SS	C	5.3	6.5
Northridge, 01/17/94	Syl-Cnvrtr, 052 (DWP Stat. 74)	601	117	0.195	R	C	6.2	6.7
Northridge, 01/17/94	Syl–Hosp., 360 (CDMG Stat. 24514)	827	130	0.157	R	C	6.4	6.7
Northridge, 01/17/94	Newhall-W Pico Canyon, 046	446	92.8	0.208	R	B	7.1	6.7
Northridge, 01/17/94	Newhall-W Pico Canyon, 316	319	67.4	0.211	R	B	7.1	6.7
Imp. Val. 10/15/79	Holtville PO, 225 (USGS Stat. 5055)	248	48.8	0.197	SS	C	7.5	6.5
Imp. Val. 10/15/79	Holtville PO, 315 (USGS Stat. 5055)	217	49.8	0.229	SS	C	7.5	6.5
Imp. Val. 10/15/79	EC CO Center FF, 092 (CDMG Stat. 5154)	230	68.8	0.299	SS	C	7.6	6.5
Imp. Val. 10/15/79	Brawley Airport, 225 (USGS Stat. 5060)	157	35.9	0.229	SS	C	8.5	6.5
Imp. Val. 10/15/79	EC Array #10, 050 (USGS Stat. 412)	168	47.5	0.283	SS	C	8.6	6.5
Imp. Val. 10/15/79	EC Array #10, 320 (USGS Stat. 412)	219	41	0.187	SS	C	8.6	6.5
Northridge, 01/17/94	Sepulveda VA, 270 (USGS Stat. 0637)	738	84.8	0.115	R	C	8.9	6.7
Northridge, 01/17/94	Canyon Country-W Lost Canyon, 270	473	45.1	0.095	R	C	13	6.7
Loma Prieta, 10/18/89	Saratoga Aloha, 090 (CDMG Stat. 58065)	318	42.6	0.134	RO	B	13	6.9
Loma Prieta 10/18/89	Corralitos, 000 (CDMG Stat. 57007)	632	55.2	0.087	RO	B	5.1	6.9
Imp. Val. 10/15/79	EC Diff Array, 230 (USGS Stat. 5165)	471	40.8	0.087	SS	C	5.3	6.5
Northridge, 01/17/94	Syl.-Cnvrtr Sta, 142 (DWP Stat. 74)	880	102	0.116	R	C	6.2	6.7
Northridge, 01/17/94	Syl.-Hospital, 090 (CDMG Stat. 24514)	593	78.2	0.132	R	C	6.4	6.7
Northridge, 01/17/94	Newhall, 090 (CDMG Stat. 24279)	572	75.5	0.132	R	C	7.1	6.7
Northridge, 01/17/94	Newhall, 360 (CDMG Stat. 24279)	579	97.3	0.168	R	C	7.1	6.7
Imp. Val. 10/15/79	EC CO Center FF, 002 (CDMG Stat. 5154)	209	37.5	0.179	SS	C	7.6	6.5
Northridge, 01/17/94	Pac.Kagel Canyon, 090 (CDMG Stat. 24088)	295	31.4	0.106	R	B	8.2	6.7
Northridge, 01/17/94	Pac Kagel Canyon, 360 (CDMG Stat. 24088)	424	51.5	0.121	R	B	8.2	6.7
Imp. Val. 10/15/79	Brawley Airport, 315 (USGS Stat. 5060)	216	38.9	0.180	SS	C	8.5	6.5
Northridge, 01/17/94	Sepulveda VA, 360 (USGS Stat. 0637)	921	76.6	0.083	R	C	8.9	6.7
Loma Prieta 10/18/89	Gilroy array #2, 000 (CDMG Stat. 47380)	360	32.9	0.091	RO	C	12.7	6.9
Northridge, 01/17/94	Canyon Country - W Lost Canyon, 000	402	43	0.107	RO	C	13	6.7
Loma Prieta 10/18/89	Saratoga Aloha, 000 (CDMG Stat. 58065)	503	41.2	0.082	RO	B	13	6.9
Loma Prieta 10/18/89	Saratoga W Valley Coll, 000 (CDMG Stat. 58235)	250	42.4	0.170	RO	B	13.7	6.9
Loma Prieta 10/18/89	Saratoga W Valley Coll, 270 (CDMG Stat. 58235)	326	61.5	0.189	RO	B	13.7	6.9
Loma Prieta 10/18/89	Gilroy array #3, 000 (CDMG Stat. 47381)	544	35.7	0.066	RO	C	14.4	6.9
Loma Prieta 10/18/89	Gilroy array #4, 000 (CDMG Stat. 57382)	409	38.8	0.095	RO	C	16.1	6.9
Loma Prieta 10/18/89	Gilroy array #4, 090 (CDMG Stat. 57382)	208	37.9	0.182	RO	C	16.1	6.9
Northridge, 01/17/94	Tarz.-Cedar Hill Nurs A, 090 (CDMG Stat. 24436)	1750	114	0.065	R	B	17.5	6.7
Northridge, 01/17/94	Tarz.-Cedar Hill Nurs A, 360 (CDMG Stat. 24436)	971	77.6	0.080	R	B	17.5	6.7

[1] The border in the middle shows the division between the records that have pulse signals and that do not have pulse signals. The records that are above the division line have pulse signals.

2 The abbreviations “R”, “RO”, and “SS” stand for reverse, reverse-oblique and strike-slip, respectively.

3 The abbreviation D stands for the closest distance between the recording station and the fault.

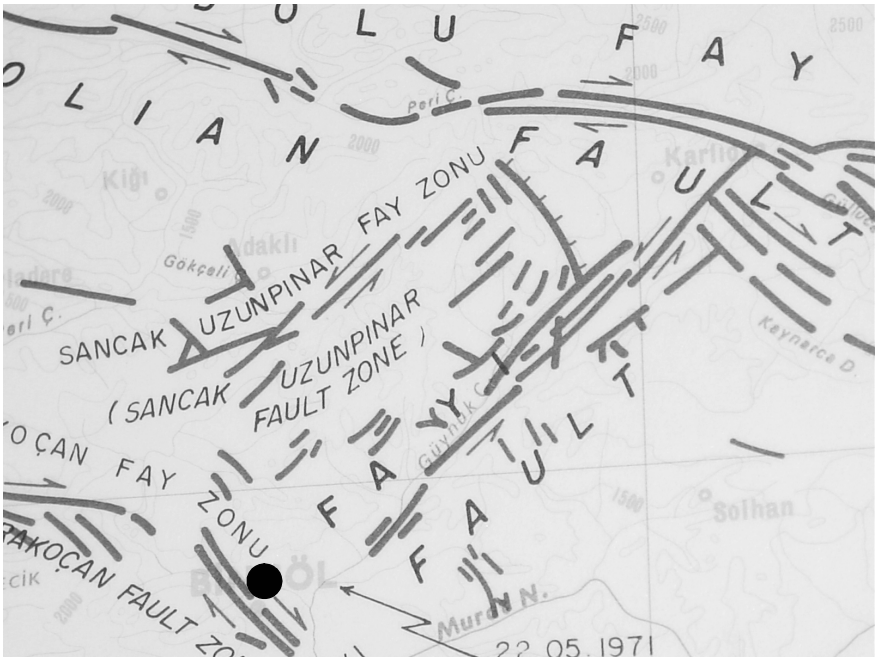

Figure 2.1 The general tectonics of the region. The approximate location of the city of Bingöl is shown by the black circle.

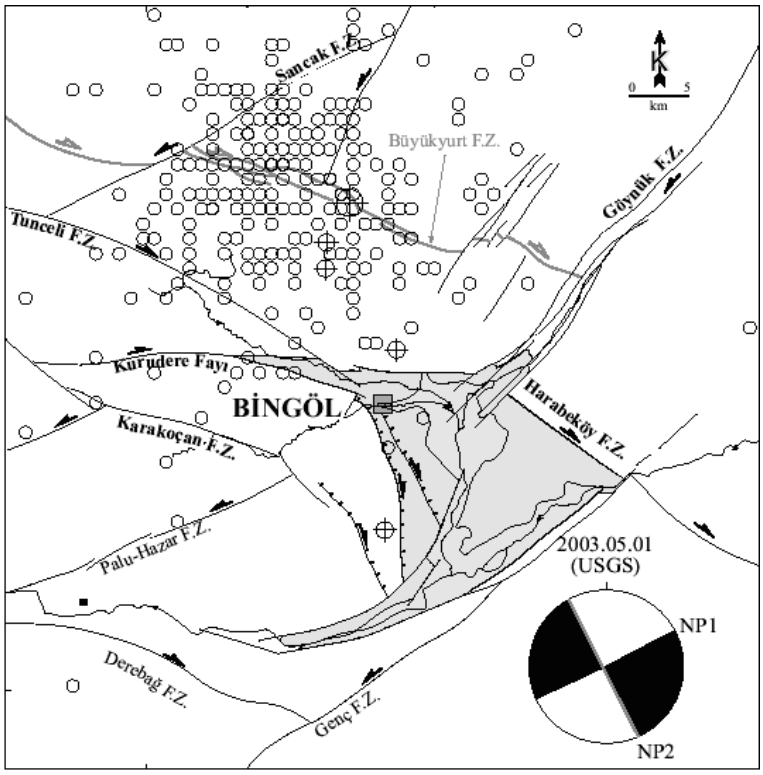

Figure 2.2 Distribution of aftershock data of the 05/01/2003 Bingöl event. The aftershock epicenters are denser in the area confined by Sancak, Göynük and Kurudere fault zones. These faults are conjugate faults that extend from the EAF and NAF. The complexity of the faulting systems is noteworthy. Koçyiğit and Kaymakçı (2003) reported that the right lateral strike-slip Büyükyurt fault zone was ruptured during the Bingöl earthquake. The rectangular block that is approximately 12.5 km to the Büyükyurt fault zone shows the Bingöl recording station. The USGS fault plane solution is shown on the lower right corner. (The map is taken from Koçyiğit and Kaymakçı, 2003).

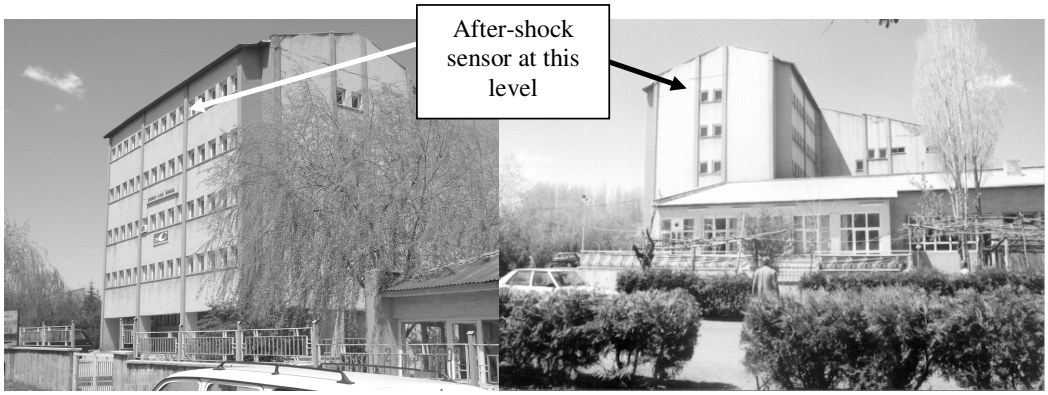

(a) (b)

(c)

Figure 2.3 Bingöl Public Works and Settlement branch office complex. Figure 2.3a shows the 5-story reinforced concrete main office building. Figure 2.3b describes the way the 5-story structure is connected to the adjacent 4-story office building in the rear. The accelerometer sensor is deployed inside the 1-story auxiliary building (Figure 2.3c) situated approximately 15 m from the mid-rise office buildings shown at the rear. The two mid-rise buildings experienced severe pounding during the main event. The effects of this pounding are not discernible in the main shock accelerogram. (Courtesy of Prof. Mete Sozen, Purdue University)

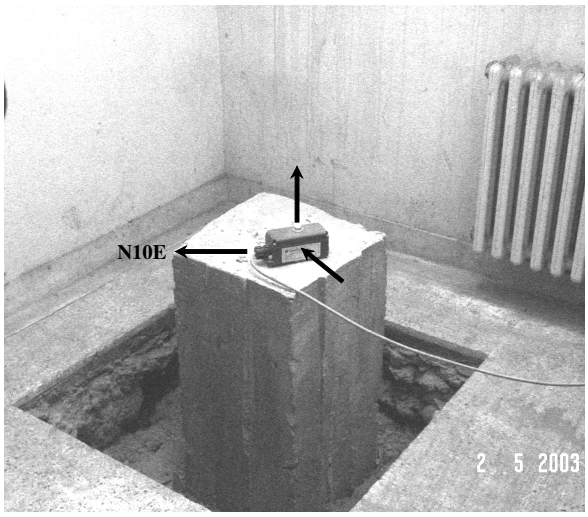

Figure 2.4 The deployment of the sensor in the Bingöl station and the directions of the principal axes. The instrument is placed on a reinforced concrete pedestal inside a 0.5 m deep, 1x1m foundation. Interaction between the structure and the sensor is minimized. The authors considered the effect of sensor's electric field on the compass while establishing these directions. ERD reported the NE10 direction as NS, and E10S direction as EW in the raw acceleration data posted at their website.

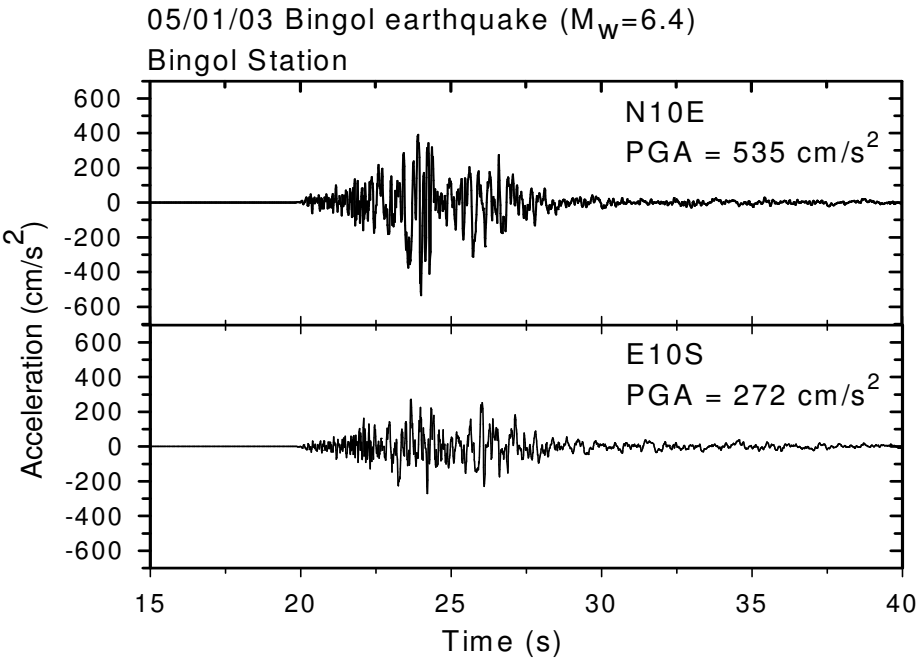

(a)

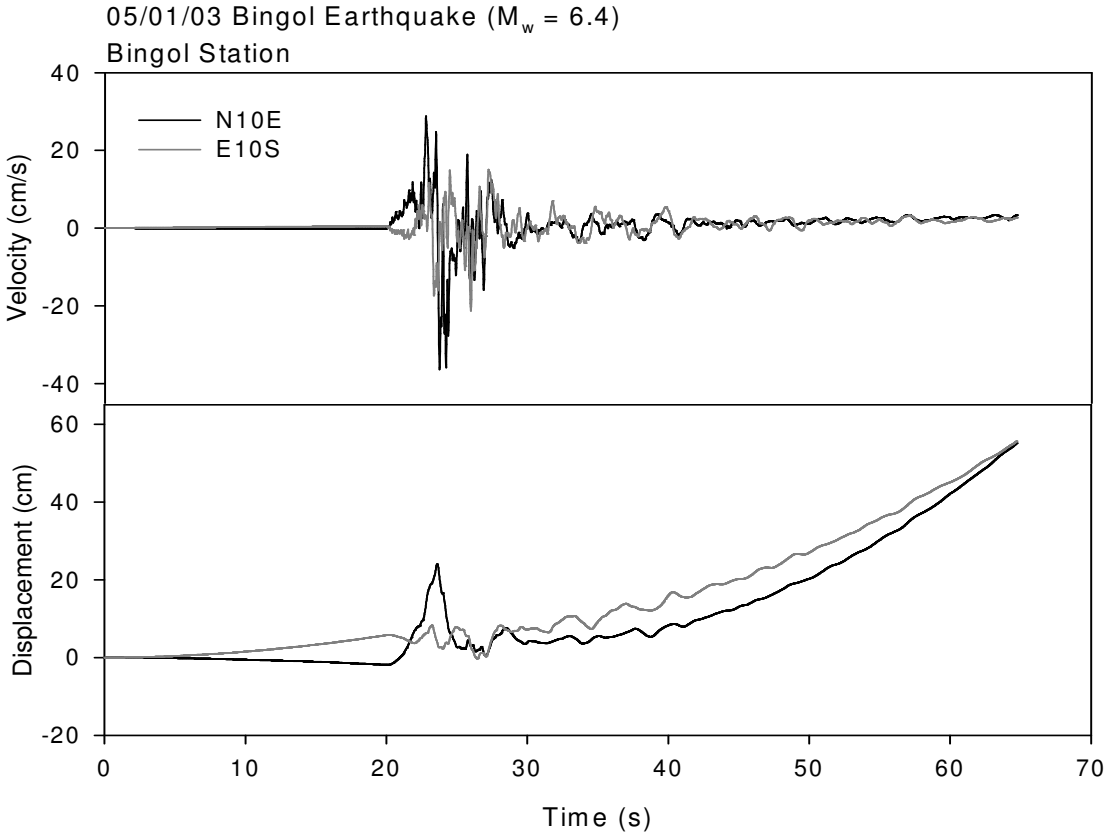

(b)

Figure 2.5 (a) Acceleration traces of the unprocessed horizontal components; (b) Velocity and displacement traces of the unprocessed horizontal components. Integrations were computed by a simple trapezoidal rule. The unrealistic linear shift in the velocity traces causes significant shifts in the displacements. These are pronounced for both components.

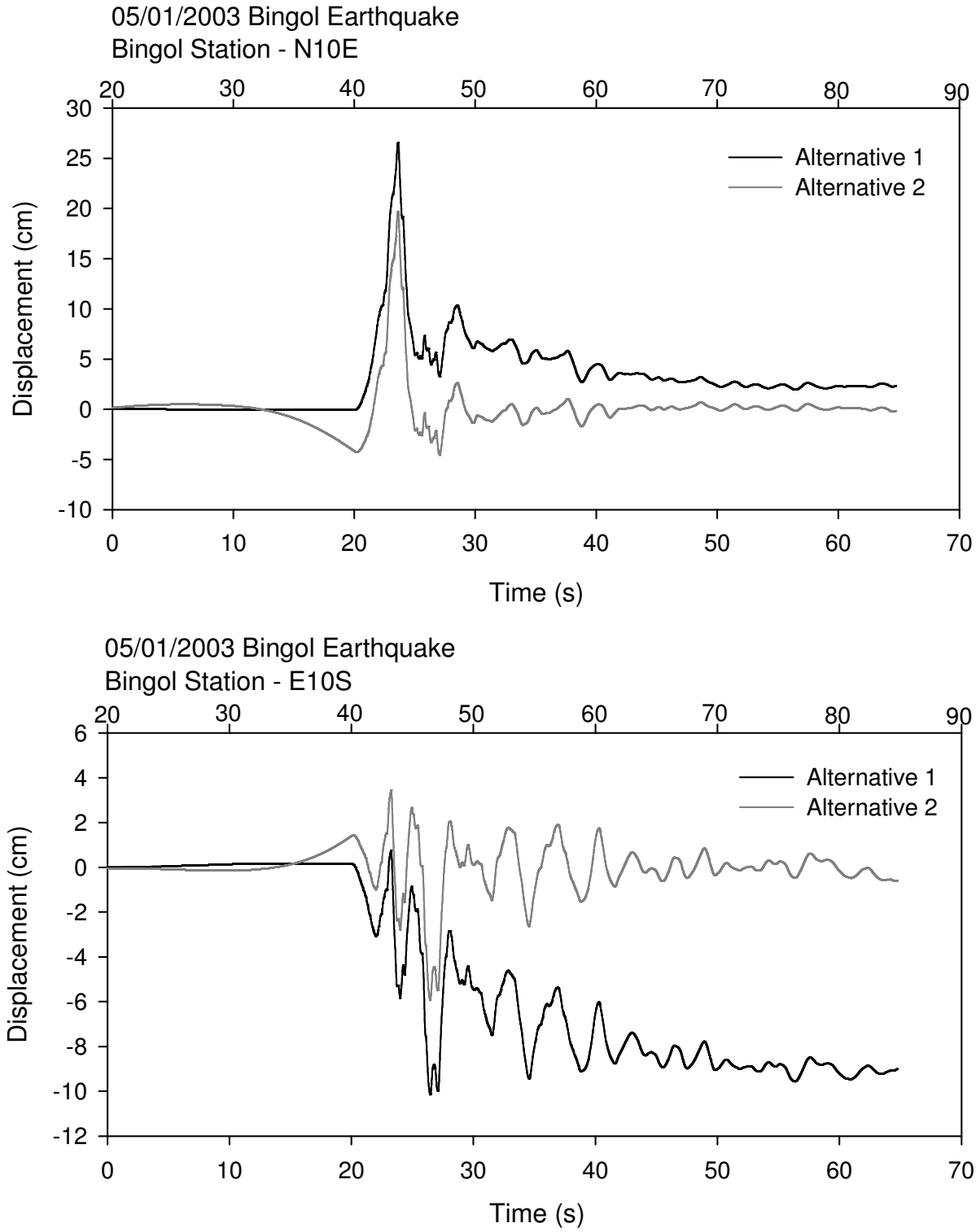

Figure 2.6 Comparisons of the displacement signal obtained from alternative correction procedures. Alternative 1 fits a straight line on the raw velocity between 50 and 64.73 s (i.e., the time interval where the ground motion is about to terminate). The fitted straight line is used to find the time (referred to as t2) at which the velocity becomes zero. This implausible shift is thus removed from the acceleration, velocity and displacement traces. Alternative 2 processes the raw acceleration data by acausal filtering, adding 20 s leading, and 40 s trailing zeros as required by the acausal Butterworth filter. The order of filtering is 1, where response runs according to f^4 at low frequencies.

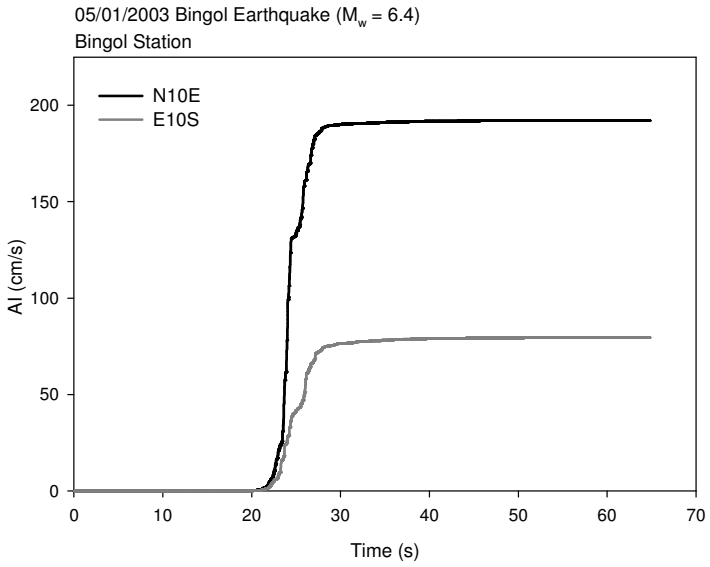

Figure 2.7 The Husid plots for the horizontal components.

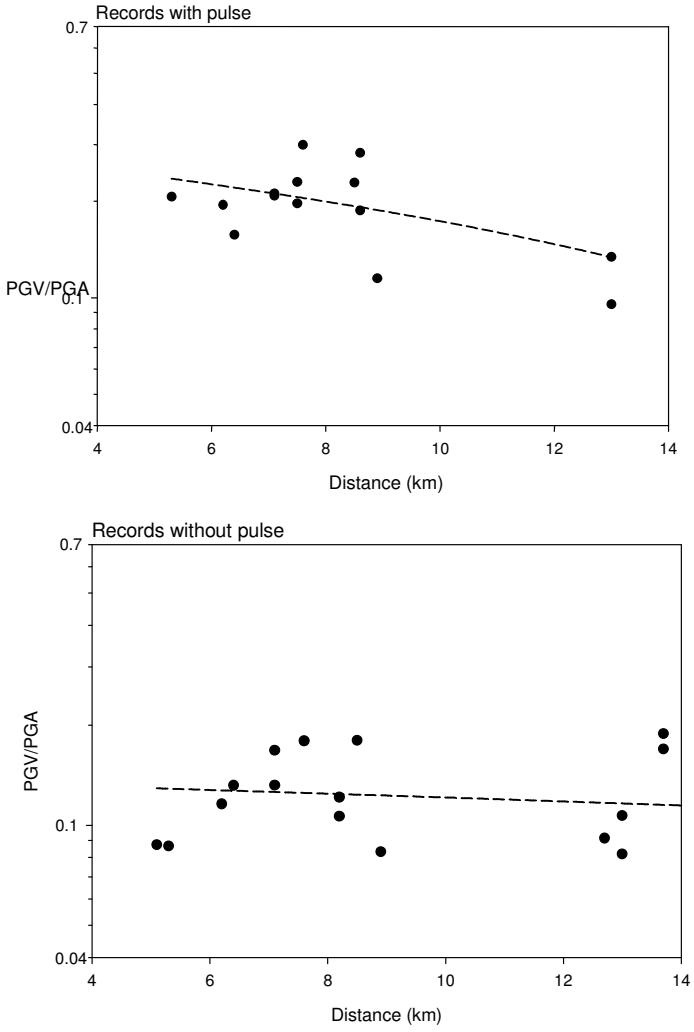

Figure 2.8 PGV/PGA ratios for ground motions in Table 2.3. The dashed curves in the scatter diagrams show the general trend for records with and without pulse. The magnitude and site conditions of the records chosen are fairly representative for Bingöl.

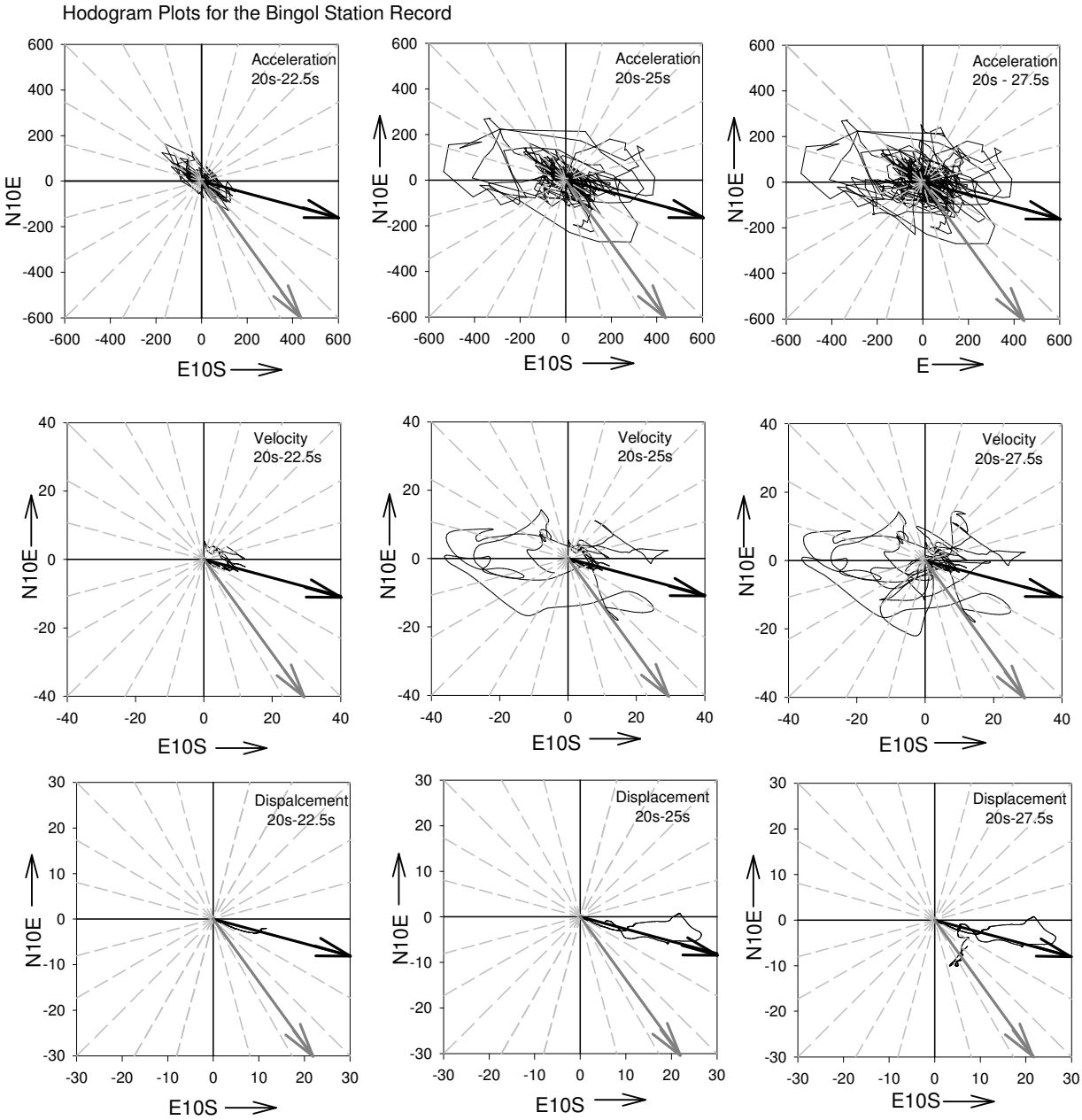

Figure 2.9 The hodographs of the horizontal motions. The plots are drawn for three consecutive time intervals that represent the strong ground motion duration of the Bingöl event. The diagrams also display the strikes of the inferred fault rupture reported by Koçyiğit and Kaymakçı (dark arrow) and the theoretical strike derived by the USGS from the fault-plane solution (light arrow). The dashed lines are drawn at every 15 deg.

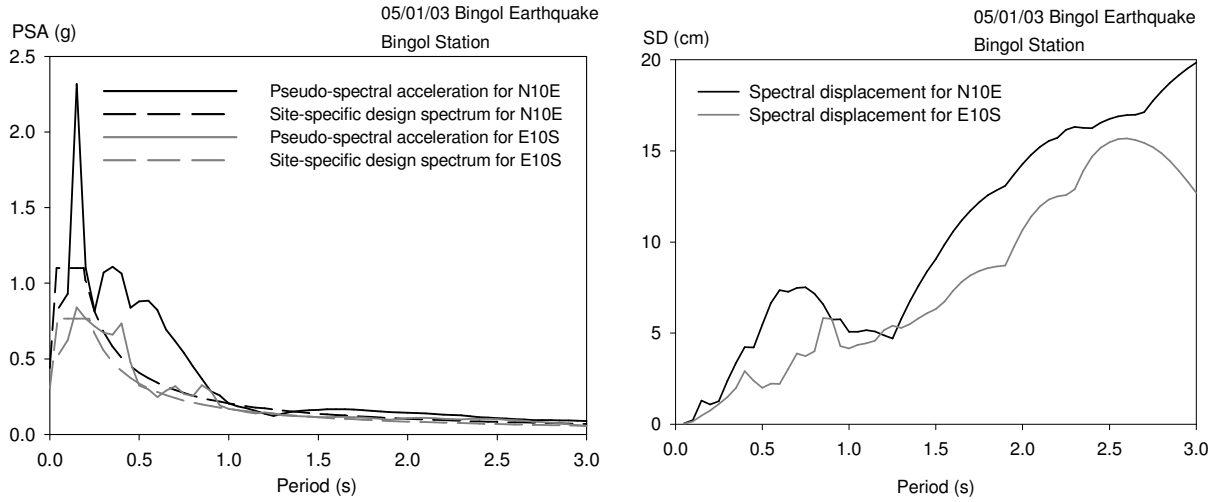

Figure 2.10 The 5-percent damped elastic spectra for the horizontal components.

Figure 2.11 Evidence of pounding between the mid-rise office buildings of the Bingöl Public Works and Settlement branch complex. The photograph on the left is taken from the enclosed garden surrounded by the office buildings and the 1-story auxiliary structure where the strong ground motion instrument was located. The distance between the office buildings and the auxiliary structure is approximately 15m. The image on the right shows that the effect of pounding grows with height. The pounding is significant in the NS direction.

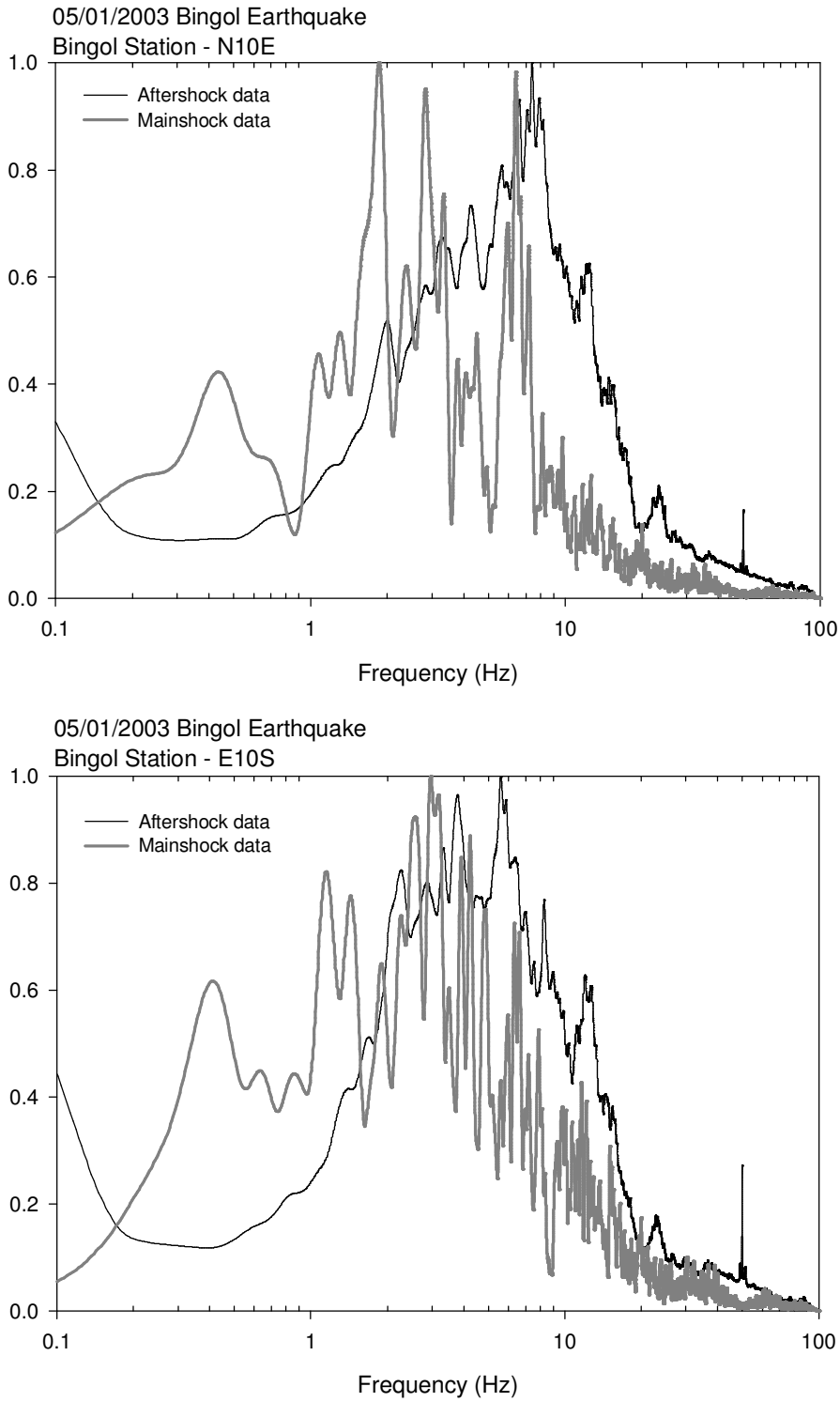

Figure 2.12 Nondimensional Fourier amplitudes for the horizontal components of main shock and aftershock data. The aftershock data is the geometric mean of 59 events. The data is normalized with respect to the maximum amplitude. For the aftershock data, the normalization is done with respect to the maximum amplitude of the mean data. The aftershock data is not processed for baseline. Both curves represent the smoothed data by Parzen's lag window with a bandwidth of 0.2 Hz. The smoothing process did not destroy any important peaks in the data. The artificial amplification of the aftershock data in the lower frequencies is due to the lack of baseline correction.

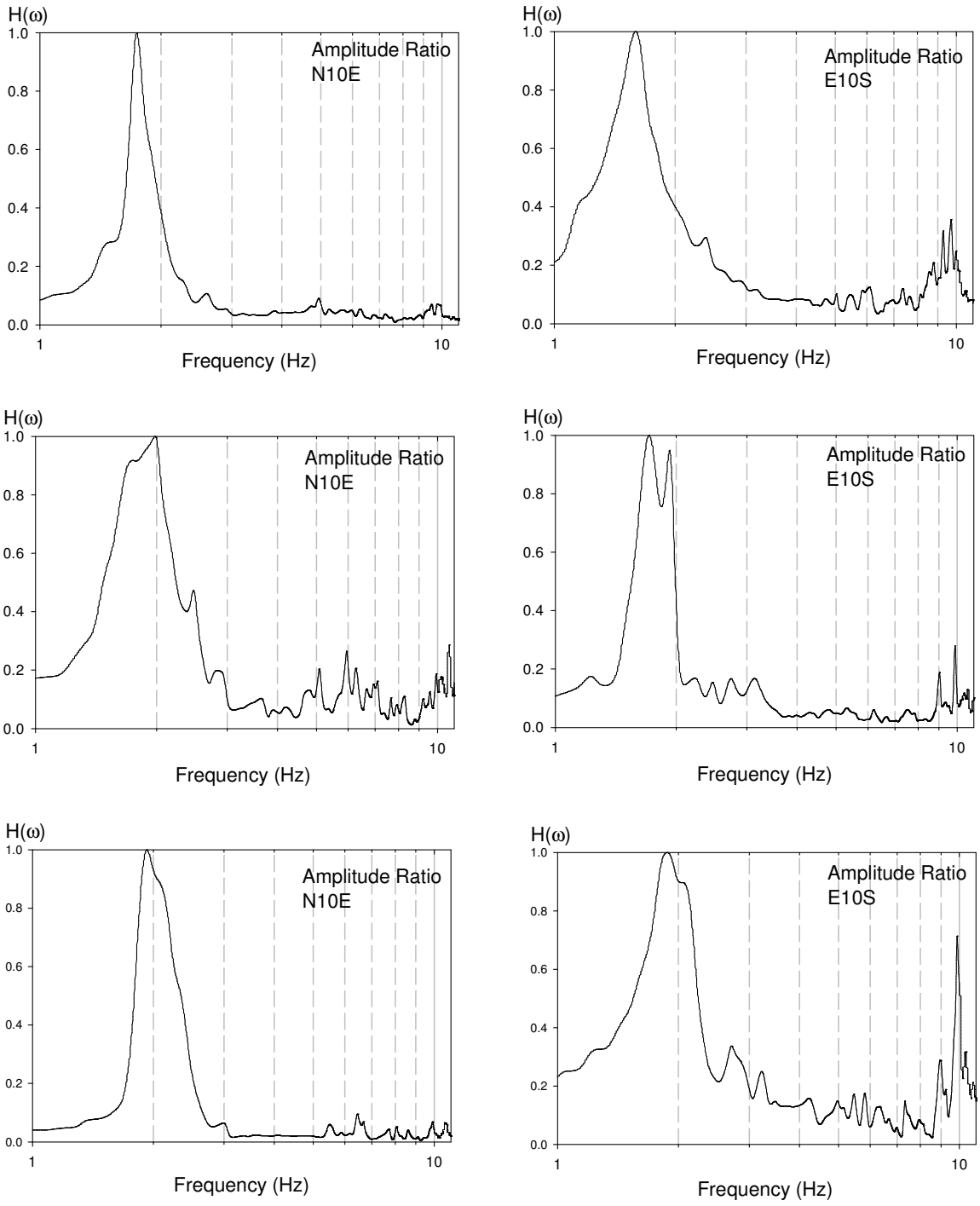

Figure 2.13 Spectral ratios of the fourth floor and ground level records obtained during the aftershock events. The floor records were obtained from the 5-story office building. The ground level records were from the 1-story adjacent building nearby.

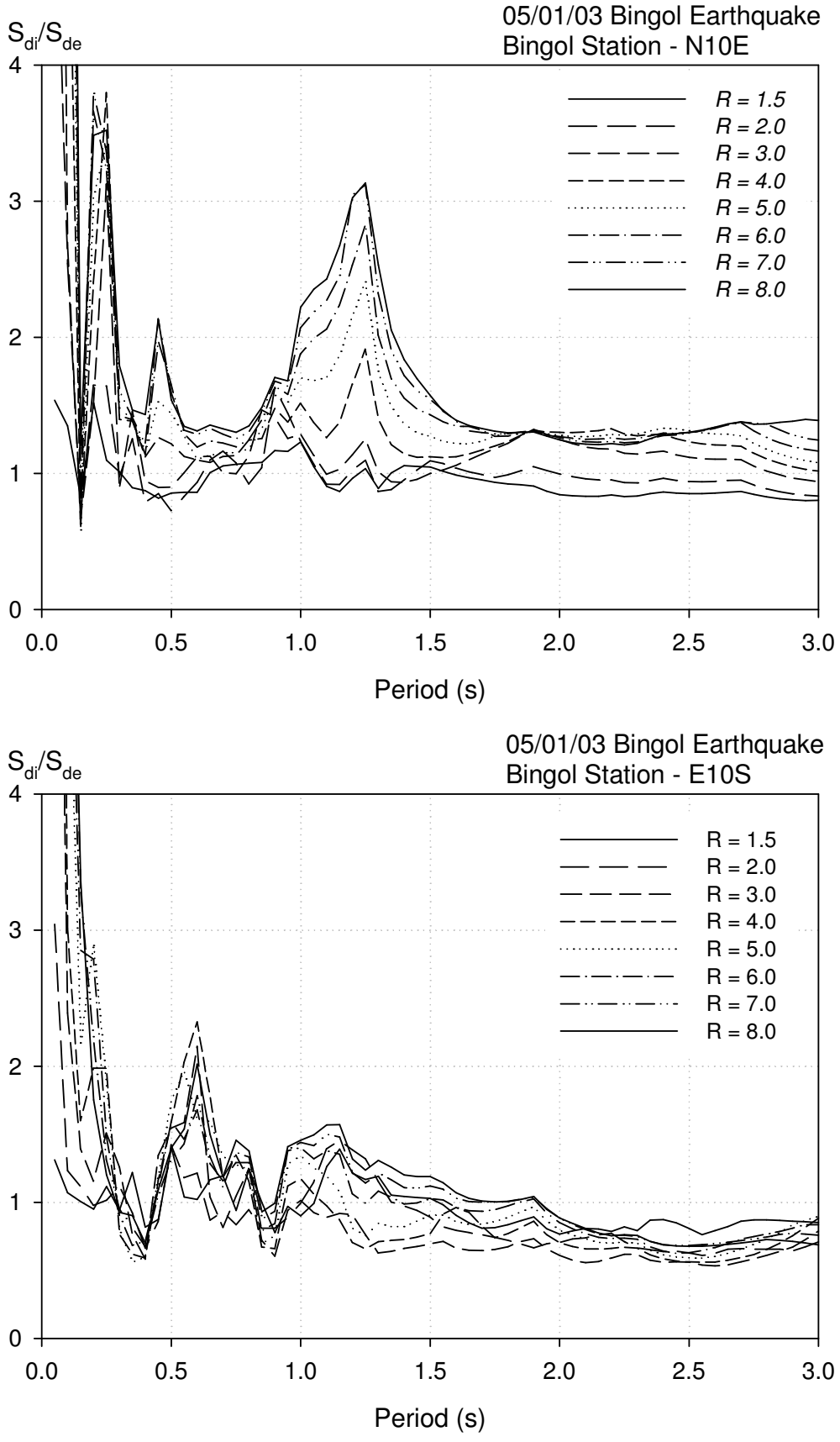

Figure 2.14 Constant strength spectral displacement amplifications.

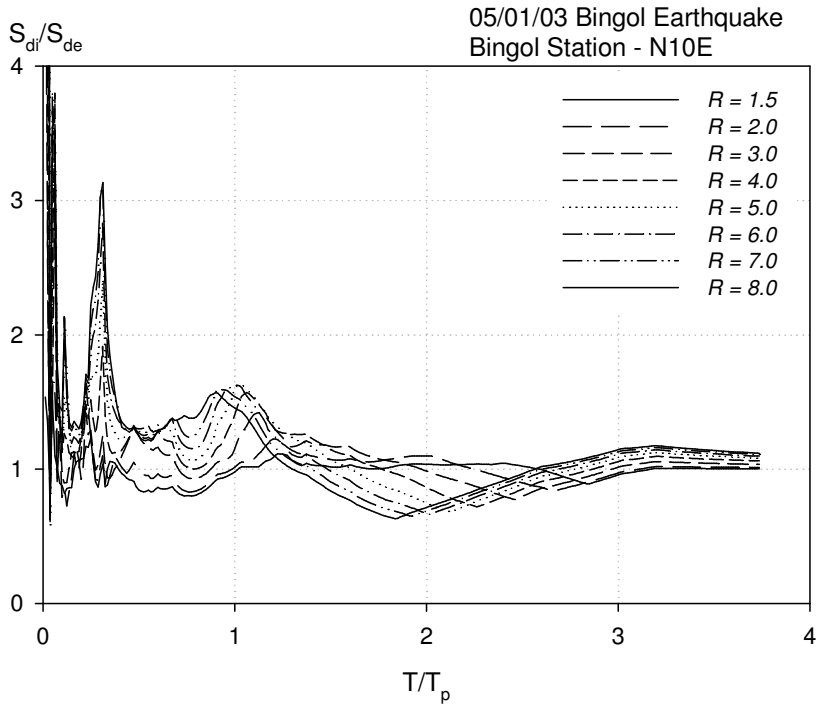

Figure 2.15 Constant strength spectral displacement amplification of the N10E component for periods normalized with respect to the pulse period.

3

GEOLOGY OF BİNGÖL AREA

3.1 GEOLOGY

The Upper Oligocene – Lower Miocene volcanic rocks represent the main geologic units in the earthquake-affected Bingöl region. These rocks are basaltic, and partly andesitic and trachy-andesitic lavas, tuffs and agglomerates (Seymen and Aydın, 1972). They exhibit varying degrees of weathering which have resulted in shallow to moderately deep - seated soil-like materials (residual soils) in different parts of the region.

The Plio-Quaternary aged terrace deposits are observed in the city of Bingöl and its close vicinity between the elevations of 1040 -1100 m. These deposits are composed of a dark brown colored clay matrix containing rounded and semi-rounded blocks. The city is founded on these stiff deposits (Figure 3.1a). Natural and man-made slopes in this material seem to be considerably stable even under seismic loads (Figure 3.1b). This unit is not liquefaction susceptible.

(a) (b)

Figure 3.1 (a) A view from the terrace deposits and (b) natural and man-made stable slopes in these deposits at the northern part of Bingöl

As can be seen from the geological map (Figure 3.2), more recent alluvial deposits cover the southern and southeastern parts of the city. These deposits have been carried and accumulated mainly by the Gayt and Göynük Rivers, and consist of gravel, sand, silt and clay sized materials in different fractions.

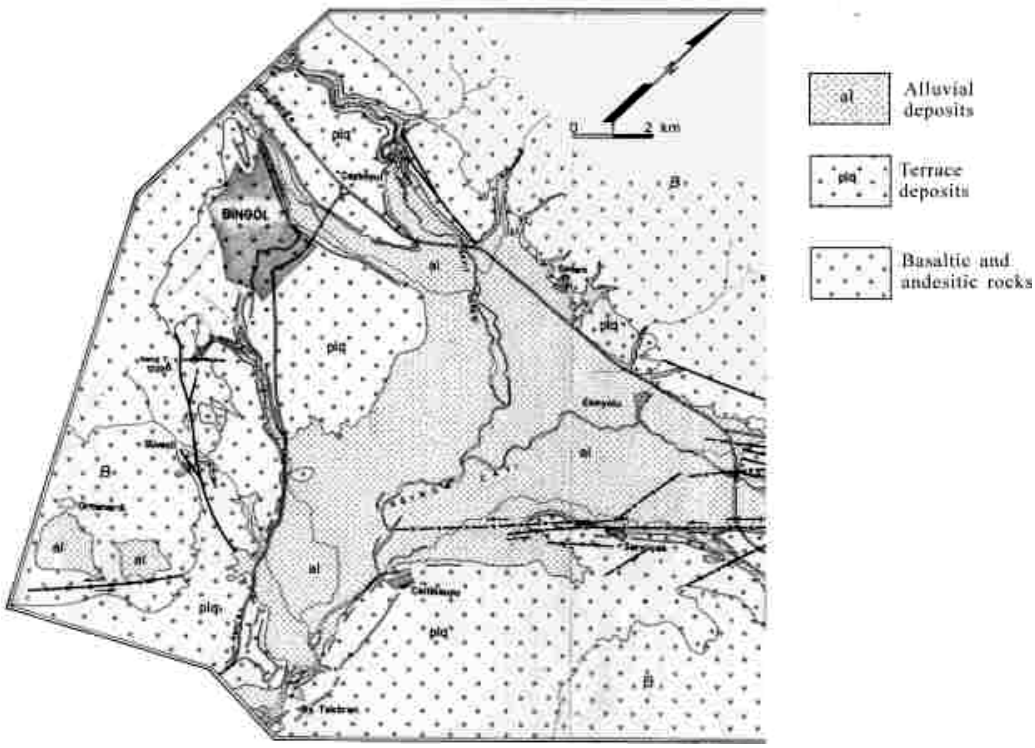

Figure 3.2 Geological map of Bingöl and its close vicinity (after Seymen and Aydın, 1972)

3.2 SEISMOTECTONICS

The earthquake-affected region is located within the Bingöl-Karlıova-Erzincan triangle, where two major strike-slip faults, NAF and EAF, intersect. In this region there are a number of conjugate active left-and-right lateral strike-slip faults extending in the NE-SW and NW-SE directions as shown in Figure 3.3. While NAF is a right-lateral strike slip fault, EAF is a left-lateral strike slip fault. The NE-SW trending Göynük segment of the EAF has a length of about 65 km and passes by the east of Bingöl city.

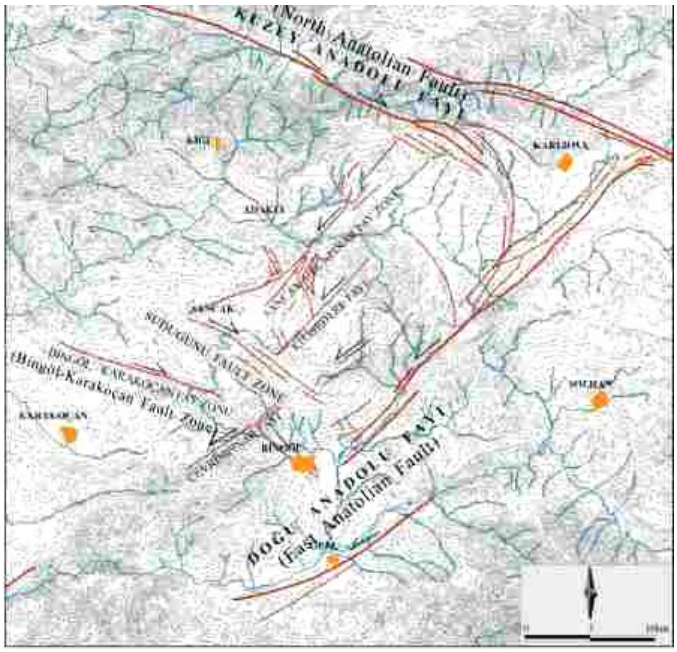

Figure 3.3 Active fault map of the Bingöl-Karlıova-Erzincan triangle (after Emre et al. 2003)

The NW-SE trending active conjugate faults show right-lateral strike slip characteristics (Şaroğlu et al., 1987 and 1992). The Bingöl-Karakoçan fault zone has a length of 40 km, while the Sudüğünü fault zone is 20 km long and consists of five segments (Emre et al. 2003; Figure 3.3). The Sancak-Uzunpınar and Kilisedere faults are the other conjugate left-lateral strike-slip faults running in the NE-SW direction.

Due to the presence of several active faults, the Bingöl-Karlıova-Erzincan triangle is a region where destructive earthquakes occur quite often. The 1971 Bingöl earthquake was the previous major event in the area and the causative fault of that earthquake was the Göynük segment of the EAF and the epicenter was about 10 km south of the city center (Seymen and Aydın, 1972). Following the earthquake, short rupture surfaces were observable along a 40-km line to the southeast of Bingöl.

3.3 MAIN CHARACTERISTICS OF THE EARTHQUAKE AND FAULTING

The magnitude of the earthquake was M_w = 6.4. The locations for the epicenter estimated by the Earthquake Research Department of Turkey (ERD), Kandilli Observatory and Earthquake Research Institute of Bogaziçi University (KOERI) and USGS are shown in Figure 3.4. Considering the distribution of damage and locations of the earthquake-triggered landslides in the region, the epicenter locations provided by KOERI and USGS seem to be quite acceptable. Table 3.1 compares the seismic parameters from focal plane solutions released by different institutions. Most fault plane solutions, which can be provided from Internet, predict a right lateral strike-slip fault (Figure 3.4). However, these solutions suggest two possible faults striking in the NW-SE and NE-SW directions. The depth of the focus released by several institutions ranges between 5 and 15 km probably due to different methods employed (Table 3.1).

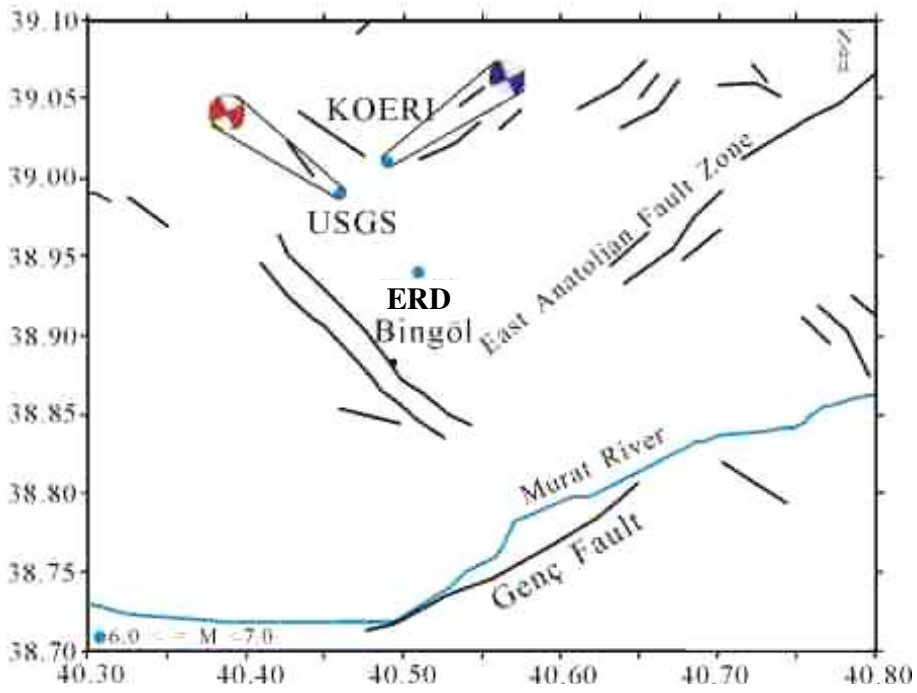

Figure 3.4 Epicentral locations of main shock released by ERD, KOERI and USGS and focal plane solutions of KOERI and USGS

Table 3.1 Seismic parameters of the Bingöl earthquake of May 1, 2003

Institute	Latitude	Longitude	Depth (km)	Magnitude			Strike	Dip	Slip
				M_d	M_s	M_w			
KOERI	39.01	40.49	10	-	6.4	-	NP1 225^0 NP2 135^0	90^0 62^0	28^0 180^0
ERD	38.94	40.51	6	6.1	-	-	-	-	-
USGS	38.99	40.46	10	-	-	6.4	NP1 64^0 NP2 154^0	88^0 90^0	0^0 -178^0
HARVARD	39.01	40.53	15	-	-	6.3	NP1 332^0 NP2 236^0	68^0 75^0	-164^0 -22^0
ETHZ	39.00	40.50	10	-	6.1	-	-	-	-

Based on the records released by KOERI, 384 aftershocks with magnitudes greater than 3.0 occurred between 40.20 and 40.65 longitudes, and 38.8 and 39.25 latitudes until May 19, 2003. As seen from Figure 3.5, the aftershocks took place over a large area around the epicenter of the main shock near the juncture of the NE-SW and NW-SE trending faults. Therefore, it seems difficult at this stage to estimate an evident faulting strike from this distribution. However, based on the evaluation of the aftershocks with M>4 by KOERI (http://www.koeri.boun.edu.tr/sismo/Bingol.htm), these show an alignment in the NW-SE direction, which is consistent with the general trend of Sudüğünü fault. Koçyiğit and Kaymakçı (2003) reported that very short and discontinuous surface ruptures ranging between a few meters to 40 m length are aligned in the N60-70W direction and extend in a zone of 50 to 500 m wide. According to their observations, these surface ruptures were located between Kuşkondu and Kurtuluş villages at NW and SE, respectively. During the observations of the authors of the present report, a few short cracks were observed at the north and south of a major lateral spread that occurred at the locality of Hanoçayırı near Sudüğünü village. One of these cracks has a strike of N60W. Although a vertical drop of 1-6 cm in the southern side of the crack was observed, no lateral offset was evident. The length of this crack is about 10 m. The second group of cracks appears at the toe of a slope near the southern boundary of the lateral spread. Along this N30E trending 250 m long crack a vertical drop of 1-3 cm towards the north and 2 to 3 cm right lateral offset (Figure 3.6a) are observed. However, the trend of the crack (N30E) is not consistent with that of the Sudüğünü fault and occasionally parallel cracks are also visible (Figure 3.6b). Therefore, based on these preliminary observations, it seems difficult to consider that these local cracks were the surface ruptures associated with the causative fault. It also seems possible that due to the heavily fractured and weathered nature of the rock units in the region the fault rupture may not have reached the surface.

3.4 ENGINEERING GEOLOGY OF BİNGÖL AREA

3.4.1 General

Bingöl is surrounded by volcanic rocks (age unknown) according to the Geologic Map of Turkey.[5] The rocks to the south, west and east are basaltic whereas those to the north are andesitic. Approximately 25 km south of Bingöl are Paleozoic metamorphic rocks, which apparently were thrust south over Upper Cretaceous rocks, which, in turn, were thrust south over Miocene Marine rocks. The thrusting is part of the Zagros suture zone.

The geologic map shows Pleistocene alluvium in a large, triangular-shaped basin, with a base approximately 40 km in the NE-SW direction and an apex approximately 25 km high from the base. Bingöl is near the apex. Most of the clasts in alluvium in the Bingöl area are volcanic.

[5] Institute of Mineral Research and Exploration, Ankara, Turkey.

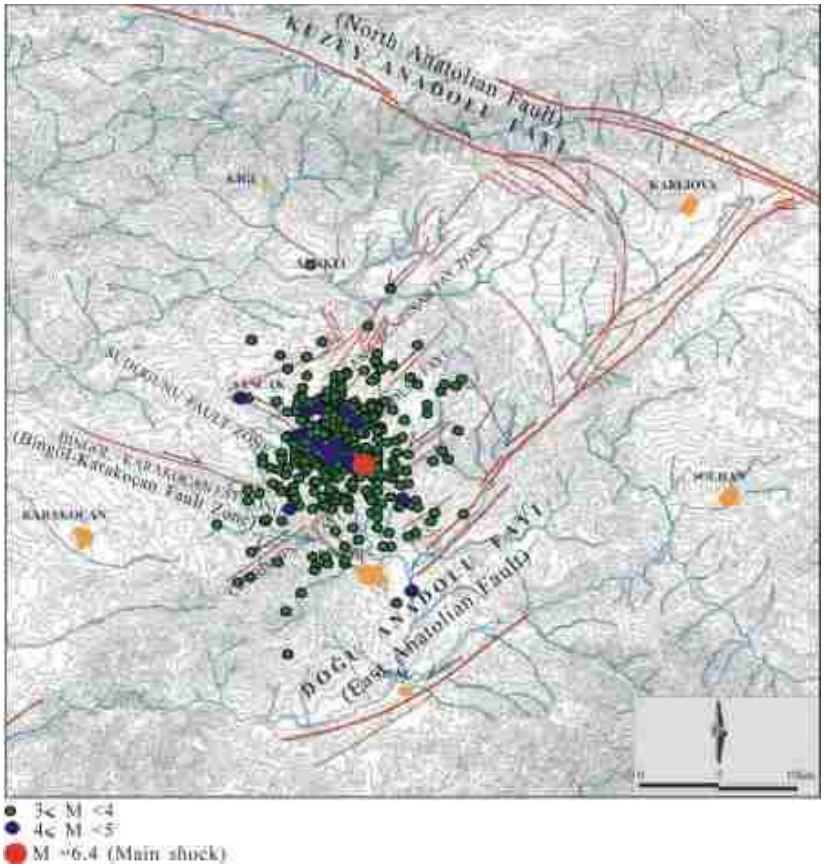

Figure 3.5 Distribution of the aftershocks occurring between May 1-15, 2003 (the base map is from Emre et al., 2003).

(a) (b)

Figure 3.6 Views from N30E trending short cracks at Hanoçayırı

3.4.2 Geologic Materials

In order to determine whether there is a correlation between geologic foundation materials and damage to structures in Bingöl, surficial deposits and relevant landforms in the area were mapped on topographic base maps with scales of 1:1000 or 1:5000. The elevations of the topographic contours are unreadable on the map, but they did provide useful information about the landforms.

The relevant materials in the area are young gravel along the major streams, alluvium along creeks and washes, old gravel (presumably Pleistocene), colluvium and volcanic bedrock (Figure 3.7).

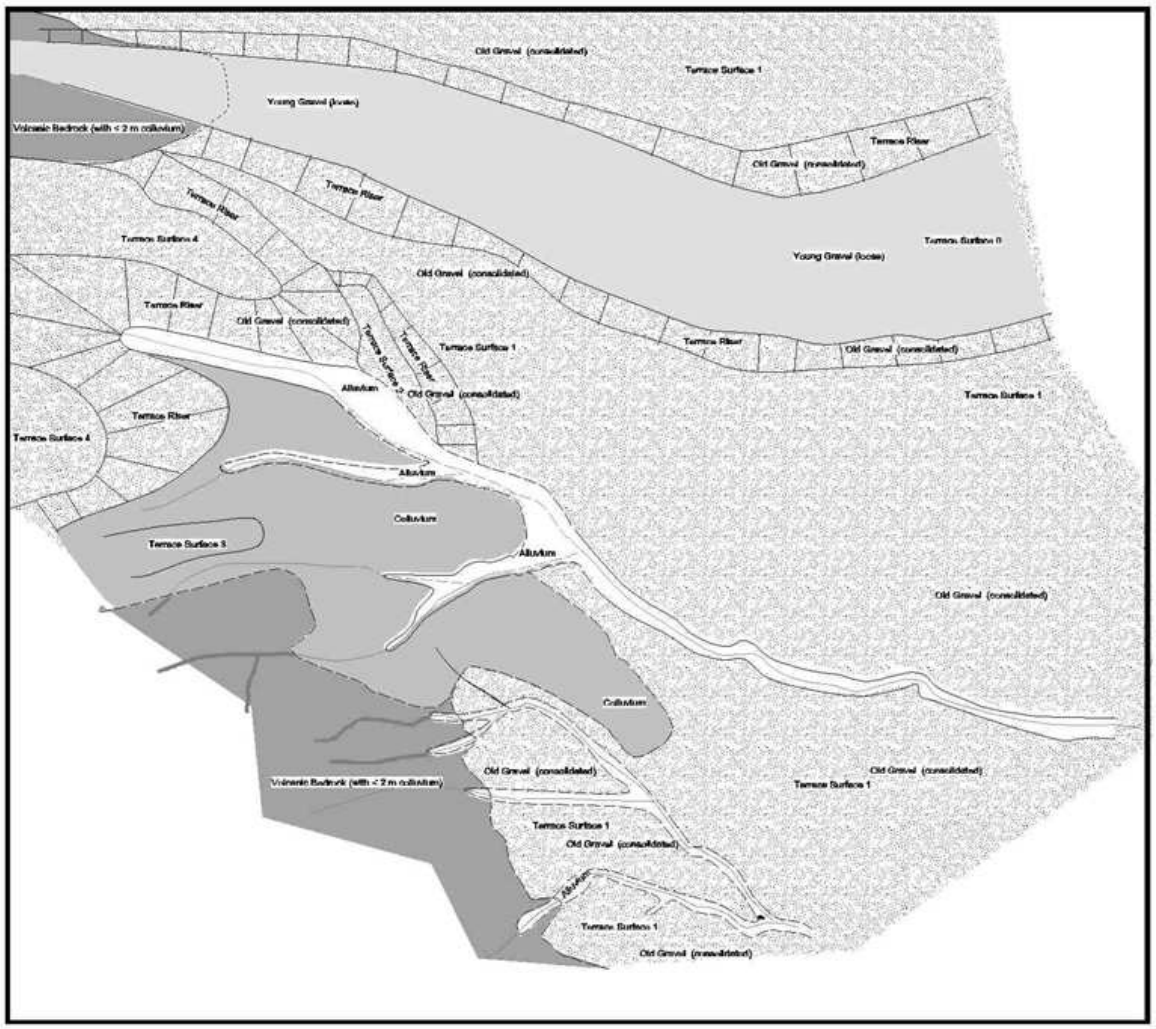

Figure 3.7 Deposits and terraces in western part of Bingöl.

3.4.1.1 Young Gravel

The major streams are the Çapakçur Çayı, which is the larger stream in the valley separating the north and south parts of Bingöl, and the Gayt Çayı, which is a smaller stream in the valley to the north of Bingöl. Both stream valleys are incised. The young gravel is largely reworked Pleistocene deposits and consists of various mixtures of sand, pebbles, cobbles and boulders within these major stream valleys. The gravels are poorly consolidated and poorly graded. The young gravels along the larger stream, Çapakçur Çayı, are shown in the upper part of Figure 3.8.

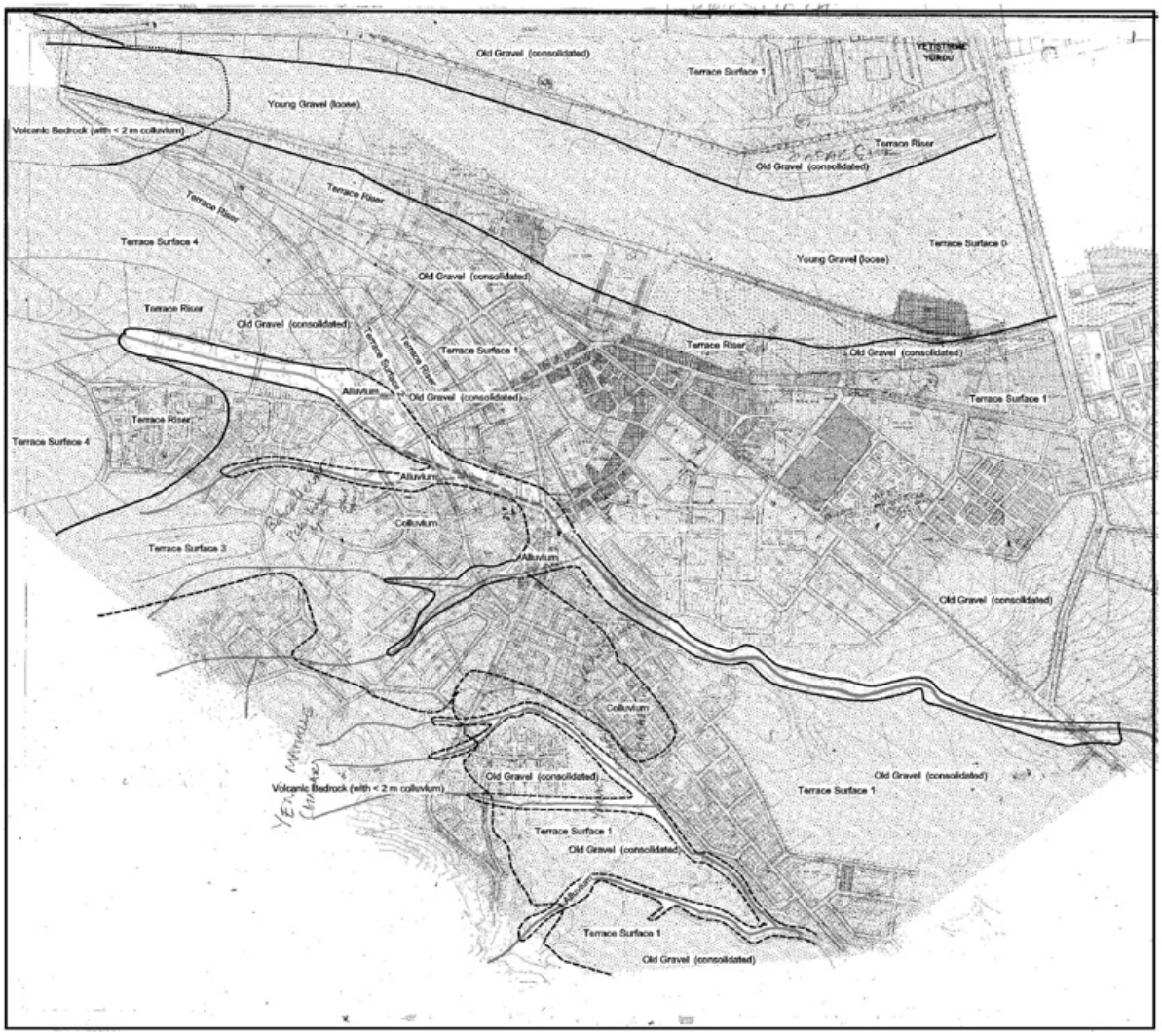

Figure 3.8 Terraces and geologic materials[6] shown on topographic base of south part of Bingöl.

3.4.1.2 Older Gravel

The older gravel, apparently of Pleistocene age, is a thick fill in the Bingöl basin, which is the triangular basin shown on the geologic map of Turkey and is approximately 40 km long and 25 km wide. The gravel is characteristically brownish red in color and contains particles ranging from clay, presumably, up to cobbles, boulders and even blocks up to 0.5 m in maximum dimension. In general it is a cobbly, bouldery conglomerate with the interstices filled by fined-grained, brownish red matrix. The gravel is consolidated.

The gravel was deposited in a basin, so its thickness would be expected to vary from place to place. The only place where a contact between the gravel and underlying bedrock was seen was along the Çapakçur Çayı, in the İnönü District (Figure 1.3; Figure 3.10), at the western edge of Bingöl (upper left in Figure 3.8). There the gravel wedges out westward and is overlying the volcanic rocks. The thickness of gravel reaches approximately 60 m where the volcanic rocks extend beneath the ground surface, but the maximum thickness of the gravel is not known.

[6] Details of the map are visible on a PDF version that can be viewed and downloaded at: http://www.eas.purdue.edu/physproc/HTM%20Files/2003_bingol_turkey.htm

Figure 3.9 Older (Pleistocene) gravel exposed in steep bank in tributary stream valley of Gayt Çayı in northern part of Bingöl.

Figure 3.10 View southwest over Çapakçur Çayı at western edge of Bingöl. Gravel in steep bank on right of view. Volcanic bedrock in shadow in steep bank on left of view. Contact slopes toward viewer.

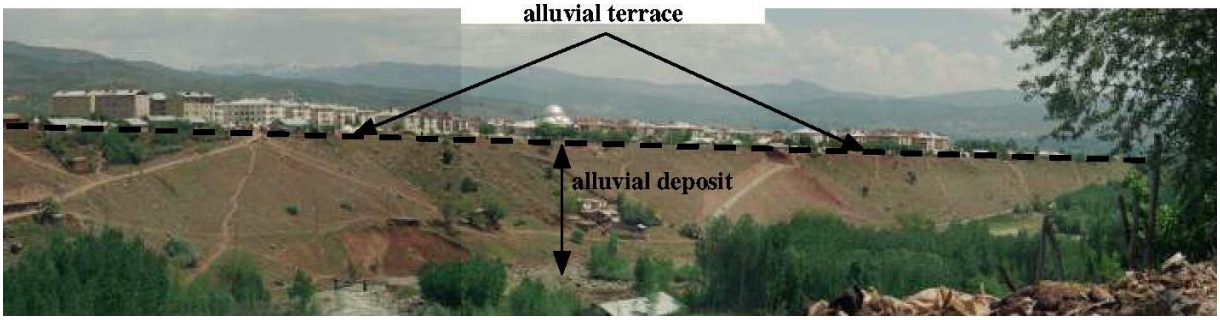

Figure 3.11 View north across Çapakçur Çayı at northern part of Bingöl. Gravel at least 60 m thick here. Apartments were built on terrace 1.

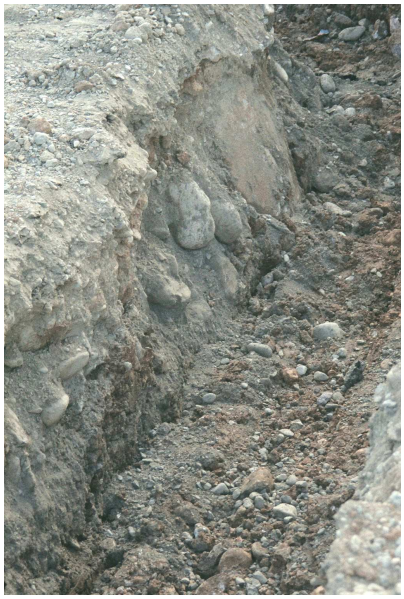

Figure 3.12 Old gravel in ditch dug along main highway through northern Bingöl.

3.4.1.3 Colluvium

Colluvium is a sedimentary deposit, formed generally by slope processes such as weathering, soil creep and sliding. These materials are the product of downhill transport of the basaltic bedrock found at a higher elevation at the limit of the urban development in the southwest part of Bingöl, and of the older alluvial deposits that form another alluvial a terrace at a higher elevation. The clast sizes range from pebbles through boulders and blocks. Much of the colluvium contains rounded clasts because of the source in older alluvium.

The contact between colluvium and the older gravel is unclear. Therefore, it is not known whether the older gravel was deposited on colluvium, or the colluvium was deposited on the older gravel. Probably both age relations pertain in different parts of the area. However, the fact that there is a high terrace in colluvium, on the hill protruding northward with a graveyard on top of it, in the Mirzan District of Bingöl (Figure 1.3), suggests that some of the colluvium is as old as the older gravel.

3.4.3 The relevant landforms

There are two landforms that might be relevant to ground shaking in Bingöl during the 2003 earthquake. One is the terrace and its attendant features and the other is the stream valley.

3.4.2.1 Terrace Surfaces

The terrace surfaces appear to have been eroded into the Pleistocene gravels that were deposited in the Bingöl basin. The terrace surfaces probably were formed as the major streams, the ancestral Çapakçur Çayı, the large stream in the valley separating the north and south parts of Bingöl, and the ancestral Gayt Çayı, the stream in the valley to the north of Bingöl.

Terrace surface 1 (Figure 3.8; Figure 3.11) is the lowest and, therefore, probably the most recent one carved into the older gravels (Figure 3.12). It is the terrace level immediately above the gravels along the major streams. It includes the level of the entire area between the two large streams, in Uydukent, Düzağaç and Saray Districts, and the level of approximately half the area of south part of Bingöl, in Yenişehir, Kültür and Yeşilyurt Districts (Figure 1.3). The downtown area of Bingöl, including the large mosque, is largely built on this terrace level.

The terrace riser of this terrace is the steep apron covered by talus along each of the major modern stream valleys. The terrace risers are labeled in the map in Figure 3.7. The terrace risers probably increased the ground shaking locally and may have been responsible for damage to some of the buildings, as noted later on in this report.

Terrace surface 2 is a distinct but very small terrace remnant that is north of the place where the modern alluvial channel of a small stream crosses the southern part of Bingöl from west to east, draining roughly parallel to the major stream Çapakçur Çayı. The terrace surface is approximately 400 m long (NW-SE) and 125 m wide.

Terrace surface 2 is adjacent to terrace level 4, which is the highest terrace level in our mapped area. Terrace level 4 forms the relatively flat top of two ridges that protrude toward the east from near the western edge of the map area (Figure 3.7). The northern ridge is in the Bahçelievler District and the southern ridge is in the Mirzan District of Bingöl (Figure 1.3). The risers of terrace level 4 are up to approximately 70 m high above terrace level 1.

Terrace surface 3 is the flat summit of the ridge underlain by colluvium, with the cemetery, in the western part of the area (Mirzan District of Bingöl, Figure 1.3). It is higher than 2 but lower than 4.

3.4.2.2 Small Stream Valley

The topographic feature that may be of most concern to earthquake shaking in Bingöl is the stream valley that heads in a cemetery between the two ridges capped by terrace surface 4 and drains along the boundary between Bahçelievler and Mirzan Districts, eastward to terrace surface 2 in the İnönü District, where it turns toward the ESE and cuts through terrace surface 2 and its riser and into terrace level 1. It extends ESE to E across the rest of the southern part of Bingöl, within the Kültür District.

The trace of the stream valley is easily observed in the far western and far eastern parts of Bingöl, but not in the downtown area. In the far western and far eastern parts its flow is largely contained in a concrete conduit with a square cross section. In the downtown area, though, a 600 m stretch of the stream valley was obliterated with man-made fill, presumably containing a subsurface drain. Its trace was determined there by study of the 1971 topographic base map (base of Figure 3.8).

The condition of the man-made fill is unknown. It is not known whether the fill was placed as engineered fill, with proper compaction, or whether it was placed loosely. The team members could not ascertain if there were any buildings placed on top of the fill because the trace of the conduit was lost in the downtown area.

CHAPTER AUTHORS

Coordinators

A. Johnson, Purdue University
R. Ulusay, Hacettepe University

Contributors

K. Ö. Cetin, Middle East Technical University
A. Bobet, Purdue University
A. Irfanoglu, WJE Assoc., Inc.
A. Matamoros, University of Kansas
J. A. Ramirez, Purdue University
M. A. Sozen, Purdue University

4

GEOTECHNICAL ASPECTS OF BİNGÖL EARTHQUAKE

4.1 GEOTECHNICAL CONDITIONS IN BİNGÖL

4.1.1 Colluvium and Alluvium

Most of the city of Bingöl is built on top of an alluvial terrace (identified in earlier pages as terrace level 1), approximately 40 to 60 m above the current level of the Çapakçur Çayı that flows through the middle of the urban area. North of the Çapakçur Çayı all the buildings foundations lie on this old (Pleistocene) alluvial deposit.

Figure 3.12 given in the previous chapter is a photograph of such a deposit. The deposit can be described[7] as a GP, a brown, poorly graded rounded gravel with small amounts of sand and traces of clay and silt, with maximum size of the particles of 1 to 2 m. The deposit is dense to very dense. Figure 3.10 also in the previous chapter shows the terrace and thickness of the deposit. Cuts excavated in this terrace are stable with angles of 40^o to 50^o.

Figure 4.1 Steel in the foundation of a new hospital under construction in the north side of Bingöl. The foundation includes a grid of reinforced concrete beams with columns at the grid intersections. The alluvial deposit can be seen on the far end of the excavation; note the almost vertical cut in the granular material.

The south part of Bingöl is built on a terrace at the same elevation as the north. In this terrace most of the subsurface materials are similar to those found in the north.

Towards the southwest the buildings are founded on moderately weathered bedrock or on stiff, colluvial deposits, which locally can be several meters thick. The colluvial deposits can be classified as CL, brown stiff clay, with variable percentages of sand or gravel, which in many cases can be described as sandy or gravelly clay.

[7] Soil classifications in this report are provided from visual observations based on the experience of the members of the geotechnical team; no soil identification tests were performed, although it is expected that the classifications are accurate enough.

4.1.2 Foundations

The buildings in the region usually have a basement that extends approximately 3 m below the ground surface (Figure 4.1). The type of foundation is very uniform throughout the area and consists of a grid of reinforced concrete beams with the structural columns at the intersections of the grid (Figure 4.2). The lateral walls of the basement are made of reinforced concrete.

Figure 4.2 The basement of a building under construction in the south part of Bingöl. The lines mark the grid of foundation beams. The space between the beams is generally filled with gravel (from river deposits), sometimes on top of a small layer of concrete placed at the bottom of the excavation.

Figure 4.2 is a photograph of the basement of a building under construction where the reinforced concrete grid of the foundation has been highlighted. Note that the grid may not be regular, but follows the layout of the columns. The dimensions of the beams of the grid are variable since they have to accommodate the dimensions of the columns; they range from 0.4 to 0.6 m wide and 0.4 to 0.5 m deep. The space between the beams is generally filled with gravel (from river deposits), sometimes on top of a small layer of concrete placed at the bottom of the excavation.

The type of foundation shown in Figures 4.1 and 4.2 is common in Turkey. This was also observed in Adapazarı, Düzce, and Bolu during the survey for the August and November 1999 earthquakes. It is interesting to note that Bingöl is in the far east of Turkey while Adapazarı, Düzce, and Bolu are in the west, which indicates that this type of design and construction of the building foundations is widespread in Turkey (note that in Adapazarı the buildings had no basement; this is because the water table was on the surface).

The most important characteristic of the foundation is that it is very stiff, and differential settlements can be easily accommodated without much distress to the upper structure. In fact in Adapazarı there were numerous examples of buildings substantially tilted due to liquefaction with

minor damage to the structure. In addition the lateral wall of the basement provides significant stiffness against lateral movements, and as a consequence the foundation-basement system is very effective in transmitting the ground movements to the upper structure.

Inspection of a number of buildings in the north and south sides of Bingöl showed no signs of distress, settlement, excessive deformations, or any other sign of foundation damage. At most light damage to the lateral walls of the basement was observed, even on buildings with severe damage. The damage was entirely concentrated in the structure above the basement.

Additional geotechnical inspections were conducted on an urban development on the northeast, a couple of miles from the center of the city. The buildings in this area had foundations on a much lower alluvial terrace, 1 to 3 m above the river. The soils in this terrace, as observed in the banks of the river, were constituted by a layer of medium stiff brown sandy silt or clay, approximately 1 to 1.5 m thick; below, at a level close to river there was a layer of gravels, seemingly ranging from dense to very dense.

Two buildings were examined: a police station that suffered severe damage and a school building that collapsed. The police station and the school showed no damage or distress to the foundation.

The only noticeable ground deformation was found in the school (Figure 4.3). There was a crack in the ground, approximately 3 to 4 m from the perimeter of the building, which indicated settlement. The school had a basement, and thus the foundation was likely placed on the gravel deposit; the crack was the result of the settlement of the backfill behind the basement wall.

Figure 4.3 School with collapsed first floor in NE Bingöl. Note that first floor is missing. Windows were in the first floor. Cracks in soil near foundation were at far end of building.

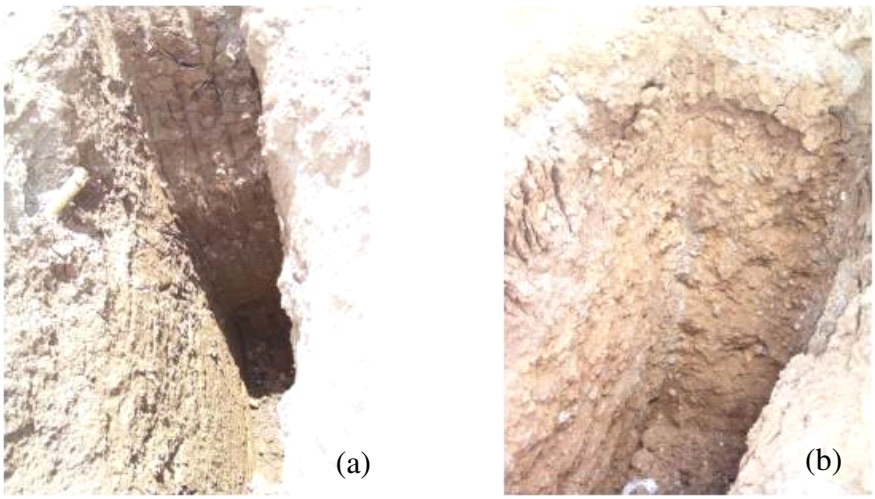

Figure 4.4 Trenches excavated near the collapsed dormitory building.

4.1.3 Collapsed Dormitory

A number of schools were surveyed at different locations far from the urban area. Some of the schools suffered collapse. Of particular interest was the site where the Çeltiksuyu Boarding School dormitory failed, killing more than eighty students. There were other two buildings in the same location: a school that collapsed, and the teacher's building that suffered light damage. The three buildings were placed on top of an alluvial deposit. Figure 4.4 shows pictures of two trenches excavated near the buildings. The first trench (Figure 4.4a) shows a stiff fine grained soil on the surface (note the marks of the teeth of the excavator on the front wall and the vertical walls of the trench), and a gravel at the bottom of the trench; there is also a fill on the top meter or so (note the yellow plastic pipe), but this is local to the site where the trench was excavated. The second trench (Figure 4.4b) was excavated on gravel, dense to very dense. Note that in none of the trenches are there signs of water. This is expected because of the nature of the soils in the area: alluvial deposits, predominantly granular, with high permeability. The location of the buildings was on an elevated terrace, and thus it is likely that the water table in this area was very low, closer to the level of the river.

4.2 EXAMINATION OF FEATURES IN EPICENTRAL AREA

According to geologists from METU[8], the fault responsible for the earthquake extends from Günören, to Kuşkondu through and Çimenli in the NW, through Sudüğünü, Hanoçayırı, Oğuldere and Kurtuluş at midlength to Ortaçanak, Samanlı, Ilıcaköyü, Kaplıcalar and Ağaçeli in the SE, a total distance of some 40 km. They cited the same kinds of evidence of fault rupture along this fault during the earthquake as that mentioned by the geophysicists from KOERI.

Two members of the NSF-TÜBİTAK team[9] examined some of the evidence of earthquake rupturing reported in the epicentral area but found no field evidence of such rupture in the locations visited.

At Çimenli there were supposed to be ground cracks reflecting earthquake rupture. A young man from the village acted as guide and conducted the team to the location where the evidence of earthquake rupturing had been described. The team found two cracks near a ridge crest, trending roughly NW-SE that were perhaps a meter long and about a mm wide. The cracks were not related to right- or left-lateral shearing parallel to the ridge; had they been, they would have been oriented on the

[8] A. Koçyiğit and N. Kaymakçı, http://www.metu.edu.tr/home/www64/reports/bingöl_depremi.pdf, in Turkish.
[9] A. Bobet and A. Johnson

order of 45° to the trend of the ridge crest. Their traces were parallel to the ridge crest, suggesting relative lateral movement of the ground, perhaps due to ground shaking or merely shrinking of the soils.

Figure 4.5 Head of flowslide channel at Hanoçayırı.

Figure 4.6 Main flowslide channel just below the head. On far side are slices of grass sod that began to detach and become mobilized when sliding stopped.

Figure 4.7 More of the flow channel. View south. The flow moved debris to vicinity of buildings visible in distance on the left in photo.

Figure 4.8 Farther down the flow channel. View north. A sheet slide mass on left.

Figure 4.9 Head of flowslide. In distance, to right of copse of trees in center, is narrow graben that connects to head and extends eastward across much of the pasture in the distance. The narrow graben is the so-called "fault ground rupture" that was supposed to be evidence of surface faulting during the Bingöl earthquake.

Figure 4.10 Closer view of graben[10]. The diagonal tension cracks in mid-distance suggest right-lateral shearing as well as opening.

At Hanoçayırı there was reported ground rupture trending roughly E-W and an associated landslide, all indicating earthquake rupturing. The ground rupturing was reported to reflect right-lateral shearing.

[10] Taken by unknown source.

Members of the NSF-TÜBİTAK team visited the site and briefly examined the ground ruptures and the landslide mass. The landslide is an excellent example of a flowslide, which is almost certainly a result of liquefaction on long-range flowage. The flowslide started as a landslide mass along a shallow valley in an open meadow (Figure 4.5). Parts of the flowing mass moved some hundreds of meters from the source (Figure 4.7; Figure 4.8) landslide so the liquefied debris was highly mobile.

The most fascinating feature, though, is the so-called ground rupture (Figure 4.9). A brief examination indicated that, in fact, the ground rupture did not represent deep-seated strike-slip faulting but a sheet-like slide, perhaps only one to two meters thick. The ground rupture represents the pull-away of sheet-like slide masses in the meadow on either side of the valley down which the flowslide moved. The interpretation of a sheet-like movement was supported by the observation that an electric pole (Figure 4.8) within the western sheet slide, perhaps 100 m south of the pull-away, had apparently moved laterally because the tension in the wires was higher between that pole and the pole north of the source of the landslide than between that pole and the next pole to the south.

The relative movement across the ground rupture above the western slide sheet indicates left-lateral shearing, rather than the right-lateral shearing that was supposed to have occurred along the rupture. Indeed the movement of the western sheet apparently was directly down the ground slope, which would have produced both opening and left-lateral shearing.

Probably the right-lateral shearing was inferred from observations of ground ruptures to the east of the flowslide (Figure 4.9; Figure 4.10). Although the feature was not examined on the spot, a photograph (Figure 4.10) supports that interpretation. However, the ground slope there would have produced opening and right-lateral shearing at the head of the sheet slide as the slide moved down the slope, so right-lateral shearing there would be expected. Perhaps observation of right-lateral shearing there misled the investigators into interpreting the fracturing as a result of tectonic rupturing.

Search for evidence for fault rupturing in the vicinity of Kaplıcalar and Ağaçeli was also conducted. No fault rupturing crossing the main road was observed in that area. While driving westward from the main road toward Ilıcaköyü, several fresh landslide scarps along very steep valley walls were visible. Supposedly the landslides reflect fault rupturing. It is suggested that they may well represent ground shaking, but they need not reflect fault rupturing.

Thus, NSF-TÜBİTAK team found no evidence to indicate the surface trace of a fault that ruptured during the 2003 earthquake. Furthermore, the Team knows of no convincing evidence for distinguishing between left-lateral and right-lateral source mechanisms of the 2003 earthquake.

4.3 EFFECTS OF GEOTECHNICAL CONDITIONS ON STRUCTURAL DAMAGE IN BİNGÖL

The observations on both the trenches opened near some collapsed or heavily damaged government buildings after the earthquake (Figure 4.11) and the open cuts by highways (Figure 4.12), supported the geological evidences revealing the fact that Bingöl city center is located on deep alluvial fan deposits composed of coarse gravel to boulder with sand and some to traces of silt and clay. Also the deep water table level in conjunction with the none to limited strain softening character of Bingöl alluvial fan deposits limited the foundation deformations. However, a clear concentration of the structural damage on the cliff side of the flat hill where the city center is located suggests a possible amplification of ground shaking at the cliff side pronouncing the contribution of topographical effects on the observed damage.

Figure 4.11 Observation Trench opened at Hulusi Bey (Point 7 in Figure 4.13) primary school (N 38^0 53.784′, E 40^0 30.396′),

Figure 4.12 Views of open cuts (alluvial fan deposits) near the district of Hacıçayır (Koçan Creek) (Point 12 in Figure 4.13) (N 38^0 54.03′, E 40^0 36.93′)

4.4 SEISMICALLY INDUCED GROUND DEFORMATIONS

Numerous seismically induced ground deformations in the forms of landslides, rockfalls, mudflows, and liquefaction-induced lateral spreading were documented after the earthquake. The location and classification of these ground deformations are shown in Figure 4.13. Heavy rains within a ten day period before the earthquake are thought to have exacerbated the occurrences of these ground deformations.

The mechanism and the depth of the landslides were governed by the degree of rock weathering, topography and soil layering. While rotational slides and flow type of failures were observed to have occurred in soil slopes originated from highly weathered volcanic rocks, rock falls were observed near steep slopes in jointed and fresh or slightly weathered volcanic rocks. The majority of the landslides are concentrated particularly close to the epicenter of the earthquake (Figure 4.13). In addition to a brief discussion of the main features of these landslides presented in Section 4.2.1, a brief summary of the main characteristics of these cases are also presented in Table 4.1.

4.4.1 Landslides

Soğukçeşme Landslide

One of the most significant seismically-induced landslides was documented near the Soğukçeşme section of the country roadway extending from Bingöl to Karlıova, and occurred in a highly weathered volcanic rock transformed into cohesive soil (Figure 4.14 (a) and (b)). It was originally a rotational failure followed by a flow running about 70-80 m towards west, and occurred on the SE bank of the Göynük River. It is a 25 m high slope with an inclination of about 30^0. A few local slides of small volume were also observed on the NW bank of this river near the same locality (Figures 4.15 and 4.16).

Table 4.1 Main features of the earthquake-triggered landslides observed in the Bingöl Region.

Location and Reference number*	Type	Slope forming material	Slope Parameters			Landslides			Remarks
			H (m)	α (deg)	Strike	W (m)	(L) (m)	M.D	
4 km north of Yolçatı village (Gökçekanat) (5)	Rock fall	Volcanic	20	45	E-W	15	8	N	Small sized rock blocks from heavily jointed basalt (Figure 4.22)
South of Yazgülü village (4)	Rotational sliding	Highly weathered volcanic	15	30	NW-SE	20	20	S35W	Overall angle of the stable part of the slope is 40^0 and consists of moderately weathered rock (Figure 4.17)
Arıcılar village (2)	Rock fall	Volcanic	>20	25	E-W	-	-	S	(Figure 4.23)
Hanoçayırı - Kurtuluş villages (16)	Rock fall	Volcanic	>50	>50	NW-SE	-	-	SW	(Figure 4.24 (a)-(b))
Kurtuluş village (15)	Flow slide	Highly weathered volcanic	50	45-50	SW	5-15	250	NW-SE	Highly weathered tuff between two relict discontinuity systems (see Figure 4.20) flowed down

* Numbers in the parentheses indicate the location numbers appearing in Figure 4.13.
H: Slope height; α : Slope inclination; W, L : Width and length of landslide, respectively; M.D.: Movement direction

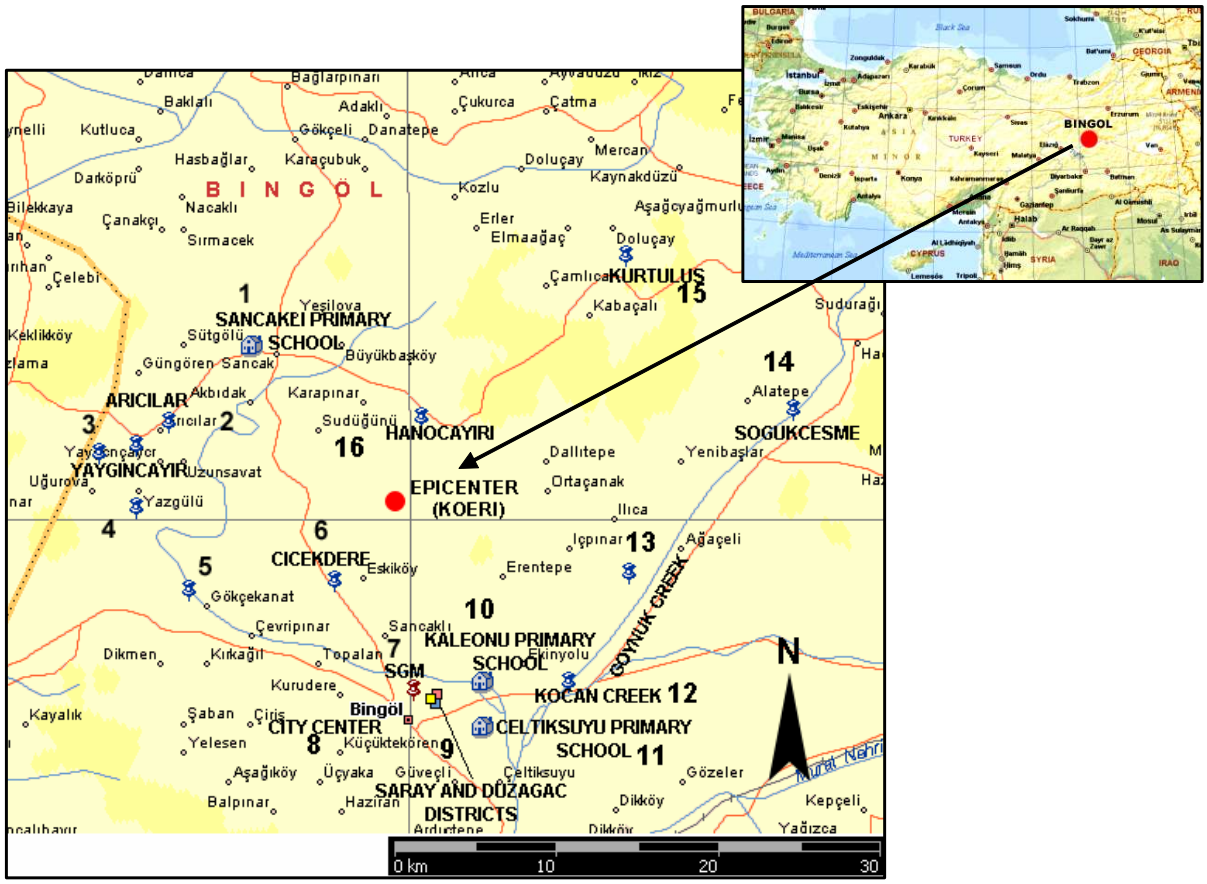

Figure 4.13 Map of Bingöl region

(a) (b)

Figure 4.14 Different views of Soğukçeşme landslide, (Point 14 in Figure 4.13) (N 39^0 03.380′, E 40^0 46.908′) (Slope = 30 degrees to the west, H= 25 m, L = 70 m)

Figure 4.15 A small scale landslide in the Soğukçeşme region (Point 14 in Figure 4.13), (N 39^0 03.380′, E 40^0 46.908′)

Figure 4.16 A landslide by the Göynük River (Point 13 in Figure 4.13) (N 38^0 57.808′, E 40^0 39.586′)

Yazgülü Landslide

The Yazgülü landslide was mapped at the southern exit of Yazgülü village. The movement was towards the highway cut, in the South 35 degrees West direction. The slope after the slide was measured as 30 degrees whereas some slopes composed of similar but less weathered material were stable at 40 degree inclinations (Figure 4.17)

Çiçekdere Landslide

The head of the Çiçekdere landslide has jeopardized the stability of the Çiçekdere Village road. Cracks as wide as 38 cm and vertical offsets as high as 10 cm were mapped (Figure 4.18).

Figure 4.17 Landslide at the south exit of Yazgülü village (Point 4 in Figure 4.13) (N 39^0 00.5′, E 40^0 17.85′)

(a) (b)

Figure 4.18 View of the head of Çiçekdere landslide (Point 6 in Figure 4.13) (N 38^0 57.53′, E 40^0 26.65

Kurtuluş Landslide

Ground deformations mapped at Kurtuluş Village as wide as 5 cm with a vertical offset of 2 to 5 cm extending to the North 40 degrees West direction suggest a potential slide at Kurtuluş Village. Another possible explanation for these ground deformations could be the surface expression of faulting; however lack of surface evidence for strike slipping has weakened this alternative (Figure 4.19).

Figure 4.19 Ground deformations at Kurtuluş (Point 15 in Figure 4.13) village (N 39^0 06.66′, E 40^0 39.48′)

4.4.2 Mudflows

Kurtuluş Village

Seismically-induced mudflow was observed at Kurtuluş village where mud covered a horizontal extent of hundreds of meters. Villagers reported that mudflow started immediately after the earthquake and continued till the morning of the night of the earthquake (Figure 4.20).

Figure 4.20 Mudflow at Kurtuluş village (Point 15 in Figure 4.13) (N 390 06.66′, E 400 39.48′)

Soğukçeşme

A similar but a smaller scale mudflow took place after the earthquake in the hills of Soğukçeşme. Figure 4.21 shows the extent of the flow through the steep hills of Soğukçeşme.

Figure 4.21 Mudflow at Soğukçeşme (Point 14 in Figure 4.13) (N 390 03.380′, E 400 46.908′)

4.4.3 Rock falls

Various small volume rock falls were documented along the village and intercity roads. Figures 4.22, 4.13 and 4.14 show pictures from rock falls at Gökçekanat, Arıcılar and Kurtuluş village roads.

Figure 4.22 Rock falls near Gökçekanat (Point 5 in Figure 4.13) (N 380 58.6′, E 400 17.05′). Joint has a dip angle of 50 degrees to the North; strike is from east to west

Figure 4.23 Arıcılar village (Point 2 in Figure 4.13), northeast exit (N 390 03.83′, E 400 18.96′),

(a) (b)

Figure 4.24 Rock fall by Hanoçayırı (Point 16 in Figure 4.13) to Kurtuluş road (Point 15 in Figure 4.13) (N390 03.1′, E 400 30.46′)

4.4.4 Liquefaction-Induced Ground Deformations and Slope Instabilities

Locations of the liquefaction-induced ground deformations and lateral spreading are shown in Figure 4.13. Luckily, due to the existence of these ground deformations in rural areas, no liquefaction-induced ground deformations were observed to have resulted in structural damages.

Yaygınçay Village

One of the typical examples of liquefaction-induced lateral spreading occurred near Yaygınçay village on the northern bank of Uğuroba Stream (Figure 4.25). Sand boiling was observed along the southern bank of the stream (Figure 4.26), which confirmed triggering of soil liquefaction. Three distinct zones of lateral spreading were identified. The maximum lateral spread displacement at this place was mapped to be 30 cm, whereas the inclination of the stream bank was measured as 15º.

(a) (b)

Figure 4.25 Different views of liquefaction-induced lateral spreading by Uğuroba stream (N 390 03.3′, E 400 17.88′)

Figure 4.26 Sand boiling mapped near Uğuroba stream (N 390 03.3′, E 400 17.88′)

Hanoçayırı Village

The other significant lateral spreading along a sloping ground was mapped at a locality called Hanoçayırı near Sudüğünü village (see Figures 4.13 and 4.27 (a)-(d)). This place is located in the close vicinity of the earthquake epicenter. The presence of a shallow-seated silt and sand sized nonplastic surficial layer (grain size distribution is shown in Figure 4.27 (e)) originated from the tuffs and combined with shallow water table depths makes this material highly vulnerable to liquefaction. Even under relatively very mild slopes ranging between 3º and 7º, as a result of soil liquefaction, mudflow and lateral spreading were observed. The presence of traceable sand accumulations with a very small extent on the eastern flank of this ground failure and other observations suggest that a 0.2 to 3 m thick sandy silt layer moved over an unknown thickness of liquefied ground. Due to the loose nature of the liquefied ground and heavy rains before the earthquake, the material flowed down in the S55W direction and the trend of flowing material then directed towards the SE. The width and length of this flow were about 35 m and 400 m, respectively. Also sand boiling was observed by the lateral spreading area (Figure 4.28).

Hanoçayırı Village Liquefaction-induced Lateral Spreading

Behind the northern hills from the Hanoçayırı liquefaction-induced lateral spread and mudflow area, another set of ground deformations, suggesting a possible liquefaction-induced lateral spreading mechanism was observed. 4 cm wide cracks with a 1 to 10 cm vertical offset were mapped in this area. The movement was downhill on a mild 3 to 5 degree slope (Figure 4.29).

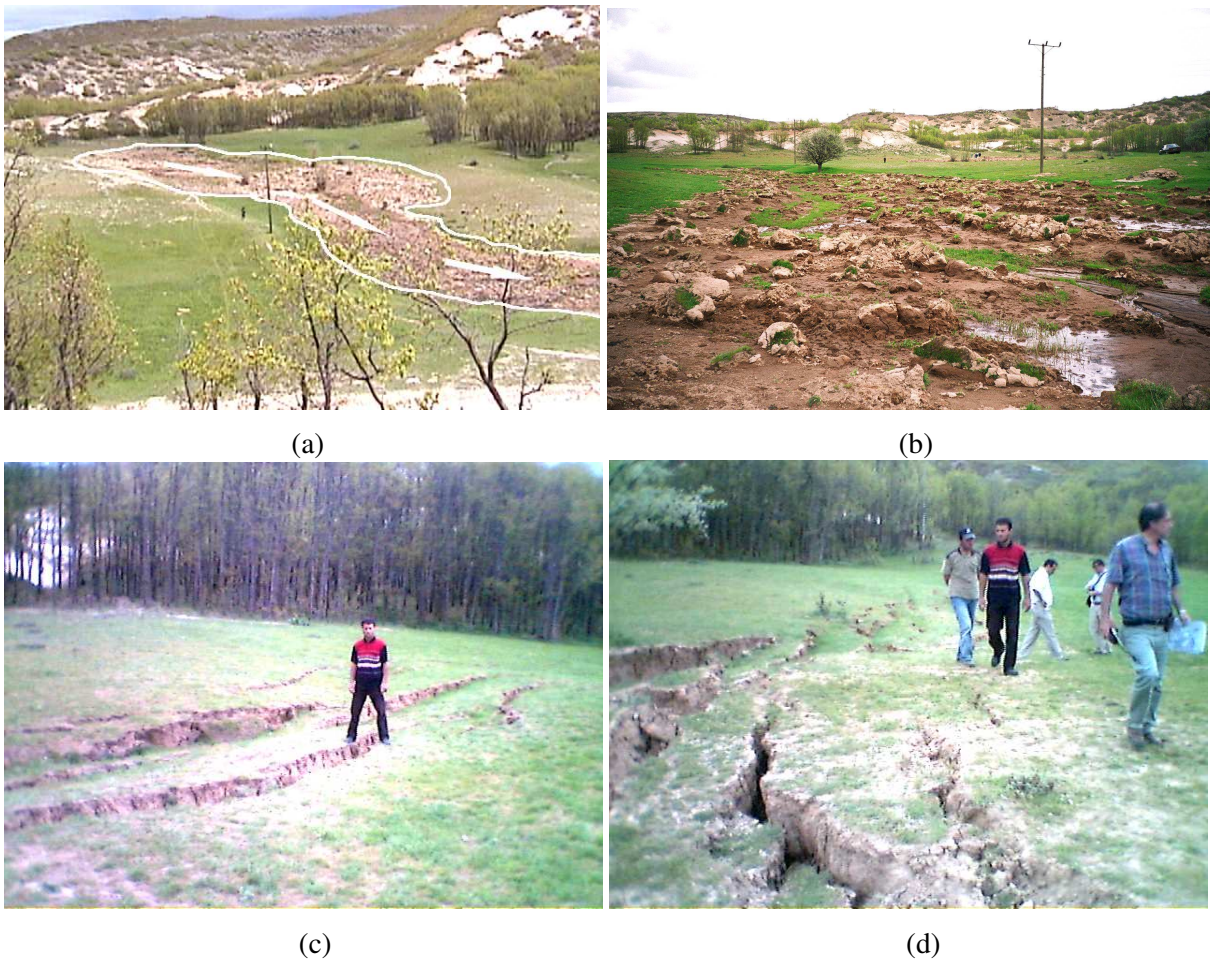

(a) (b)

(c) (d)

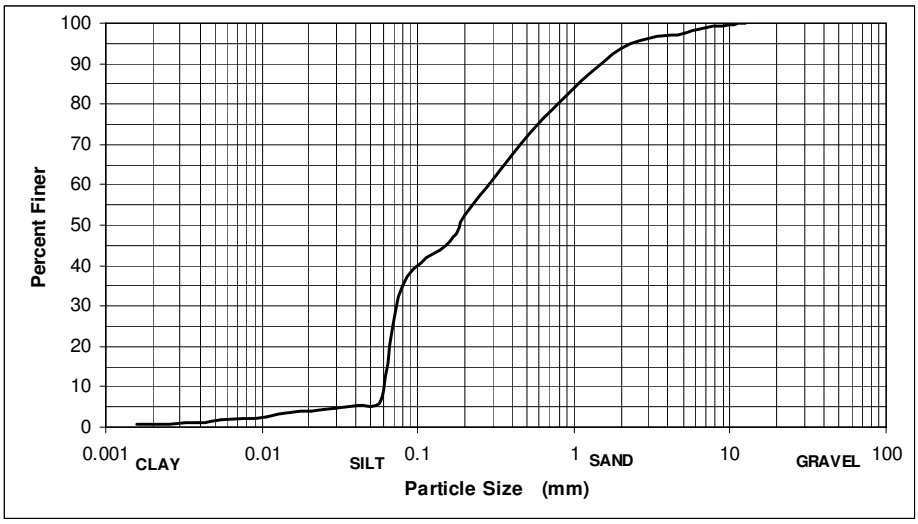

(e)

Figure 4.27 Lateral spreading and mudflow at Hanoçayırı (Point 16 in Figure 4.13) (N 390 03.1′, E 400 30.46′)

Figure 4.28 Sand boil at Hanoçayırı (Point 16 in Figure 4.13) (N 390 03.1′, E 400 30.46′)

(a) (b)

Figure 4.29 Ground deformations at Hanoçayırı valley (Point 14 in Figure 4.13). (N 390 03.1′, E 400 30.46′)

4.5 SUMMARY

The investigation of the engineering geological and geotechnical conditions in Bingöl indicates that soil conditions in the area are quite uniform, predominantly granular alluvial deposits, dense to very dense. Because of the characteristics of the soil it is not likely that they amplified the ground motions. Furthermore it is expected that the ground motions in the area were quite uniform. The only exceptions perhaps are areas close to the edge of very tall slopes where some amplification might have occurred; for example, buildings on top of the slopes near the river.

Several buildings were examined in the north and south sides of Bingöl to determine whether there were signs of distress, settlement, excessive deformations, or any other indication of foundation damage. The most damage observed was light damage to the lateral basement walls, even in buildings with severe damage. The damage was invariably concentrated in the structure above the basement.

Further, no evidence was found in the epicentral area of the earthquake to indicate the surface trace of a fault that ruptured during the earthquake.

Thus this study suggests that differences in damage to buildings from place to place in Bingöl due to the 1 May 2003 earthquake were a result of characteristics of the structures, not of foundation conditions or gross ground deformation of any kind.

CHAPTER AUTHORS

Coordinators

A. Bobet, Purdue University
K. Ö. Çetin, Middle East Technical University

Contributors

S. Bakır, Middle East Technical University
A. Irfanoglu, WJE Assoc., Inc.
A. Johnson, Purdue University
A. Matamoros, University of Kansas
M. A. Sozen, Purdue University

5

TYPES OF STRUCTURES AND OBSERVED DAMAGE

5.1 PRELIMINARY REMARKS

In all, the TÜBİTAK team inspected a total of 96 buildings in Bingöl, of which 57 were residential buildings, 21 were schools and 18 comprised other government or official buildings. The NSF team inspected a total of 62 buildings, of which 29 were schools and dormitories, and 33 were reinforced concrete residential buildings. The grand total of buildings entered and inspected was not; however, 158 as 14 buildings were jointly assessed by the two teams. Of these 14 buildings, 4 were residential and the remainder were school buildings.

Because of limited time available to the teams for inspection, only visual damage assessments were made. Here it was neither necessary nor practical that both teams utilize exactly the same assessment philosophy or procedures. In general it may be stated that though the assessment principles used by each team were consistent in themselves, the NSF team adopted a stricter approach to damage than the TÜBİTAK team. It will later be shown in the present chapter that for buildings which were common to both teams, the NSF assessment was more stringent, and the same damage state while described as 'moderate' in the NSF assessment could often be described as 'light' in the TÜBİTAK assessment. Needless to add, the assessments of both teams converged when the damage was identified as very light or very severe. Furthermore, there were occasional differences in emphasis when it came to terminology. The TÜBİTAK team preferred the use of "short column" to indicate the stub or part of a column that resisted high shear forces because the infill walls did not laterally support it completely over its height, whereas the NSF team used "captive column" in similar circumstances. No attempt has been made to homogenize every item of technical usage in the present report, as the literature in this area uses both short column and captive column.

In the sections that follow, assessments by both teams are presented separately. Since the majority of the buildings covered by both teams are different, this will not introduce any duplications as common buildings are included only once.

5.2 CLASSIFICATION OF STRUCTURAL SYSTEMS [UBC]

The structural assessments made by the NSF team refer to building systems as mentioned in the Uniform Building Code [UBC]. In order to relate descriptions better with those given by the TÜBİTAK team, sketches of the main types of structural systems defined by UBC are shown in Figure 5.1 below. Table 16-N of the UBC may also be consulted.

I. BEARING WALL SYSTEM: A bearing wall system is a structural system without a complete vertical load carrying space frame. Bearing walls or bracing systems provide support for most gravity loads. Resistance to lateral load is provided by shear walls or braced frames.

II. MOMENT-RESISTING FRAME SYSTEM: A structural system with an essentially complete space frame providing support for gravity loads. Moment resisting frames provide resistance to lateral load primarily by flexural action of members.

III. BUILDING FRAME SYSTEM: A structural system with an essentially complete space frame providing support for gravity loads. Resistance to lateral loads is provided by shear walls or braced frames.

IV. DUAL SYSTEM: A structural system with the following features:

- A complete space frame which provides support for gravity loads.
- Resistance to lateral load is provided by shear walls or braced frames and moment-resisting frames. The moment resisting frames shall be designed to resist ≥ 25 percent of the design base shear.
- The two systems shall be designed to resist the total design base shear in proportion to their relative rigidities considering interaction at all levels.

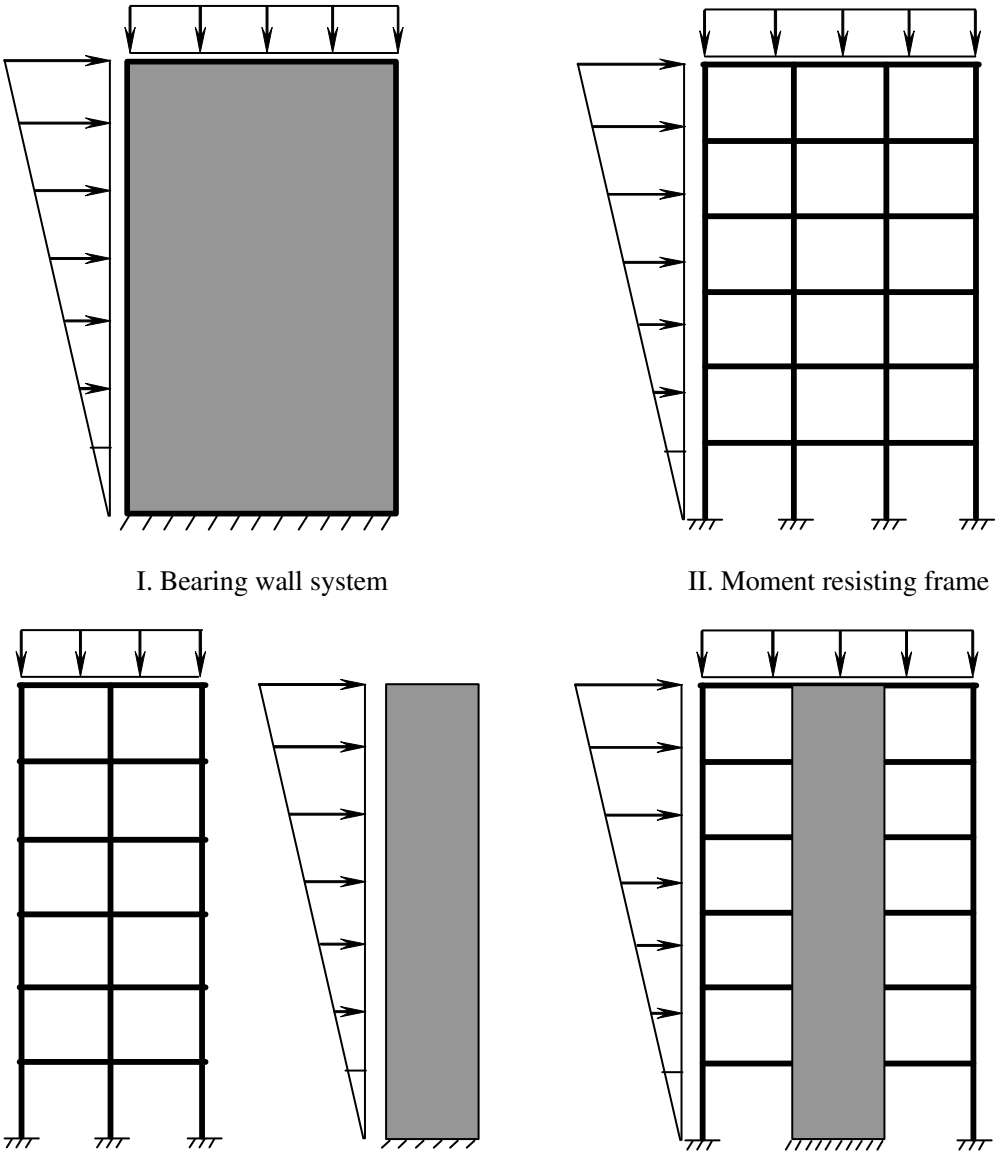

I. Bearing wall system

II. Moment resisting frame

III. Building frame system

IV. Dual system

Figure 5.1 Structural system definition of UBC

5.3 PERFORMANCE OF RESIDENTIAL BUILDINGS

5.3.1 Introduction

The performance of buildings within the provincial area of Bingöl was investigated through post-earthquake damage assessment conducted shortly after the earthquake. The Bingöl provincial area

mostly contains reinforced concrete buildings of up to 6 stories in height. The majority of these buildings were built within the last decade. Therefore the influence of changes introduced in the 1998 Turkish Seismic Code is expected to be reflected in some of the surveyed buildings. In this section of the report, a brief discussion of the typical reasons for damage observed in reinforced concrete buildings in Turkey is given first, the damage assessment methodology employed is explained and the performance of buildings with emphasis on the causes of observed damage is presented.

5.3.2 Reasons for Damage Observed in Reinforced Concrete Buildings

The peculiarities of the architectural configurations in Turkey, which follow the legal restrictions on land use for housing are known to affect the performance of buildings negatively. This enforces the designers to make an improper choice of structural configuration that in turn results in discontinuity in the lateral load resisting elements, irregular framing in the principal lateral direction, weak and soft stories arising from sudden changes in the stiffness and strength, overhangs, captive or short columns and irregularity in the plan and elevation.

The second major cause of damage results from improper and poor detailing and proportioning of the reinforced concrete components. This might be introduced at two different stages. In the design phase, the requirements of the code are not implemented and thus the reinforced concrete sections designed do not comply with the ductility and strength requirements of the code. In the construction stage, poor workmanship and the tendency to disregard the detailing in the design drawings both intentionally and due to ignorance is another reason that leads to improper detailing and proportioning. Insufficient transverse reinforcement at the critical sections of the members and at the connections is a common practice that is a major reason for the damage pertaining to poor detailing. Inadequate anchorage and splice length are other factors that lead to damage related with detailing.

Turkey has a modern seismic code that is periodically revised and upgraded to reflect new findings and changes that come into existence in the field of earthquake resistant design. Code enforcement, on the other hand, has become a prominent concern that can be linked to several factors including lack of technical control and supervision, problems with the legal framework, low income rates, the cultural and sociological nature of the society, improper regional construction practice and irregular practices. When these factors are combined in the construction phase of buildings, the built structure does not reflect many aspects of the design it is supposed to comply with. As a result, its resistance to earthquakes becomes inferior and the consequence is unpredicted damage or failures under the loads that are most of the time below the design loads. These deficiencies can be summarized as follows:

a. Altering the member sizes from what is foreseen in the design drawings
b. The detailing does not comply with the design drawings
c. Inferior material quality and improper mix-design
d. Changes in the structural system by adding/removing components
e. Reducing quantity of steel from what is required and shown in the design
f. Poor construction practice

Observations made in Bingöl after the earthquake revealed that the factors mentioned above played significant role in the damage of many reinforced concrete buildings. In the sections to follow several examples of these cases are illustrated.

5.3.3 Assessments of TÜBİTAK team

5.3.3.1 Damage Assessment Methodology

Post-earthquake damage assessment involves a great deal of challenge because it requires from the assessor necessary expertise to convert physical damage visible in terms of cracks, deformations and

failures to the loss in the capacity of the components and, in turn, of the whole building. This introduces judgment into the evaluation process and renders it somewhat subjective. Thus the final decision regarding the state of damage or condition of the building is not certain and depends on the person conducting the survey. The uncertainty can be minimized if certain general criteria are set and followed in the assessment. Therefore, the damage assessment criteria used in our survey after the Bingöl earthquake is explained to evaluate better the distribution and extent of the damage presented in this report.

Three damage states, namely light/none, moderate and heavy/collapse were employed when assigning damage for both structural and nonstructural components. In assigning a damage state to the structural system of the building, usually the most severely damaged floor, in most cases the ground floor, was studied, its structural components were examined for any visible cracks, deformations or spalling/crushing of concrete and the decision was made for the building's damage state. Damage state definitions employed are given in Table 5.1 for each component. It is worth noting that a single component itself does not dictate the damage level of the whole building, thus the condition of many components is taken into account when assigning the damage states.

In the post-earthquake damage assessment when assigning damage state to the building under consideration, the reparability status and the life-safety performance criteria have been taken into account together. Therefore, a cost-effectively repairable building is deemed to have served satisfactorily in meeting the life-safety performance criteria.

Table 5.1 Damage state definitions employed

Damage State	Column	Beam	Shear Wall	Infill Wall
Light/none	Visible flexural hairline cracks	Visible flexural and inclined hairline cracks	Visible flexural hairline cracks	Surface cracks along the boundaries
Moderate	Clear flexural and shear cracks	Wide flexural and inclined cracks, spalling of concrete	Visible inclined hairline cracks and clear flexural cracks	Diagonal cross cracks, separation from the frame
Heavy/collapse	Wide cracks, spalling and crushing of concrete, buckling of reinforcement, excessive deformation	Large cracks, plastic hinge formation, crushing of concrete	Complete diagonal cracks, spalling of concrete, exposure of reinforcement	Through cross cracks, rupture of bricks

5.3.3.2 Damage Statistics

This section presents examples of typical and noteworthy damage to reinforced concrete frames with masonry infill and shear wall structures. The areas studied were selected as the location of high concentration of damage within the city as indicated in Figure 5.2. An overall summary that contains observed damage, structural system, number of floors and apparent material quality of the residential concrete buildings surveyed is given in Table 5.2. The table also contains wall and column indexes given in Hassan and Sozen (1997) for those buildings that were surveyed in detail. The buildings that are identified with two separate ID's indicate common buildings with NSF team; the identifications in the parentheses correspond to the NSF team designations.

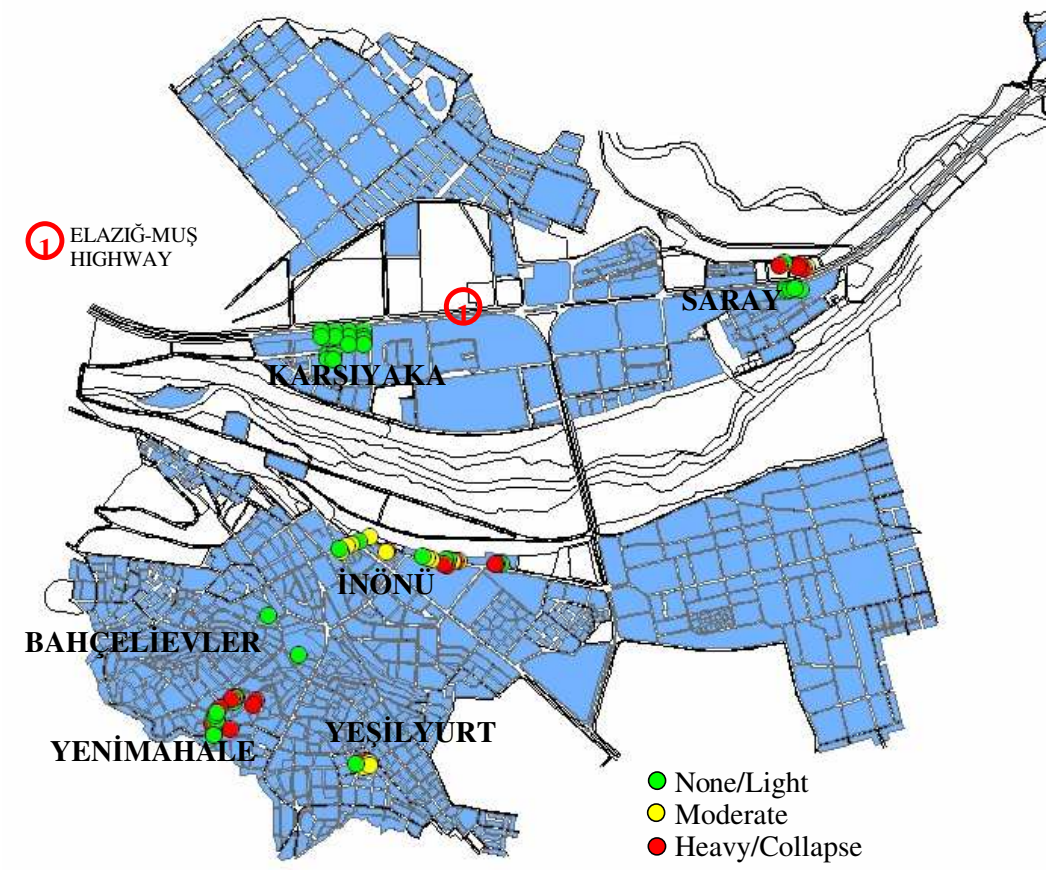

Figure 5.2 City map of Bingöl and sub-districts visited

Table 5.2 Damage Survey Summary

Building ID	Location	Const. Year	No. of Floors	Type	Apparent Quality	Damage	Minimum WI (%)	CI (%)
BNG-10-4-4	İnönü	1998	4	RCF	average	moderate	0.01	0.22
BNG-10-4-5	İnönü	1997	4	RCF	poor	severe/collapse	0.02	0.28
BNG-10-4-6	İnönü	1976	4	RCF	average	moderate	0.01	0.15
BNG-10-4-7	İnönü	1988	4	RCF	average	light	0.03	0.14
BNG-10-4-8	İnönü	NA	4	RCSW	poor	severe/collapse		
BNG-10-4-9	İnönü	2002	4	RCSW	good	light	0.01	0.21
BNG-10-3-10	İnönü	NA	3	RCF	poor	moderate	0.00	0.25
BNG-10-5-11	İnönü	1988	5	RCF	average	light	0.03	0.29
BNG-6-3-1	Yenimahalle	1991	3	RCF	poor	severe/collapse	0.00	0.26
BNG-6-4-2	Yenimahalle	2001	4	RCF	poor	severe/collapse	0.03	0.27
BNG-6-4-3	Yenimahalle	2003	4	RCF	poor	severe/collapse	0.00	0.33
BNG-6-3-4	Yenimahalle	2003	3	RCF	average	light	0.16	0.12
BNG-6-4-5	Yenimahalle	1996	4	RCF	good	light	0.01	0.28
BNG-6-4-6	Yenimahalle	1996	4	RCSW	poor	severe/collapse	0.01	0.26
BNG-6-4-7	Yenimahalle	1996	4	RCSW	poor	severe/collapse	0.00	0.46
BNG-6-2-8	Yenimahalle	1992	2	RCF	poor	severe/collapse	0.02	0.22
BNG-6-4-9	Yenimahalle	NA	4	RCF	poor	severe/collapse	0.02	0.18
BNG-6-3-10	Yenimahalle	1995	3	RCF	average	light	0.00	0.29
BNG-6-3-11	Yenimahalle	NA	3	RCF	poor	light	0.03	0.26
BNG-6-3-12	Yenimahalle	NA	3	RCF	average	light	0.01	0.16
BNG-5-5-1	Bahçelievler	Pre 1990	5	RCF	poor	light		

Table 5.2 Damage Survey Summary - cont'd

Building ID	Location	Const. Year	No. of Floors	Type	Apparent Quality	Damage	Minimum WI (%)	CI (%)
BNG-11-4-1	Yeşilyurt	1998	4	RCSW	poor	severe/collapse		
BNG-11-4-2	Yeşilyurt	1989	4	RCF	poor	severe/collapse	0.02	0.16
BNG-11-2-3	Yeşilyurt		2	RCF	poor	moderate	0.02	0.14
BNG-11-4-4	Yeşilyurt	2000	4	RCF	poor	moderate		
BNG-11-4-5	Yeşilyurt	1997	4	RCF	average	moderate	0.02	0.21
BNG-3-4-1	Karşıyaka	1998	4	RCF	poor	light	0.00	0.32
BNG-3-4-2	Karşıyaka	1996	4	RCF	poor	light		
BNG-3-4-3	Karşıyaka	NA	4	RCF	poor	light	0.03	0.18
BNG-3-4-4	Karşıyaka	NA	4	RCF	Poor	light	0.04	0.23
BNG-1-5-1 (A-12-01/02)	Saray	NA	5	Tunnel Form	Poor	light		
BNG-10-I-4-1	İnönü	NA	4	RCF	average	light		
BNG-10-I-4-2	İnönü	NA	4	RCF	poor	severe/collapse		
BNG-10-I-4-3	İnönü	NA	4	RCF	poor	severe/collapse		
BNG-10-I-4-4	İnönü	1984	4	RCF	poor	severe/collapse		
BNG-10-I-4-5	İnönü	1998	4	RCF	average	moderate		
BNG-10-I-4-6	İnönü	1995	4	RCF	poor	moderate		
BNG-10-I-4-7	İnönü	2000	4	RCSW	average	light		
BNG-10-I-8	İnönü	Pre 1971	4	RCF	average	severe/collapse		
BNG-10-I-9	İnönü	NA	4	RCF	poor	moderate		
BNG-10-I-10	İnönü	1985	4	RCF	poor	moderate		
BNG-10-I-11	İnönü	1980	3	RCF	poor	moderate		
BNG-10-I-12	İnönü	1982	4	RCF	poor	moderate		
BNG-10-I-13	İnönü	1973	4	RCF	poor	light		
BNG-I-3-1	Yenimahalle	NA	3	RCF	NA	light		
BNG-I-3-3	Yenimahalle	NA	3	RCF	NA	light		
BNG-I-3-5	Yenimahalle	NA	3	RCF	NA	light		
BNG-I-4-7	Yenimahalle	NA	4	RCF	poor	light		
BNG-I-2-11	Yeşilyurt	NA	2	RCF	NA	light		
BNG-I-4-12	Bahçelievler	NA	4	RCF	average	light		
BNG-I-5-13	Saray	1999	5	RCSW	poor	moderate		
BNG-I-5-14 (C-12-9)	Saray	NA	5	RCF	NA	severe/collapse		
BNG-I-4-15	Saray	NA	4	RCF	poor	moderate		
BNG-I-4-16	Saray	NA	4	RCF	poor	severe/collapse		
BNG-I-4-17	Saray	NA	4	RCF	NA	severe/collapse		
BNG-I-5-18 (C-12-10)	Saray	NA	5	RCF	NA	light		
BNG-I-4-19	Saray	1998	4	RCF	NA	severe/collapse		

Notes: RCF: Reinforced Concrete Frame with Masonry Infill Walls
RCSW: Reinforced Concrete Frame with Shear Walls
NA. Not available or could not be determined

A total of 57 residential buildings of 2-5 stories with varying degrees of damage were examined. As displayed in Figure 5.3, the majority of buildings surveyed comprised of four story reinforced concrete frame buildings. Each building was assigned a damage degree based on the criteria mentioned earlier, and a quality classification of the materials was made by visual inspection whenever possible. Three levels of material quality were employed; poor, average and good. Nineteen buildings were judged heavily damaged/collapsed, 14 were assigned moderate damage and the remaining 24 were identified as either undamaged or lightly damaged. The relationship between the

damage level and material quality is illustrated in Figure 5.4. Although a rough trend between damage and material quality is evident, the lack of quality assessment for the buildings that had collapsed or had no damage prevents us from making a general conclusion.

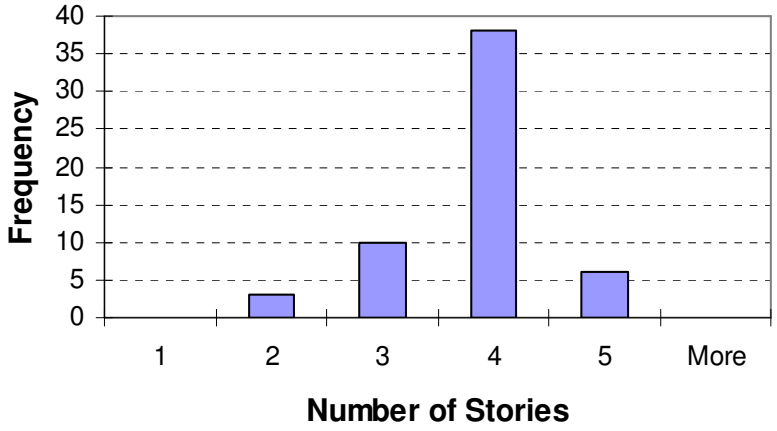

Figure 5.3 Height distribution of the buildings surveyed

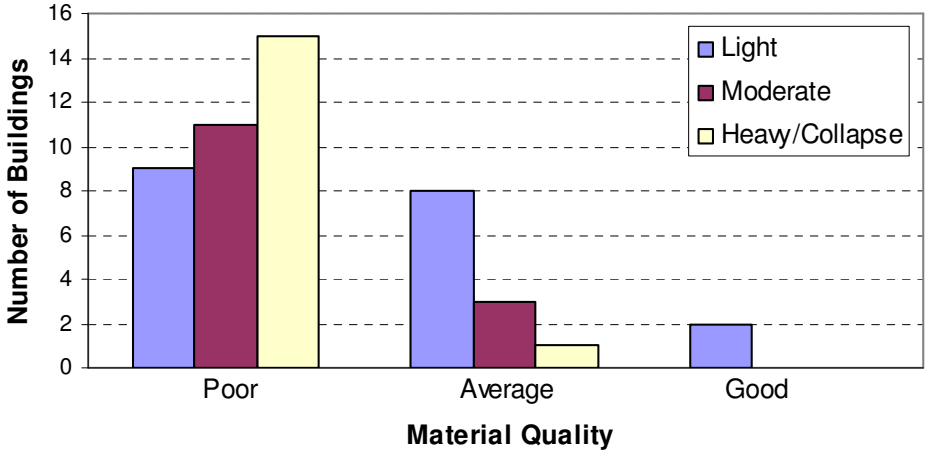

Figure 5.4 Damage versus material quality distribution

Twenty-five of the buildings were surveyed in detail to collect information about their layout, plan area, sizes of vertical members, infill wall area and other relevant architectural features. In order to investigate the adequacy of the lateral load-carrying members several existing methods can be employed. An index called the Priority Index (PI), obtained by adding wall index and column index, proposed by Hassan and Sozen (1997) is used here to obtain a relative indication of the adequacy of the structural system and to see if there is any trend that relates to the observed damage. Although it is expected to have a reverse relation between PI and damage, i.e. as PI increases damage should decrease, the outcome of surveyed buildings does not reveal any consistent trend (Figure 5.5a). Similar plots were obtained also in a different format (Figure 5.5b). An additional chart is given in Figure 5.5c in order to display the indexes computed for all residential buildings surveyed (except two tunnel form buildings) by both the TÜBİTAK and the NSF teams. Although a boundary is drawn to classify heavily damaged buildings, it also inevitably traps many lightly damaged buildings. This is not unexpected because the index basically relies on the structural system and disregards the effects of the material and construction quality, and detailing. Therefore a further check could be made by evaluating the PI index along with the material quality as depicted in Figure 5.6. A high priority index does not dictate low damage unless the material quality is decent. The figures presented in this plot, however, do not clearly reveal the effect of material quality due to inadequacy of content of data collected. Furthermore, the influence of subjective evaluation and probably bias introduced in the quality assessment of heavy/collapse buildings might be unavoidable.

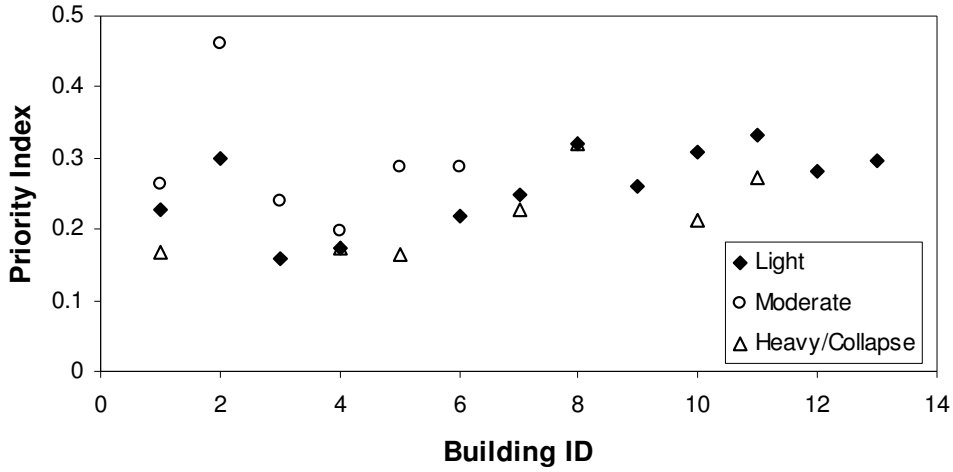

a) Priority index

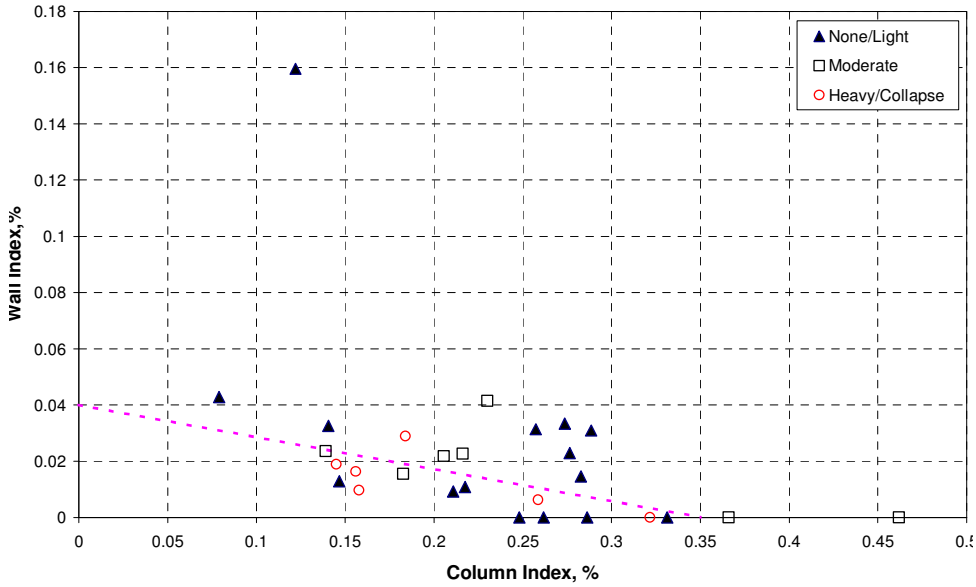

b) Wall and column indexes

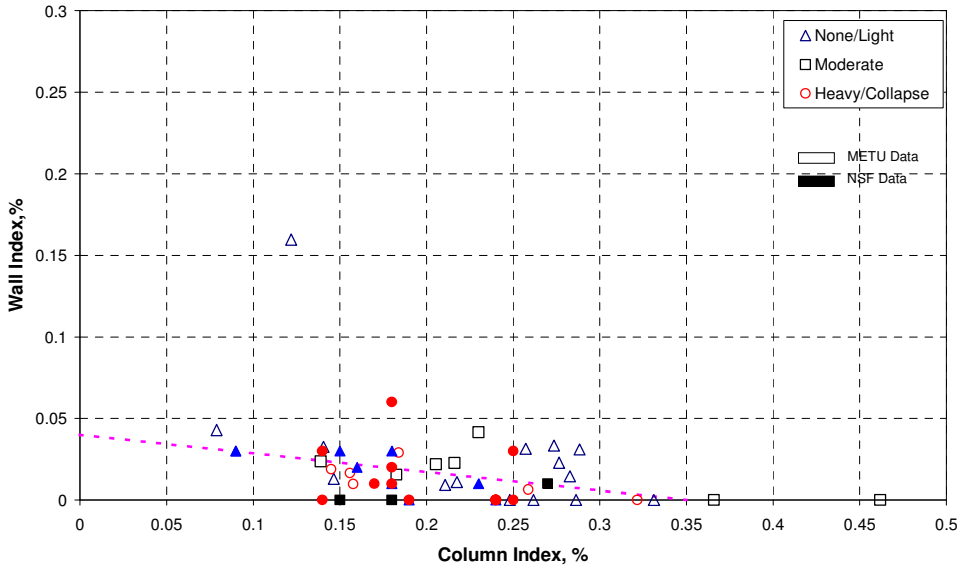

c) All residential buildings

Figure 5.5 Hassan and Sozen (1997) indexes versus observed damage

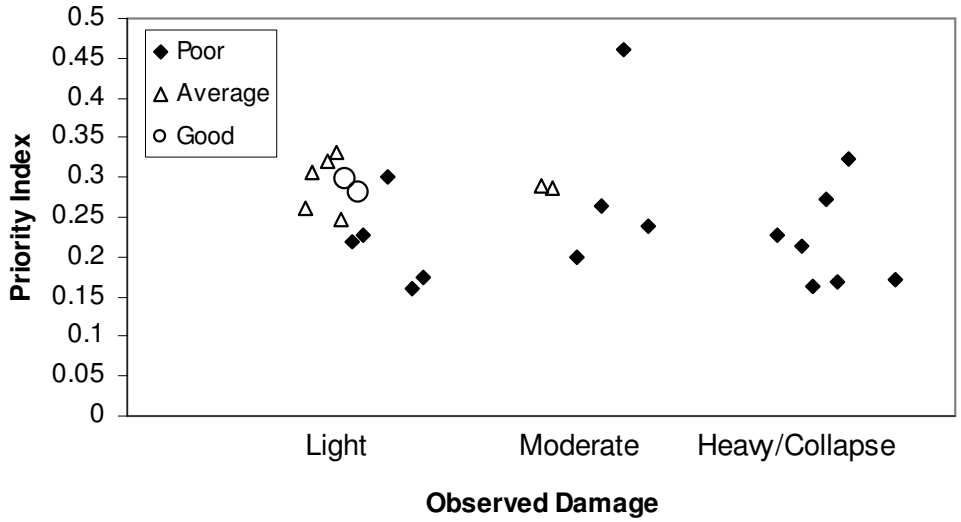

Figure 5.6 Priority index, damage and material quality

5.3.3.3 Damage Observations

The commonalities of construction practice in Bingöl resulted in some typical damage patterns observed in many buildings. The collapse of ground floor, shear cracks in columns, complete hinging at column ends, buckling of reinforcement, spalling and crushing of concrete in reinforced concrete members, diagonal cracking and separation of infill walls from encasing frames were widespread damage patterns observed. Unlike other major historic earthquakes, damage due to pounding, pancake collapses and damage due to existence of over-hangs were not very common in this earthquake. This in part is considered to be the result of the short duration of the earthquake.

Figure 5.7 shows a conventional four-story reinforced concrete building located in the İnönü sub-district, a commercial area. The building experienced moderate damage indicating that load-resisting elements performed well with respect to life-safety. The resistance to lateral loads was mainly provided by the columns and filler walls since the building does not have any shear walls. The increased strength demand in the first floor was supplied by the contribution of infill walls as evidenced by heavy infill wall damage concentration in that floor (Figure 5.7). The building has several undesired architectural features that are worth mentioning here. The presence of a mezzanine floor, commercial use of the ground floor, the penthouse and strong beam-weak column are some of those features that can be seen from Figure 5.7. The uncovered masonry infill on the side face of the building outlines the structural system. The infill walls are composed of conventional hollow clay tile, Figure 5.8, used in practice for partition walls. The ratio of holes in the tile directly affects the load carrying capacity of the wall. The nonstructural components, i.e. masonry infill, suffered severe damage (Figure 5.9) whereas reinforced concrete components had experienced moderate damage.

A three-story residential building located in the same sub-district suffered severe damage due to its poor material quality and detailing as shown in Figures 5.10 to 5.13. The building has a basement and a soft ground story where the heaviest damage was observed. A spectacular example of the diagonal tension crack at the upper end of the column due to a combination of inferior material quality and inadequate transverse reinforcement is shown in Figure 5.11. The condition of several other columns and masonry walls illustrated in Figures 5.12 and 5.13 reemphasizes the poor quality of construction combined with a high deformation demand in the ground floor. The level of damage in the beams was generally insignificant compared to the columns (Figure 5.13). Despite extremely poor performance of the columns, the masonry walls, which were made of unreinforced solid brick blocks, are believed to have prevented the collapse of the building.

Figure 5.7 Four-story residential (except ground floor) building in İnönü sub-district

Figure 5.8 Typical hollow clay tile used in infill walls

Figure 5.9 Severe infill wall damage

Figure 5.10 Two-story residential building

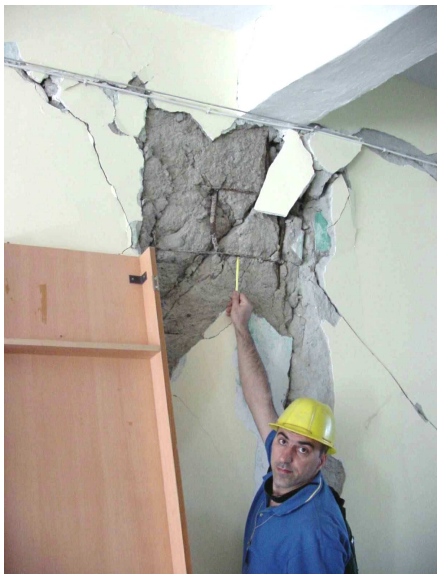

Figure 5.11 Diagonal tension crack at the upper end of the ground floor column

Figure 5.12 A clear column-end failure and masonry wall damage

Figure 5.13 Column damage and condition of beams

The damage levels observed in the sub-district of İnönü were not uniform and quite different among the buildings with the same number of stories and structural system. There were several examples of collapsed buildings due to insufficient strength in the soft ground floor. Figure 5.14 shows a four-story reinforced concrete frame building that suffered heavy damage due to a combination of poor construction quality and the presence of a soft ground story. The upper stories are intact with minor damage whereas the ground floor has collapsed. The five-story reinforced concrete frame building shown in Figure 5.15 suffered light damage despite the presence of a mezzanine floor and a soft story. The above average quality of concrete observed here might have led to the satisfactory performance.

The influence of sufficient lateral load resistance was evident from the excellent performance of reinforced concrete shear wall buildings. Two identical buildings separated by dilatation joints and possessing a sufficient area of structural walls have survived the earthquake almost unscathed. It is also worth noting that the apparent quality of material and workmanship was quite good. The building on the left was completed and being occupied but the one on the right had only its structural system finished. The pounding between adjacent buildings did not result in significant damage most likely due to short duration of the shaking (Figures 5.15 and 5.16).

Figure 5.14 First story collapse of a four-story building

Figure 5.15 Lightly damaged five-story reinforced concrete frame building

Figure 5.16 Satisfactory performance of two-identical shear wall buildings, BNG-10-4-9 in Table 5.1.

Another sub-district, Saray, located in the provincial area north of the major highway connecting Bingöl to the cities of Elazığ and Muş was visited and the buildings were evaluated. Most of the buildings along a line parallel to the highway experienced heavy/complete damage. The majority of these buildings had a reinforced concrete frame structural system and a soft ground floor where the heaviest damage was concentrated. These buildings generally had insufficient structural resistance and poor construction quality and detailing which played important part in their collapse as depicted in Figures 5.17 to 5.19.

Figure 5.17 Loss of soft story in reinforced concrete frame building

Figure 5.18 Collapse of ground floor

Figure 5.19 Insufficiently confined column of a collapsed building

Some of the sub-districts that were mainly residential areas were affected significantly, many buildings suffering great deal of damage, where some others did quite well. The building stock in Yenimahalle was generally composed of three to four story reinforced concrete buildings constructed after 1995. Those that were facing the main street all had commercial stores in the ground floor, some older masonry buildings constituted the remaining part of the building inventory. A four-story building that experienced heavy damage was built on a slope, having one basement, open on the back only (Figure 5.20). The date of construction being 2001, it was supposed to reflect the criteria of the most recent seismic code. Although the building did not collapse, the lateral load system comprising reinforced concrete frames was insufficient to survive the intensity and thus had severe damage as shown in Figure 5.21. The apparent quality of concrete was relatively poor, though the detailing and reinforcement seemed to be better than found in average practice. The increased axial load demand

during the shaking along with associated flexural demand caused high compressive loads and thus extensive damage to the columns. Additionally, the configuration of the building possesses some undesirable architectural features such as an over-hang, a soft story and construction on a slope.

Figure 5.20 A heavily damaged four-story building in Yenimahalle

Figure 5.21 Spalling and crushing of concrete due to high axial loads

The soil properties at the site and the proximity to the earthquake source might have played important roles for localized damage in certain sub-districts, but the striking difference on the performance of very similar adjacent buildings enhances the importance of other factors pertaining to the construction. One such case is shown in Figure 5.22, the building on the left survived the earthquake but the building to its right which was unoccupied due to unfinished nonstructural work, suffered a ground floor collapse and tilted backwards. The construction quality and technical inspection of the undamaged building is much superior to the damaged one as observed by the NSF-TÜBİTAK teams and confirmed by the local people who had witnessed the construction of these buildings.

Figure 5.22 a) Lightly damaged four story RC building constructed in 1996; b, c) Complete damage to four story RC building constructed in 2003; d) Column offsetting at collapsed floor due to improper connection.

Among the concrete buildings that were surveyed throughout the city only a few had limited and in some cases primitive shear walls contributing to their lateral load resistance. The presence of these shear walls very likely prevented the collapse of the buildings (Figure 5.23 – 5.25) despite their inferior material quality. The walls picked up a significant part of the seismic force experiencing substantial damage. One unusual observation was that the wall was observed to have more significant damage in the first floor than the ground floor level (Figure 5.24). Although the building had many favorable features such as regular rectangular floors, no soft stories and continuous vertical frames, substandard construction and material quality were the major factors that led to heavy damage.

Figure 5.23 Heavily damaged reinforced concrete frame with shear wall type construction

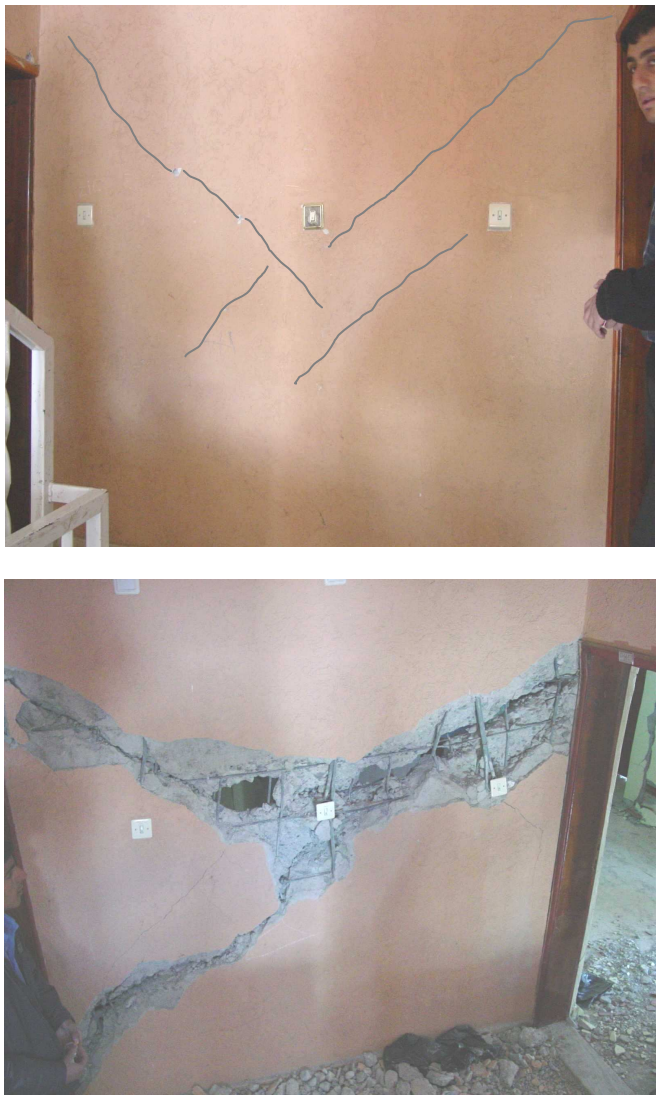

Figure 5.24 Shear failure of ground floor (top) and first floor (bottom) shear walls

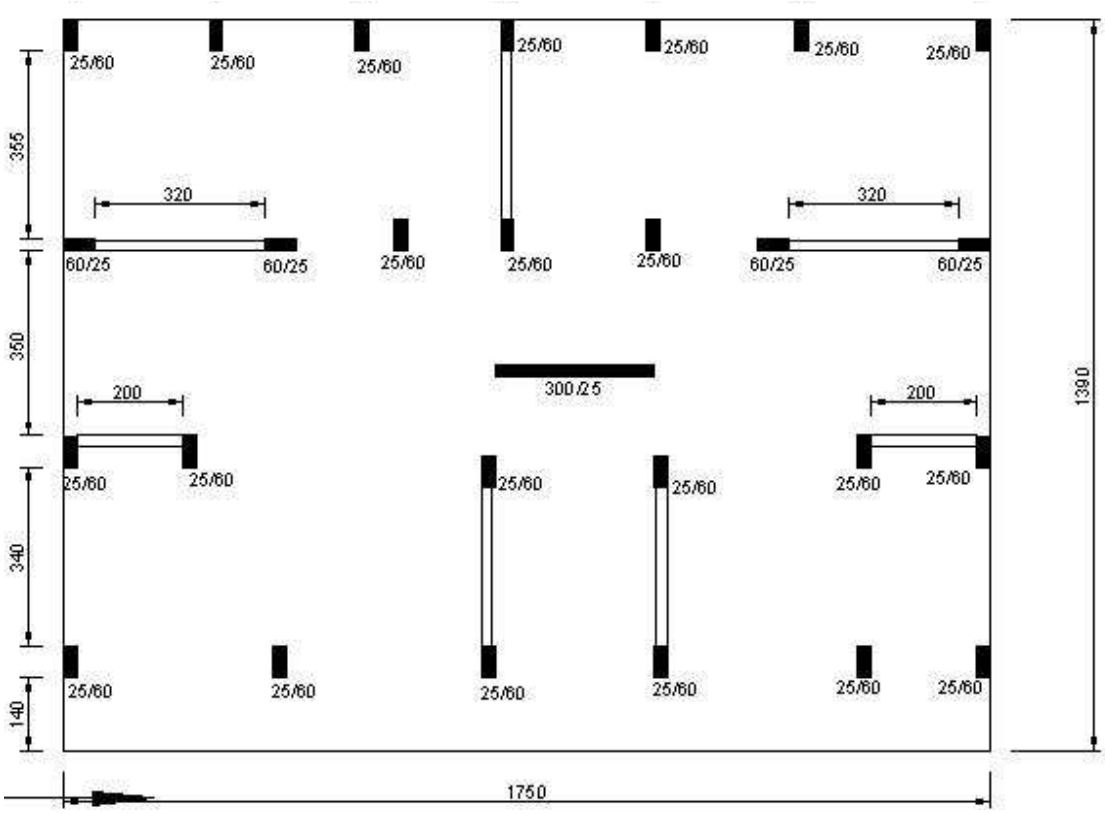

Figure 5.25 Structural floor plan of the building

A similar scheme is shown in Figure 5.26, where a four-story building with shear wall experienced heavy damage. The poor material quality and the detailing that does not reveal any lateral reinforcement are among the major factors for the observed damage. This building had a penthouse floor added on the roof, and it is likely that this is neither accounted for in the design calculations nor approved by the responsible authorities.

Figure 5.26 Heavily damaged 4 -story building (plus penthouse) and the damage experienced by its shear wall

Cases of collapsed buildings, which were generally reinforced concrete frame buildings were also observed in Yenimahalle. Figure 5.27 displays the collapse of the first floor of a frame building that was built on a slope. The floor that was facing the street had stores within it.

Figure 5.27 Collapsed 5 story building in Yenimahalle.

A unique observation from this earthquake was widespread damage to the windows. Contrary to the insignificant damage of their structural system, the windows of many buildings were broken during the shaking. This was found to be due to a peculiar regional practice of using steel framing around the windows welded to the reinforcement in the enclosing column or beam (Figure 5.28).

A few cases of damage associated with short column formation were observed. These limited short column damage observations were mainly due to local building practice in which the basements are generally either completely below ground or in case of the basement being partially embedded the part above the surface is surrounded with shear walls. A two-story building with one basement located in Yeşilyurt sub-district experienced short column damage as shown in Figure 5.29.

Figure 5.28 Window framing detail. Steel frame is welded to the rebar of the beam.

Figure 5.29 Short column damage of a two-story reinforced concrete frame building in Yeşilyurt.

As revealed by many examples and shown in Figure 5.3 the majority of the buildings surveyed are four story reinforced concrete buildings that portray the characteristics of the building stock in Bingöl. This is due to the construction regulation that places a limit on the building height. The damage patterns experienced by the components of another reinforced concrete shear wall building located in Yeşilyurt displays the most spectacular cases of damage resulting from poor material quality and improper reinforcement (Figures 5.30 to 5.33).

Figure 5.30 Four story residential building. The look from outside is quite different and misleading for a heavily damaged building.

Figure 5.31 Failure of the shear wall due to inferior material quality and detailing.

Figure 5.32 Brittle failure of the column of building shown in Figure 5.30. Buckling of bars due to insufficient lateral confinement and crushing of core concrete.

Figure 5.33 An inclined shear crack of a moderately damaged column.

In the Yeşilyurt sub-district the damage patterns were pretty similar to the examples shown above. A striking example of connection damage of a four-story building is illustrated in Figure 5.34.

Figure 5.34 A corner column on the ground floor of a four-story building. Separation of the column due to improper detailing.

5.3.3.4 Summary of Observations

The Bingöl earthquake of May 1st, 2003 resulted in substantial damage to residential buildings that were generally 3-5 story reinforced concrete frames with infill wall type construction. The most widespread damage pattern was the collapse or heavy damage confined to the ground floor occupied by the commercial stores. The cases of pounding damage, pancake collapse, and damage due to over-hangs were quite rare and might be attributed to the short duration of the earthquake. Examples of significant damage attributed to short/captive columns were also observed.

Damage was mainly concentrated in columns in the form of core crushing and buckling of longitudinal bars leading to local collapse and shear cracks confined generally to the column ends. Damage to beams was limited and insignificant.

The effect of material quality and structural configuration (including short/captive column, soft story etc.) was quite clear. All surveyed buildings with shear walls survived the earthquake without collapse but those that did not have adequate material quality and proper detailing suffered substantial damage. A general observation made by the survey teams revealed that buildings that had a combination of the typical damage inducing parameters mentioned previously experienced significant damage.

The contribution of the infill walls to the lateral load resistance of the building was once again proven because many buildings had carried on with only damage to their filler walls. Especially buildings that had unreinforced clay tile infill were observed to perform better than the ones with hollow clay tile.

5.3.4 Observations of the NSF Team

The NSF team of researchers was subdivided in units of 2 and 3 researchers for purposes of covering the damage. The building designations have the form X-NN-MM, where X is the designation of the unit that visited the site, NN is the day of the month that the building was visited, and MM represents the sequential order in which the buildings were visited each day.

For each building, the following information was acquired and made available in this report

- Location (GPS coordinates),
- Building orientation relative to north,
- Number of stories,
- Story height,
- Ground floor plan showing the structural system,
- Damage level of reinforced concrete system,
- Damage level of masonry infill walls.

The damage rating of the reinforced concrete system used in this survey aims to group the buildings with similar damage patterns rather than to define their damage states in absolute terms. Inclined cracking of columns is a very dangerous type of damage in the case of insufficient transverse reinforcement and improper detailing. Therefore, the structures with inclined cracks observed on their columns were rated to be severely damaged. The shear and flexure cracks on beams, spalling of concrete on columns and hairline cracks on shear walls were the most common damage patterns in the moderately damaged structures. The lightly damaged structures were the ones with only hairline cracks on beams.

The masonry infill wall damage of the buildings was also rated in three levels which can be defined as follows:

- Severe damage: The wide and through cracks on walls and their boundaries.
- Moderate damage: Cracks on walls and their boundaries, flaking of large pieces of plaster.
- Light damage: Hairline cracks on walls, flaking of plaster.

The building inventory includes two residential buildings (B-12-07 and C-12-03) that collapsed during the earthquake. It was not possible to obtain information on the ground floor plan of these buildings. In addition, floor plans were not developed for two other severely damaged buildings, C-12-02 and C-12-09, because it was not safe to enter these buildings. Other data from these four buildings were kept in the inventory to help define the spatial distribution of damage.

5.3.4.1 Building Damage Survey

A total of 33 reinforced concrete buildings were surveyed. The buildings were selected to investigate whether damage varied systematically from district to district or over the area of the city (Figure 5.35). The survey covered buildings with various types of lateral load resisting systems. Among the selected buildings, 23 had moment resisting frames, 8 had dual systems with moment resisting frames and structural walls, and 2 had panel wall systems. The buildings ranged in height from 3 to 6 stories above ground; with partition walls typically made of hollow clay masonry units (Figure 5.36). Common features observed in buildings were the presence of overhangs above the first story, the lack of continuity of girder lines, columns with aspect ratios ranging from 2 to 4, and relatively small tributary areas for the columns.

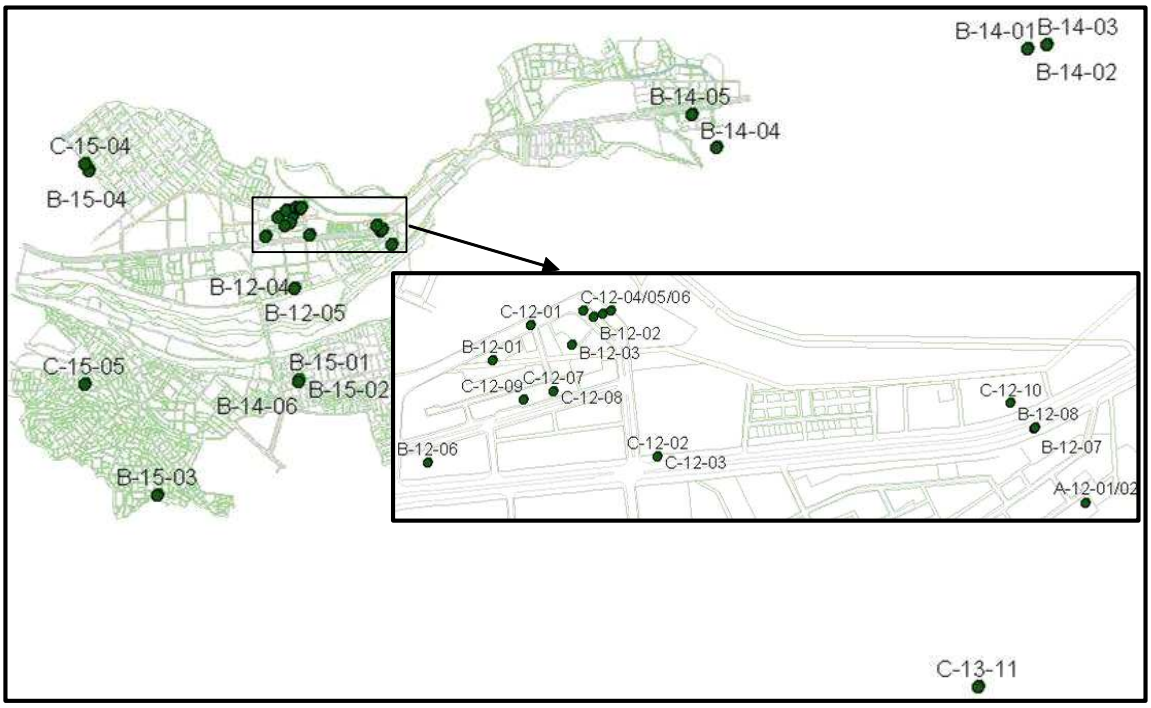

(a)

(b)

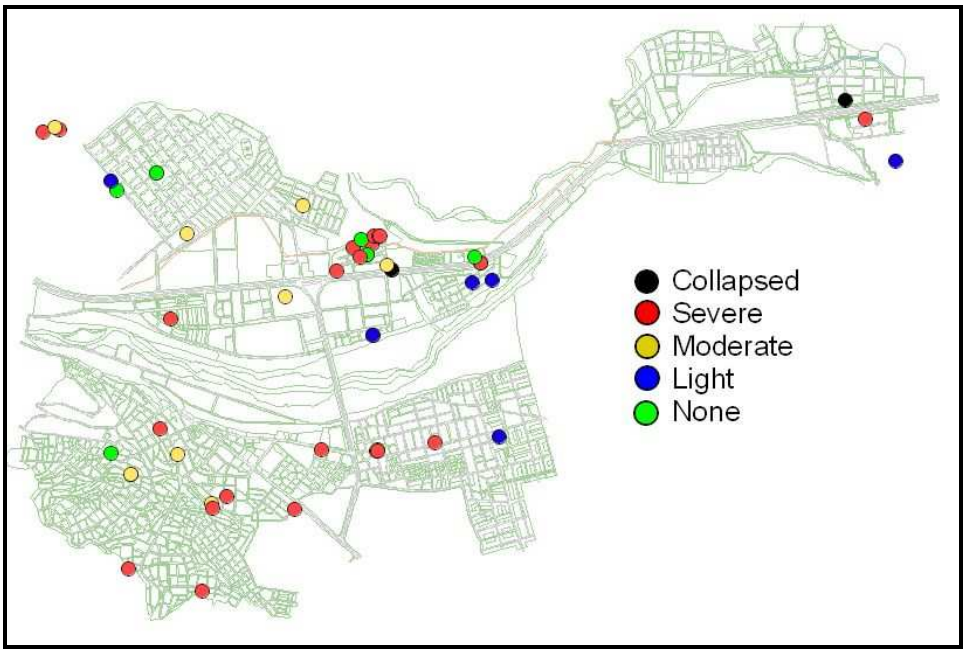

(c)

Figure 5.35 (a) Location of buildings in damage survey; (b) Overview of Bingöl from point indicated in Figure 5.35a, looking south-east; (c) Damage distribution in the city of Bingöl based on the buildings surveyed by the NSF team.

Within sampled buildings with moment-resisting frames, the ratio of column area to floor area ranged between 0.09 percent and 2.7 percent. In buildings with structural walls, the ratio of wall area to floor area ranged between 0.2 percent and 5 percent.

Damage was catalogued following a scale similar to that used in other structures, and results of the survey are summarized in Table 5.3 and 5.5. Results indicate that the level of damage was highest for structures with moment-resisting frames, and all documented cases of collapse occurred in this type of structures. The primary reason for collapse or severe damage in moment frames was the shear failure of columns in the first story. Damaged columns commonly exhibited inclined cracks ranging from barely visible to widths in the order of inches (Figure 5.37), without the presence of flexural cracks. In the majority of the cases the damage to girders was very light, without any noticeable flexural or inclined cracks.

Figure 5.36 Typical reinforced concrete moment frame building

Figure 5.37 Shear failures in unrestrained and captive columns.

Damage to nonstructural partition walls was severe in most cases. Most partition walls were made with unreinforced hollow clay masonry units that effectively restrained the motion of the frames at the start of the event. As a result of the interaction with the frames, the masonry walls suffered severe damage at very low levels of drift. The brittle behavior of the walls and low tensile strength of the masonry units were the two factors contributing to the level of damage that occurred. Two types of failure commonly observed in masonry walls were due to crushing of the masonry units near the beam-column interface (left of the column in Figure 5.38) or shear failure of the masonry panel (right of the column in Figure 5.38). The former had the unforeseen consequence of creating a captive column, which was particularly vulnerable to shear failure (Figure 5.38). Another type of failure observed less frequently was the out-of plane collapse of the masonry wall.

Structures with dual systems or structural walls suffered less damage, and no partial or total collapses were observed among this group of structures. In some instances inclined cracks were visible in structural walls, but the small width was a clear indication that yielding of the transverse reinforcement had not occurred. Damage to masonry walls in these structures was not as severe as in the case of moment frames.

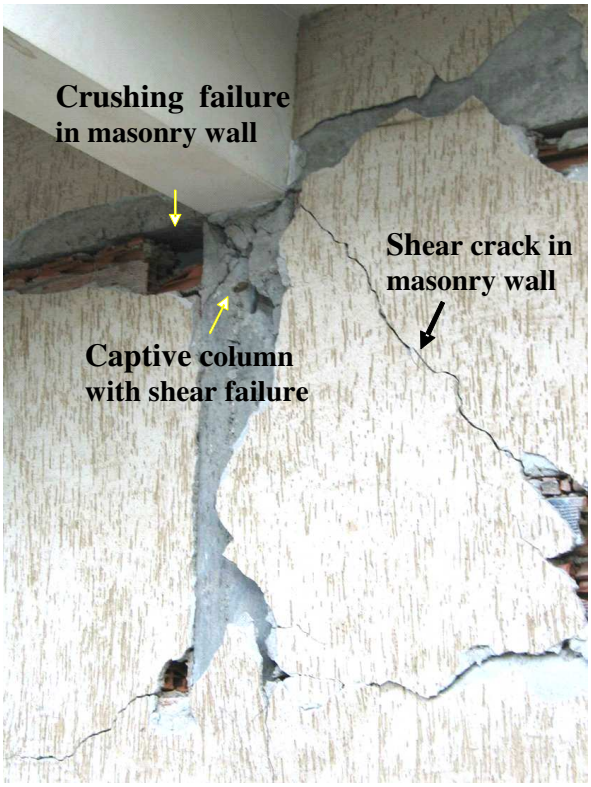

Figure 5.38 Damage to masonry walls.

A good example of the different types of response experienced by different structural systems is illustrated in Figure 5.39. Before the earthquake, there were three buildings at the site of Çeltiksuyu Boarding School, located approximately 10 km to the south east of Bingöl. The buildings were the teachers' apartments (C-13-11), the student dormitory and the school building (C-13-10). The figure shows the state of the three structures after the earthquake. Both the school building (right of the picture) and the student dormitory (center of the picture), with moment-resisting frames, collapsed with a death toll of 84 (mostly children). The apartment building for the teachers, with a dual structural wall – moment frame resisting system, survived without damage. Figure 5.40 is a photograph taken inside the kitchen of an apartment located in the second story of the apartment building. Objects violently thrown out of shelves are an indication of the high accelerations that must have taken place at the site. There is also an elevated water tank behind the apartments building that survived without any visible damage.

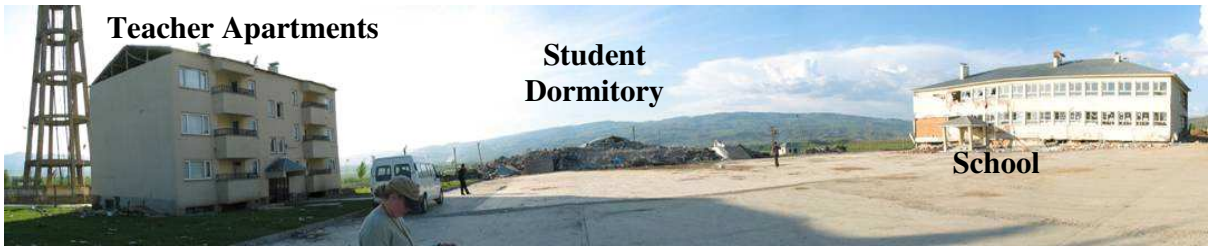

Figure 5.39 Damage to three different structures

Figure 5.40 Objects thrown on the floor of apartment building as a result of the earthquake

5.3.4.2. Characteristics that affected the performance of moment frame structures

There were many factors that affected the performance of structures with moment- resisting frames during the Bingöl earthquake. Three main categories are discussed in this report: structural characteristics, material properties, and detailing of the structural elements.

Structural characteristics

Most residential buildings surveyed had bays with relatively short span lengths, typically ranging between 2.5 and 5m. Commonly observed features include columns that were more flexible (and weaker) than the girders, which is substantiated by the observed damage patterns.

It is very common in this area of Turkey for residential buildings to have retail space in the first story (Figure 5.41). Masonry walls surrounding the apartments in the upper stories are interrupted at the first story, placing a very large displacement demand on the weak direction of the columns of the first story.

Figure 5.41 Residential/commercial buildings in downtown Bingöl

Another commonly observed feature was the presence of captive columns due to the partial restraint imposed by masonry walls discontinued to allow for window space (Figure 5.37).

Material properties

A significant problem observed in all buildings that were surveyed was the quality of the concrete. Because Bingöl is located in a remote rural area, ready-mixed concrete is not available, and material quality control is reportedly very lax. Aggregates are obtained from the adjacent river bed and used in concrete mixes without any processing. As a result fine aggregates consist of river sands with unknown gradation and fines content, and coarse aggregates have round and smooth surfaces, with observed maximum sizes of up to 15 cm (Figure 5.42). According to local engineers, concrete mixes are not proportioned on the basis of a target compressive strength. Workers determine the amount of aggregates and cement based on traditional practice and add water until a desired workability is achieved. No form of curing takes place after concrete casting.

Tolerances in forms (Figure 5.43 and 5.44) and steel cages are of the order of several centimeters, and it is common to have very small or no cover for the reinforcement. The placement of the concrete is carried out without compaction or vibration. As a result, problems in structural members such as voids in the concrete and exposed reinforcement are commonly observed (Figure 5.42).

All these factors result in very poor quality of concrete in most buildings for which proportioning and detailing rules included in modern design codes are unlikely to be applicable.

Figure 5.42 Beam-column joint in building under construction

Another problem observed in construction practice is the use of undeformed steel bars. Although the use of this type of bars presents a significant problem in terms of achieving adequate bond between reinforcement and concrete, the observed crack patterns in the members did not indicate the occurrence of bond failures. This is attributed to shear failures in columns occurring at relatively low drift levels, such that the deformation demand on the members was never large enough to cause failures due to loss of bond.

Figure 5.43 Beam and column formwork in building under construction

Figure 5.44 Slab formwork in building under construction

Element detailing

Building configurations with flexible stories or captive columns place very large displacement demands on the columns of moment resisting frames. In order to sustain large deformations without collapse, proper detailing for toughness is essential. In the case of commercial and residential buildings with moment resisting frames in Bingöl, the most common type of damage observed in structural members was observed in captive as well as noncaptive columns associated with bending about either axis of the column. This damage pattern in conjunction with the absence of flexural cracks is an indication that the most significant vulnerability of the columns was due to lack of adequate amounts of transverse reinforcement to withstand the shear demand.

As indicated previously, typical span lengths in residential buildings were below 5 m, resulting in fairly small tributary areas for the columns. Due to the relatively large column sizes employed in local construction practice and the small tributary areas, the majority of the columns in the buildings that were surveyed was subjected to axial load demands below 0.2 f'_c A_g, and had longitudinal reinforcement ratios of approximately 1 percent. Consequently, axial load did not affect the shear strength of the columns significantly. The amount and distribution of the transverse reinforcement was the primary parameter affecting shear strength.

Typical column details consisted of arrangements of 8 or 10 16-mm bars with stirrups consisting of 10 mm bars with spacing raging between 150mm and 250 mm. In order to allow the columns to blend with the masonry walls, local construction practice favored rectangular cross sections with aspect ratios ranging in most cases from 2 to 4. To maintain a width similar to that of the wall, the smallest dimension of the columns was usually 250mm or 300 mm. In many instances the smallest dimension of the column was approximately the same as the spacing of the stirrups, allowing shear cracks to form in the weaker direction of the column without intercepting any reinforcement (Figure 5.45). Given the types of aggregates commonly used and the standard practice for placing of the concrete, it is doubtful that a smaller stirrup spacing can be used without severe problems due to formation of voids in the concrete (Figure 5.42).

The lack of sufficient amount of shear reinforcement to allow the development of yield in the longitudinal column reinforcement resulted in shear failures at low drift demands. This hypothesis is consistent with the absence of damage and the type of crack patters observed in reversed cyclic loading tests of well-confined columns in the laboratory. Because columns exhibited such brittle behavior, the best performance was achieved by buildings with dual and wall systems in which the walls limited the drift.

Even if the amount of shear reinforcement had been sufficient to achieve some level of ductility, the toughness of the columns would have been questionable for several reasons. The amount of confining reinforcement provided was very light. In the case of two columns sampled in the field, the amount of confining reinforcement was approximately 30 percent of the amount required by the ACI 318-02 building code. The combination of inadequate confinement and weak concrete would have resulted in rapid deterioration of the core, and a significant loss in the maximum shear carried by the columns.

Figure 5.45 Typical column details in plastic hinge regions

Other issues that could have affected the performance of frames at larger drift demands include the location of splices in plastic hinge regions (Figure 5.46), the use of 90 degree bends to anchor bars in stirrups (Figure 5.47), and the lack of ties providing out of plane support for intermediate bars (Figure 5.45).

Similar detailing concerns were observed in shear walls (Figure 5.48). Boundary elements were not used to provide adequate confinement of the compression zone, and the spacing of the transverse reinforcement was similar to that observed in columns. However, the outcome was strikingly different in the case of structural walls. The performance of these elements was significantly less susceptible to proper detailing, and although some structural walls exhibited inclined cracks and crushing of the concrete in the compression zone, there were no signs of impending collapse. The stiffness of the structural walls was very effective in reducing the drift demand on the columns, as indicated by the significantly lower levels of damage observed in the buildings containing such walls.

Figure 5.46 Typical location of column splice

Figure 5.47 Typical detail for anchorage of stirrups

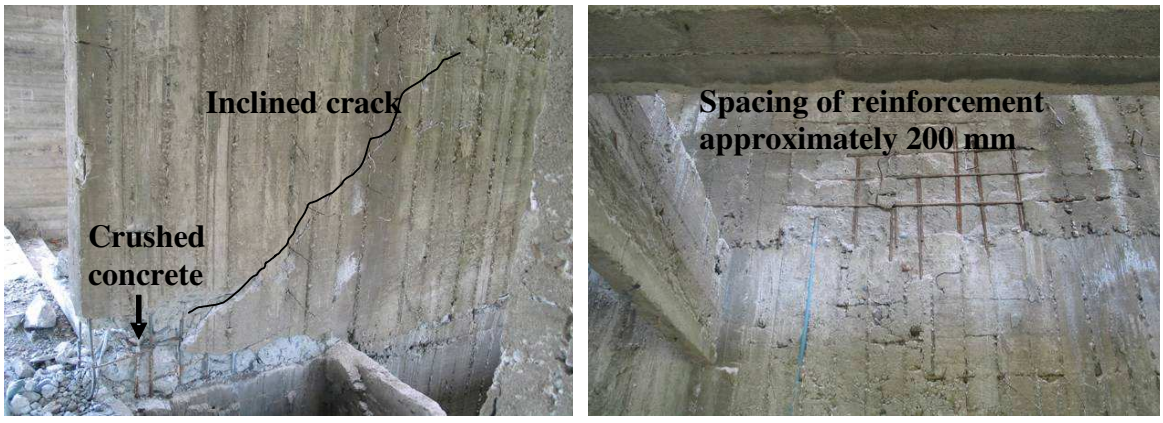

Figure 5.48 Types of damage and detailing characteristics observed in structural walls.

5.3.4.3. General observations about the performance of commercial and residential buildings

The experience provided by the Bingöl earthquake shows that there is a significant gap between the requirements established by modern seismic codes including the one in effect in Turkey and construction practice in rural areas. In the town of Bingöl this disassociation resulted in a very high toll in terms of human lives and the large number of people left homeless after the event.

Despite improvements in the fabrication of moment resisting frames over time, the current state of construction practice in this region of Turkey is not adequate for achieving collapse prevention using this type of structural system. Conversely, the performance of buildings with dual systems and structural walls was satisfactory in terms of collapse prevention. It was observed that buildings with the largest ratios of structural wall to floor area had the least amount of damage. This is because the stiffness of the lateral load resisting system was effective in reducing the drift demand and the damage to nonparticipating and nonstructural elements. Although the detailing of the walls was not in accordance with modern seismic codes, these types of structural elements showed to be considerably less sensitive to inadequate detailing practices and substandard materials.

The experience from the Bingöl earthquake showed that the state of construction practice must be an important consideration in the implementation of building regulations. In rural areas the choice of safest structural system must be consistent with local materials and construction practices. The use of systems such as moment-resisting frames, that require careful detailing and excellent construction practice to achieve the intended level of performance, must be avoided when these conditions are not likely to be met. In this case, structural systems that are less dependent on detailing to provide adequate safety against collapse should be encouraged. Finally, the clash between architectural and structural needs is another area deserving close scrutiny to ensure that structural performance is not compromised as in the case of the schools with lack of structural concrete walls.

Table 5.3 Damage characterization for lateral load resisting system

Lateral Load Resisting System Damage category	**Moment Resisting Frames**	**Dual Systems (Moment Frame – Structural Walls)**	**Structural Walls (Panel wall)**	**Total**
None	4	4	-	8
Light	4	-	2	6
Moderate	1	-	-	1
Severe	12	4	-	16
Collapse	2	-	-	2
Total	23	8	2	33

Table 5.4 Damage characterization for partition walls

Lateral Load Resisting System Damage category	**Moment Resisting Frames**	**Dual Systems (Moment Frame – Structural Walls)**	**Structural Walls (Panel wall)**	**Total**
None	1	3	2	6
Light	-	-	-	-
Moderate	5	2	-	7
Severe	15	3	-	18
Collapse	2	-	-	2
Total	23	8	2	33

Table 5.5 Inventory of Surveyed Buildings

Building Designation	**No. of Stories**	**Damage Category**		**GPS**		**Structural System**
		RC	**M**	**N**	**E**	
A-12-01	5	Light	None	38-53.796	40-31.196	Structural Walls
A-12-02	5	Light	None	38-53.810	40-31.216	Structural Walls
B-12-01	5	Severe	Severe	38-53.938	40-30.492	Moment-Frame
B-12-02	5	Light	Moderate	38-53.976	40-30.613	Moment-Frame
B-12-03	5	Severe	Moderate	38-53.951	40-30.587	Moment-Frame
B-12-04	5	Severe	Moderate	38-53.591	40-30.587	Moment-Frame
B-12-05	5	Light	Severe	38-53.591	40-30.587	Moment-Frame
B-12-06	5	Severe	Severe	38-53.844	40-30.413	Dual System
B-12-07	**4**	**Collapse**	**Collapse**	**38-53.866**	**40-31.136**	**Moment-Frame**
B-12-08	5	Severe	Severe	38-53.867	40-31.137	Dual System
B-14-01	4	Moderate	None	38-44.700	40-35.202	Moment-Frame
B-14-02	4	Severe	None	38-44.700	40-35.202	Dual System
B-14-03	3	Severe	Severe	38-64.718	40-35.329	Moment-Frame
B-14-04	3	Light	Severe	38-54.242	40-33.242	Moment-Frame
B-14-05	3	Severe	Severe	38-54.410	40-33.090	Moment-Frame
B-14-06	4	Severe	Severe	38-53.132	40-30.597	Dual System
B-15-01	4	None	Severe	38-53.137	40-30.599	Moment-Frame
B-15-02	4	Severe	Severe	38-53.134	40-30.599	Moment-Frame
B-15-03	4	Severe	Severe	38-52.588	40-29.704	Moment-Frame
B-15-04	3	None	Severe	38-54.179	40-29.305	Moment-Frame
C-12-1	5	None	Severe	38-53.970	40-30.530	Moment-Frame
C-12-2	**6**	**Severe**	**Severe**	**38-53.846**	**40-30.687**	**Moment-Frame**
C-12-3	**6**	**Collapsed**	**Collapsed**	**38-53.846**	**40-30.687**	**Moment-Frame**
C-12-4	5	Severe	Severe	38-53.987	40-30.601	Moment-Frame
C-12-5	5	Severe	Severe	38-53.979	40-30.624	Moment-Frame
C-12-6	5	Severe	Severe	38-53.982	40.30.634	Moment-Frame
C-12-7	4	None	Moderate	38-53.908	40-30.564	Dual System
C-12-8	4	None	Moderate	38-53-908	40-30.564	Dual System
C-12-9	**5**	**Severe**	**Severe**	**38-53.901**	**40-30.528**	**Moment-Frame**
C-12-10	5	None	Moderate	38-53.890	40-31.108	Moment-Frame
C-13-11	3	None	None	38-51.579	40-34.825	Dual System
C-15-04	4	Light	Moderate	38-54.216	40-29.281	Moment-Frame
C-15-05	5	None	None	38-53.138	40-29.257	Dual System

Table 5.6 Building Properties

Building Number	Structural System	Damage to RC	Damage to Masonry	Number of Stories	Floor Area (m^2)	RC Wall Area EW (m^2)	Masonry Wall Area EW (m^2)	RC Wall Area NS (m^2)	Masonry Wall Area NS (m^2)	Column Area (m^2)	Minimum WI (%)	CI
A-12-01	Panel wall	Light	None	5	332	22.49	0.00	17.42	0.00	0.00	1.05	0.00
A-12-02	Panel wall	Light	None	5	332	17.40	0.00	22.50	0.00	0.00	1.05	0.00
B-12-01	Mom-resisting frame	Severe	Severe	5	285	0.00	0.00	0.00	3.62	4.04	0.00	0.14
B-12-02	Mom-resisting frame	Light	Moderate	5	217	0.00	0.00	0.00	6.64	5.17	0.00	0.24
B-12-03	Mom-resisting frame	Severe	Moderate	5	217	0.00	6.64	0.00	0.00	5.17	0.00	0.24
B-12-04	Mom-resisting frame	Severe	Moderate	5	217	0.00	6.64	0.00	0.00	5.17	0.00	0.24
B-12-05	Mom-resisting frame	Light	Severe	5	251	0.00	6.44	0.00	1.68	6.84	0.01	0.27
B-12-06	Dual system	Severe	Severe	5	415	0.83	6.45	0.38	8.05	7.58	0.06	0.18
B-12-07		**Collapse**	**Collapse**	**4**								
B-12-08	Dual system	Severe	Severe	5	268	0.40	2.68	0.00	4.60	3.84	0.03	0.14
B-14-01	Mom-resisting frame	Moderate	None	4	192	0.00	0.00	0.00	0.00	2.84	0.00	0.18
B-14-02	Dual system	Severe	None	4	286	1.26	0.00	0.00	0.00	4.44	0.00	0.19
B-14-03	Mom-resisting frame	Severe	Severe	3	316	0.00	1.35	0.00	2.91	3.18	0.01	0.17
B-14-04	Mom-resisting frame	Light	Severe	3	134	0.00	3.37	0.00	0.00	1.20	0.00	0.15
B-14-05	Mom-resisting frame	Severe	Severe	3	258	0.00	2.04	0.00	5.13	3.94	0.03	0.25
B-14-06	Dual system	Severe	Severe	4	263	0.48	2.60	0.00	1.94	3.74	0.02	0.18
B-15-01	Mom-resisting frame	None	Severe	4	350	0.00	5.90	0.00	2.74	4.58	0.02	0.16
B-15-02	Mom-resisting frame	Severe	Severe	4	438	0.00	1.15	0.00	3.76	6.40	0.01	0.18
B-15-03	Mom-resisting frame	Severe	Severe	4	333	0.00	2.41	0.00	0.00	6.78	0.00	0.25
B-15-04	Mom-resisting frame	None	Severe	3	309	0.00	0.63	0.00	8.06	4.35	0.01	0.23
C-12-01	Mom-resisting frame	None	Severe	4	336	0.00	0.00	0.00	8.83	5.22	0.00	0.19
C-12-02	**Mom-resisting frame**	**Severe**	**Severe**	**6**								
C-12-03	**Mom-resisting frame**	**Collapsed**	**Collapsed**	**6**								
C-12-04	Mom-resisting frame	Severe	Severe	5	218	0.00	0.00	0.00	6.64	5.17	0.00	0.24
C-12-05	Mom-resisting frame	Severe	Severe	5	218	0.00	0.00	0.00	6.64	5.17	0.00	0.24
C-12-06	Mom-resisting frame	Severe	Severe	5	218	0.00	0.00	0.00	6.64	5.17	0.00	0.24
C-12-07	Dual system	None	Moderate	4	191	0.00	2.64	0.49	1.43	1.43	0.03	0.09
C-12-08	Dual system	None	Moderate	4	191	0.00	2.64	0.49	1.43	1.43	0.03	0.09
C-12-09	**Mom-resisting frame**	**Severe**	**Severe**	**5**								
C-12-10	Mom-resisting frame	None	Moderate	5	262	0.00	3.88	0.00	3.36	3.90	0.03	0.15
C-13-11	Dual system	None	None	3	194	0.90	6.16	2.52	1.65	4.76	0.26	0.41
C-15-04	Mom-resisting frame	Light	Moderate	4	336	0.00	7.11	0.00	1.73	4.75	0.01	0.18
C-15-05	Dual system	None	None	5	319	0.32	2.14	0.39	2.84	5.65	0.03	0.18

5.4 PERFORMANCE OF SCHOOL AND GOVERNMENTAL BUILDINGS

5.4.1 Introduction

The observations from earthquakes during the last decade indicated that only a fraction of existing buildings suffered severe earthquake damage while the remaining portion did not create any life-safety hazard. Unfortunately, the buildings, which suffered from the earthquakes, were mostly governmental buildings, including school buildings. This observation was also supported by the most recent earthquake in the eastern part of the country, the 2003 Bingöl earthquake. Almost 60 percent of the deaths occurred in the school buildings or at the dormitories.

The objective of this chapter is to draw and figure out the important parameters, which played significant role in contributing to the damage in school and governmental buildings. The effects of number of story, type of structure, apparent quality, and the location of the building were studied. Here it needs to be pointed out that local proper names for schools and other buildings have often been retained in the text, figures and tables for purpose of easy identification. Thus, Çeltiksuyu Primary Boarding School may also appear as Çeltiksuyu Yatılı İlköğretim Okulu.

This section reports the observations of the team sponsored by the National Science Foundation (NSF) working jointly with a team of TÜBİTAK researchers who were mainly from the Middle East Technical University (METU). As indicated earlier, a total of 68 school and government buildings in the town of Bingöl and the surrounding area were visited by the NSF-TÜBİTAK Team between May 5 and May 17. Of these buildings, 39 government buildings, among which 21 were school buildings, were investigated in detail by the TÜBİTAK team and 29 were surveyed by the NSF team. 10 buildings investigated were common to both the NSF and TÜBİTAK teams.

5.4.2 Observations of the TÜBİTAK team

5.4.2.1. Damage Distribution and Parameter Dependency

The Bingöl earthquake site was visited by the TÜBİTAK team between May 5th and May 9th, 4 days after the event. Major government and school buildings were visited for a quick condition assessment and damage evaluation. A total of thirty-nine such buildings were visited and inspection results were documented under the headings: “number of story”, “structural system”, “visual concrete quality” and “GPS coordinates”.

The building damage was categorized under three levels, namely light/none, moderate and heavy/collapse. In assigning the damage state to the structural system of the building the methodology described in Section 5.3.3.1 was used.

The number and distribution of the buildings selected from a representative subset of the general building population for the building type of interest. Among these buildings only two of them were masonry type structures. Both of these structures were used as school buildings. Seventeen buildings were Reinforced Concrete Frame (RCF) with Masonry infill Walls, and the remaining twenty buildings were Reinforced Concrete Frame with Shear Walls (RCSW). The construction year of only a few of the structures could be determined. Nevertheless none of the structures were built according to the latest version of the Turkish Seismic Code (1998 version). An overall summary that contains observed damage, structural system, number of floors and apparent material quality of the buildings surveyed is given in Table 5.7. In Table 5.7 school buildings are shown in bold letters. The cells that are filled indicate the school buildings that are common to both NSF and TÜBİTAK teams; the NSF team’s designations are shown in the parenthesis. The rest are other government buildings including Police Stations, Telecommunication Buildings, Gendarme Buildings and Hospitals. Among the investigated buildings, 5 were heavily damaged, 13 were moderately damaged, and 20 were lightly

damaged.

Table 5.7 Observed buildings summary

Building Name	Const. Year	No of Floors	Type	Apparent Quality	Damage
Anadolu Güzel Sanatlar Lisesi	NA*	2	Masonry	NA	Light
Fatih İlköğretim Okulu	1971	2	Masonry	NA	Moderate
Karayolcular Koop A-Blok	1996	5	RCF	average	Light
DSİ İdari Bina	1983	2	RCF	poor	Light
100. Yıl İlköğretim Okulu	NA	4	RCF	NA	Light
Atatürk İlköğretim Okulu	1995	3	RCF	average	Light
YIBO - Yatılı Bölge İlköğretim (D-17-04)	NA	4	RCF	poor	Light
Bingöl Anadolu Lisesi	NA	3	RCF	good	Light
Ticaret Lisesi	NA	4	RCF	NA	Light
75_Yıl İlköğretim (C-13-01)	NA	3	RCF	good	Moderate
İl Halk Kütüphanesi	NA	3	RCF	poor	Moderate
Türk Telekom	1975	3	RCF	poor	Moderate
DSİ Lojman	1984	3	RCF	poor	Moderate
Anadolu Kız Meslek Lisesi	NA	3	RCF	poor	Moderate
Sarayiçi İlköğretim Okulu (C-15-01)	1998	4	RCF	poor	heavy/collapse
Teknik Lise ve E.M.L.	1965	2	RCF	poor	heavy/collapse
Çeltiksuyu Yatılı İlköğretim Okulu	NA	3	RCF	average	heavy/collapse
Kaleönü İlköğretim Okulu	NA	3	RCF	average	heavy/collapse
Karaelmas İlköğretim Okulu (C-14-01)	NA	3	RCF	poor	heavy/collapse
Gazi İlköğretim okulu	NA	3	RCSW	good	Light
Şehit Mustafa Gündoğdu İlköğretim (C-13-05)	1994	2	RCSW	NA	Light
PTT	1990	5	RCSW	good	Light
Bingöl Devlet Hastanesi	NA	6	RCSW	good	Light
Bingöl İl Sağlık Müdürlüğü	NA	4	RCSW	NA	Light
Hükümet Konağı	1980	4	RCSW	good	Light
Rekabet Kurumu Lisesi (C-13-03)	NA	4	RCSW	NA	Light
Mustafa Kemal Paşa İlköğretim Okulu (C-13-04)	NA	3	RCSW	good	Light
Kredi Yurt Kur Bingöl Yurt Müd.	NA	2	RCSW	average	Light
Emniyet Müdürlüğü	NA	6	RCSW	good	Light
Jandarma İl komutanlığı	NA	5	RCSW	poor	Light
Bayındırlık Binası	NA	5	RCSW	good	Light
Sigorta İşleri Genel Müdürlüğü	NA	5	RCSW	poor	Moderate
Özel Harekat Binası	NA	3	RCSW	poor	Moderate
Anadolu Öğretmen Lisesi (C-13-02)	1974	2	RCSW	poor	Moderate
Belediye	1990	5	RCSW	average	Moderate
TEDAŞ	NA	4	RCSW	poor	moderate
Ziraat Bankası	1990	4	RCSW	good	moderate
Öğretmen Lisesi Ek bina (C-13-02)	NA	3	RCSW	poor	moderate
Bingöl Lisesi (C-14-08)	NA	4	RCSW	poor	heavy/collapse

* NA. Not available or could not be determined

The GPS coordinates taken from each building are used to plot the building locations on a city map. First a digital map of the Bingöl downtown area was prepared and then GPS coordinates of the buildings are placed on that digital map in a commercial computer program Arc-View. The locations of the surveyed buildings with assigned damage levels are given in Figure 5.49. In that figure the red point on the very far right bottom corner belongs to Çeltiksuyu Yatılı İlköğretim Okulu [Çeltiksuyu Primary Boarding School]. Another school building called Kaleönü İlköğretim Okulu [Kaleönü Primary School] is on the right upper corner of the figure. These two school buildings were

perfectly identical (in terms of number of story, type of structural system, apparent quality, plan of the building, orientation of the building), and they had an identical damage pattern. As this observation helps to eliminate the randomness of the damage patterns, it is believed that the effect of soil conditions is not of importance and the structural system and configuration govern the observed damage.

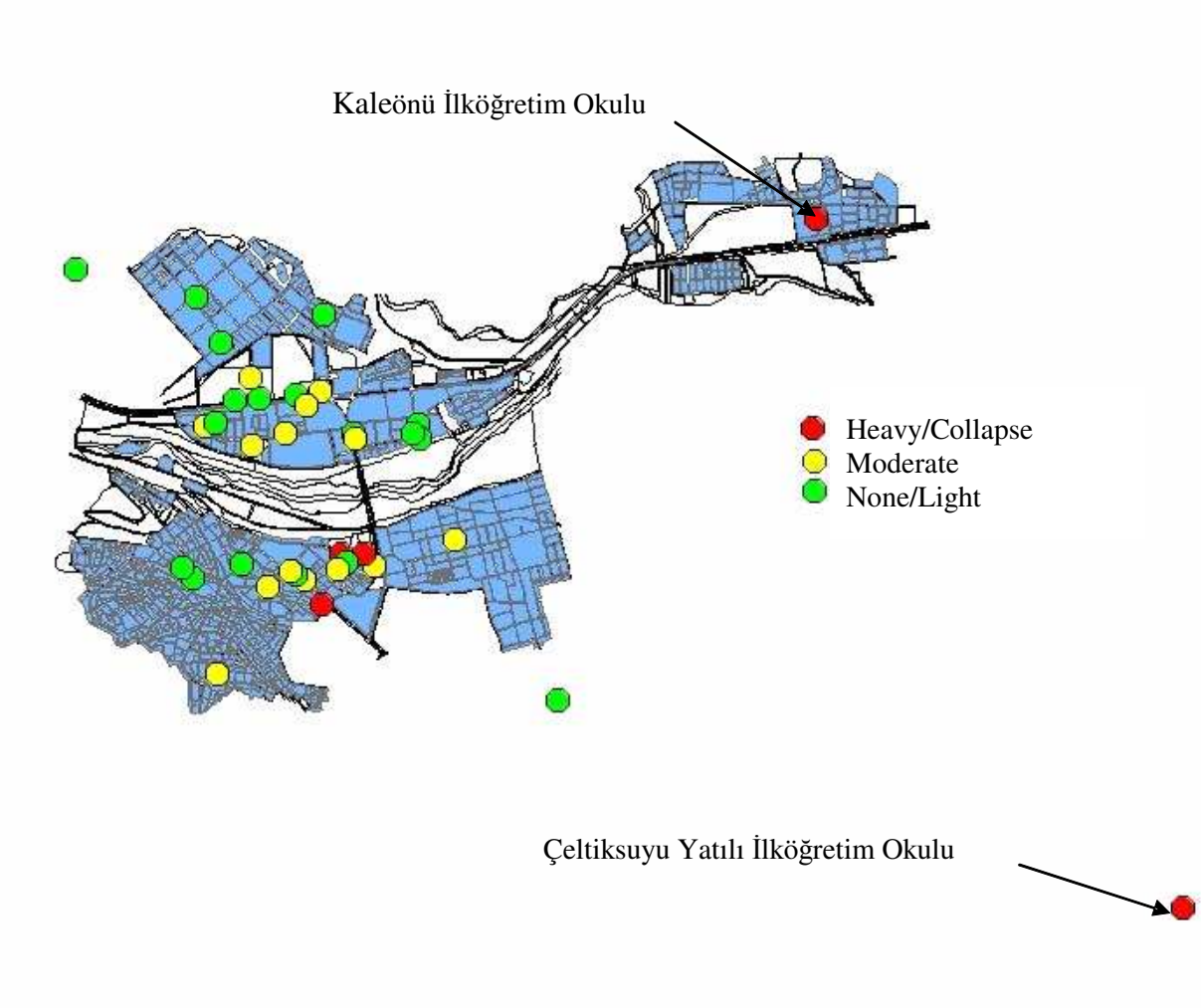

Figure 5.49 Selected building locations and the damage distribution

In Figure 5.50 distribution of the number of stories for the observed buildings is given. As is seen most of the observed buildings are mid-rise structures (3-6 story), only seven buildings are low-rise. Among these seven low-rise buildings two are masonry type, two buildings are of the reinforced concrete frame type and the remaining three are reinforced concrete frame with shear wall (Dual system) structures. Of the mid-rise buildings fifteen are reinforced concrete moment resisting frame types and the remaining seventeen are reinforced concrete frame with shear wall type.

In Figure 5.51 the relationship between the material quality and the damage observed is given. As expected, there is a good correlation between these two, even if this sole parameter may not be an indicator. When the material quality is poor the possibility of a severe damage in a building is very high. On the other hand when the material quality is good, none of the buildings studied suffered collapse or heavy damage. The majority of the buildings with observed good material quality had light damage and only a few were moderately damaged.

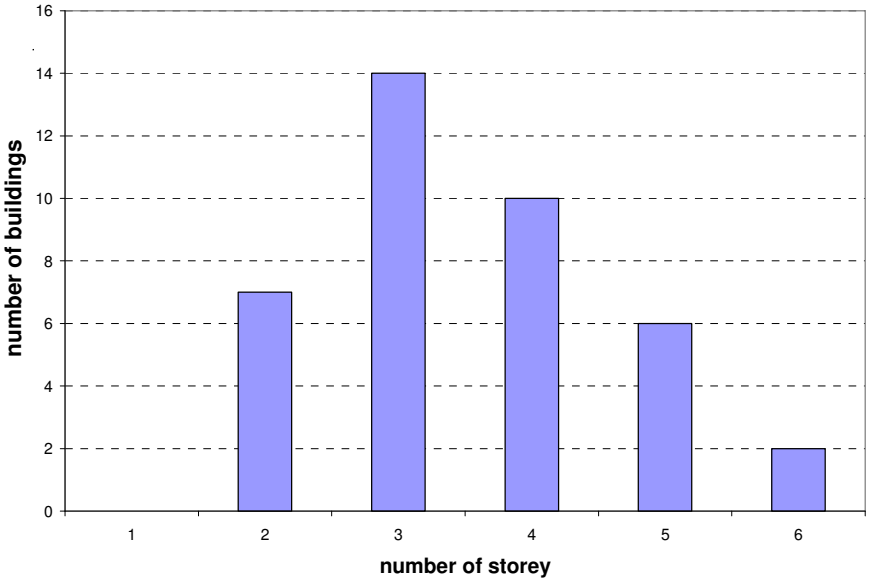

Figure 5.50 Number of story distribution of the observed buildings

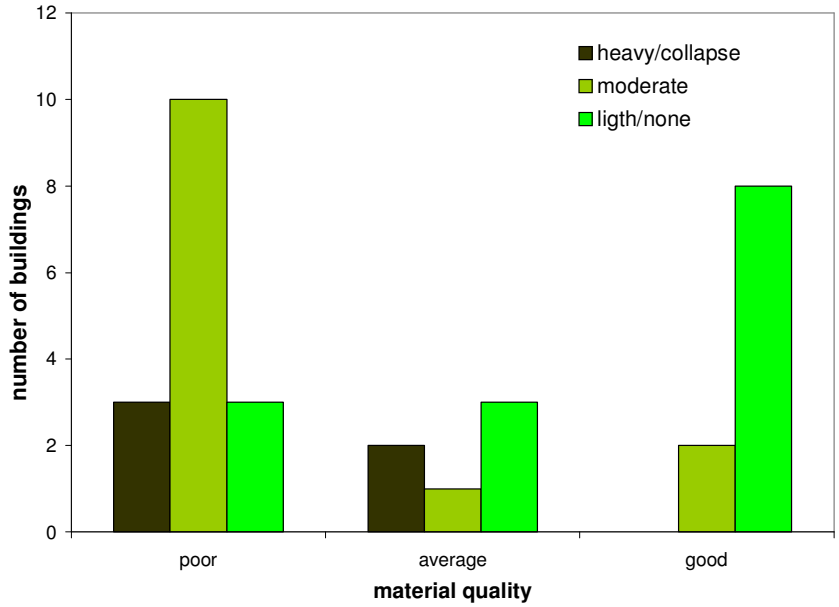

Figure 5.51 Material quality versus damage distribution

5.4.2.2 Damage Observations

The common characteristics of construction practice in Bingöl resulted in some typical damage patterns observed in many buildings. Soft story collapse, shear failure in short/captive columns, shear walls and infill walls, damage at the column ends, spalling and crushing of concrete in reinforced concrete members, separation of infill walls from encasing frames were widespread damage patterns observed. As in other major earthquakes in Turkey, school buildings were among the most seriously affected structures.

In this earthquake, the most tragic collapse occurred at Çeltiksuyu Yatılı İlköğretim Okulu [Çeltiksuyu Primary Boarding School] which was a primary school (Figure 5.52) with a dormitory (Figure 5.53). Since the earthquake occurred at 3:27 a.m. local time, the majority of the students were asleep inside the collapsed dormitory in which 84 (out of 195) students and 1 teacher lost their lives. In Figure 5.54, on the same block there appears a 3-story building, which was used by the teachers for

accommodation. As is seen, there was no damage observed in that building (Figure 5.54). Therefore the explanations of the damage implying the effect of soil conditions seem unreasonable.

Figure 5.52 Çeltiksuyu Yatılı İlköğretim Okulu, school building

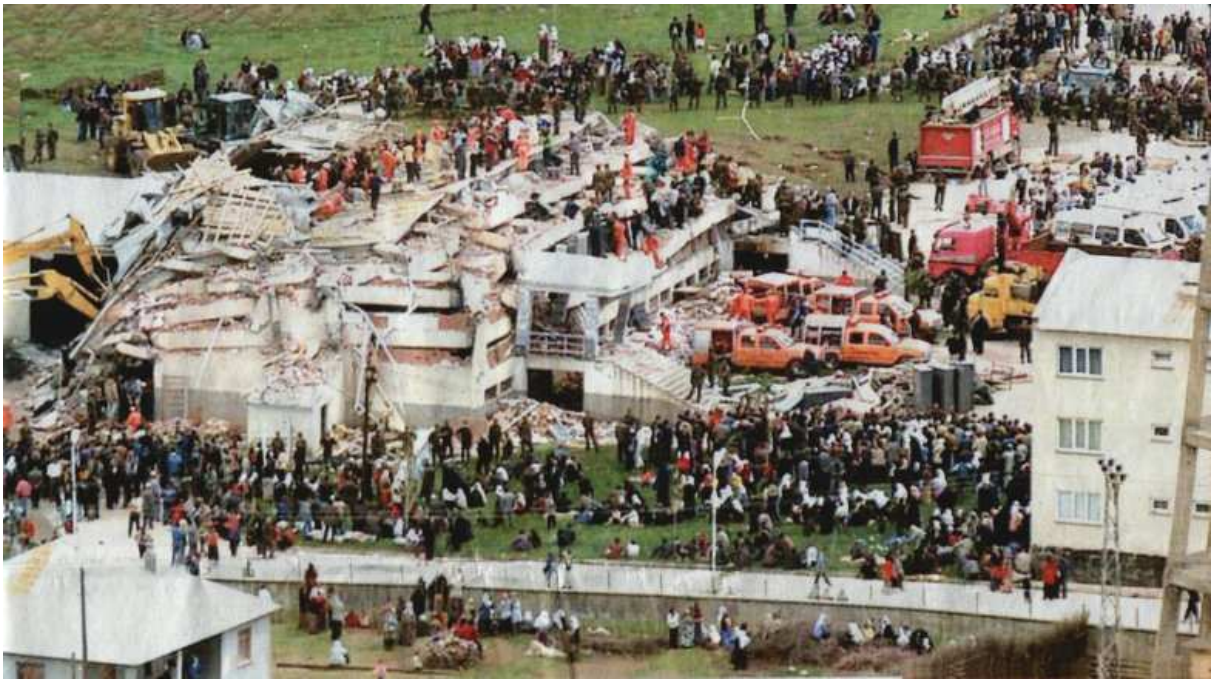

Figure 5.53 Çeltiksuyu Yatılı İlköğretim Okulu, dormitory building (Akşam newspaper)

Figure 5.54 Çeltiksuyu Yatılı İlköğretim Okulu, teachers accommodation building

Another school building which had the same number of stories, type of structural system, apparent quality, plan of the building, and same orientation with the Çeltiksuyu İlköğretim Yatılı Okulu was the Kaleönü İlköğretim Okulu. As is seen in Figure 5.55, both school buildings had the same damage although the soil conditions were different. Similar to the case of the Çeltiksuyu İlköğretim Yatılı Okulu office building, there was no damage at all in the Kaleönü İlköğretim Okulu office building (Figure 5.56).

Figure 5.55 Kaleönü İlköğretim Okulu, school building

Figures 5.57 and 5.58 show a conventional four-story reinforced concrete frame and shear wall building used as a government bank. Although the building has a soft story (Figure 5.58) it experienced light damage indicating that the load-resisting elements performed very well. The apparent material quality was good, and the resistance to lateral loads was mainly provided by the shear walls. The infill walls are composed of conventional hollow clay tile used in practice for partition walls. Diagonal cracks appear on the nonstructural components, i.e. masonry infill walls (Figure 5.58).

Figure 5.56 Kaleönü İlköğretim Okulu, office building

Figure 5.57 Ziraat Bankası (State Agricultural Bank)

Figure 5.58 Diagonal cracks on partition walls (Ziraat Bankası, State Agricultural Bank)

Another conventional four-story reinforced concrete frame and shear wall government building with poor apparent material quality is TEDAŞ (Figures 5.59 and 5.60). This building is the branch office of the Turkish Electricity Distribution Company. The building experienced moderate damage indicating that load-resisting elements performed well with respect to life-safety. The resistance to lateral loads was mainly provided by the shear walls and there was no damage in these shear walls. On the other hand, columns suffered moderate to heavy damage. The building has several inadequacies against lateral loads like strong beams-weak columns, short columns (Figure 5.60), and insufficient transverse steel (Figure 5.61). In Figure 5.62 a corner of the structure is shown. As is seen the end zone of the column was inadequately confined and damage has occurred due to the short column effect created by window openings in the hollow clay brick infill walls.

Figure 5.59 TEDAŞ Bingöl branch

Figure 5.60 TEDAŞ Bingöl branch, short column effect

Figure 5.61 TEDAŞ Bingöl branch, inadequate confinement at column ends

Figure 5.62 TEDAŞ Bingöl branch, damage in column end zone due to short column effect

In Figure 5.63, a high school building, Bingöl Lisesi is shown. This building is also a four-story reinforced concrete frame with shear wall structure. However its apparent material quality and the lateral reinforcement were poor. As a result the structural system suffered heavy damage. A spectacular example of the diagonal shear crack and crushing of the concrete core in the shear wall due to a combination of inferior material quality and inadequate transverse reinforcement is shown in Figures 5.64 and 5.65. As may be observed, the resulting gap in the shear wall easily enabled the entry of a human hand. Although the shear walls were heavily damaged their presence prevented the total collapse of the building. Also, there are diagonal shear cracks in the nonstructural members which suffered light damage (Figure 5.66).

Figure 5.63 Figure 5.63. Bingöl Lisesi, high school building

Figure 5.64 Bingöl Lisesi, school building, core concrete crushing and resulting gap in the shear wall

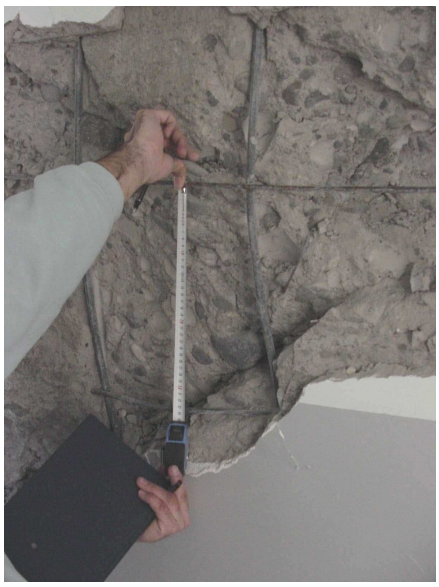

Figure 5.65 Bingöl Lisesi, school building, inadequate lateral reinforcement in the shear wall (spacing is greater than 30 cm.)

Figure 5.66 Bingöl Lisesi, school building, diagonal cracks in the infill masonry walls

5.4.2.3 Summary

Most of the government buildings in Bingöl suffered moderate to heavy damage during the May 1st 2003 Bingöl earthquake. A large number of children lost their lives due to preventable mistakes made in the construction practice in Bingöl. Reinforced concrete buildings having poor concrete quality, inadequate detailing of both longitudinal and transverse reinforcement and improper structural configurations like soft story and short/captive column experienced heavy damage or total collapse.

The soil properties at the site and the proximity to the earthquake source might have played some roles for localized damage in certain buildings, but the striking difference in the performance of very similar adjacent buildings enhances the importance of other factors pertaining to the construction. One such case is shown in Figures 5.52 to 5.54 where the school building suffered heavy damage, the dormitory collapsed totally but the adjacent teacher accommodation house had no damage at all. The construction quality and technical inspection of the undamaged building is much superior to the damaged one as observed by the TÜBİTAK team and confirmed by local people who had witnessed the construction of these buildings.

Parameters obtained by visual inspection show promising correlations with the recorded damage states, pointing to increased chances of identifying damage prone structures and damage estimation prior to a possible earthquake.

5.4.3 Observations of the NSF team

The team visited 27 schools and dormitory buildings in Bingöl and its close vicinity, one school in Ilıcalar (20 km away from Bingöl) and one school in Sancak (25 km away from Bingöl) between May 13 and May 17 (Figure 5.67). The complete list of the schools is given in Table 5.8.

The structural system of the schools can be grouped as:

1) RC Moment resisting frame systems (17 buildings)
2) RC Dual systems (11 buildings)
3) Masonry (1 building, not surveyed)

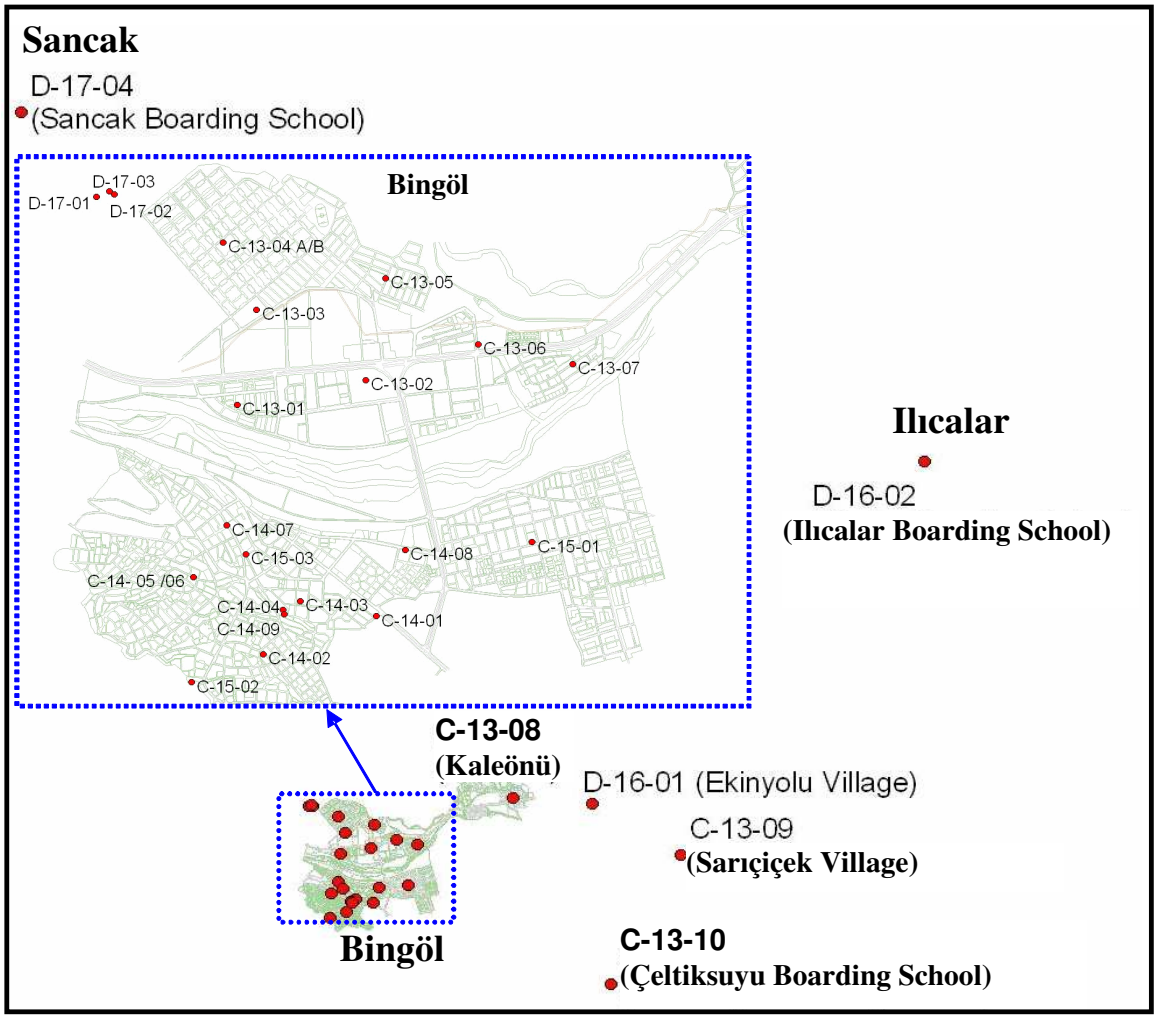

Figure 5.67 The location of the school and dormitory buildings surveyed.

5.4.3.1. School Buildings with RC Moment-Resisting Frame System

Of the 17 buildings in this category, 16 had the same column layout (Figure 5.68 and 5.69). As the floor plan indicates, the lateral load resisting system in these buildings can be categorized as regular in plan. The majority of the columns were aligned in regular bays, and most of the beams framed into columns. The dimensions of the columns in the buildings were typically 0.3m x 0.5m. The orientation

of the columns was the same in all buildings, with the exception of a corner column in building C-13-01. The locations of the masonry infill walls varied depending on the use of the space in these schools. The exterior masonry walls were typically thicker than the interior walls.

The only school building with a different column layout was C-13-02. The school complex was a combination of two separate buildings. The separation afforded by the expansion joint between the two buildings was not sufficient to avoid pounding between the two structures. The floor plan of the northern building is shown in Figure 5.70. All the columns shown in the figure have dimensions of 0.2m x 0.5m.

The total column area of buildings with moment-resisting frames was approximately 1 percent of the floor area, regardless of the number of floors. Consequently, the performance of the structures during the earthquake was significantly influenced by the number of floors. The level of damage of the lateral load resisting system with respect to the number of floors can be categorized as follows:

1) 5 two-story schools: 4 moderately damaged, 1 lightly damaged
2) 11 three-story schools: 3 collapsed, 6 severely damaged, 2 moderately damaged
3) 1 four-story school: severely damaged.

Damage to the masonry walls was rated separately. The three- and four-story buildings typically sustained severe masonry wall damage (Table 5.6). This indicates that earthquake placed a significant displacement demand on these structures.

There were several construction and structural design deficiencies commonly observed in the school buildings. In most of the structures surveyed, the quality of construction practices was uniform. Specific problems noted were:

1) Use of unwashed aggregate,
2) Use of aggregates with large maximum size (up to 10 cm),
3) Use of undeformed bars,
4) Inadequate preparation of cold joints.

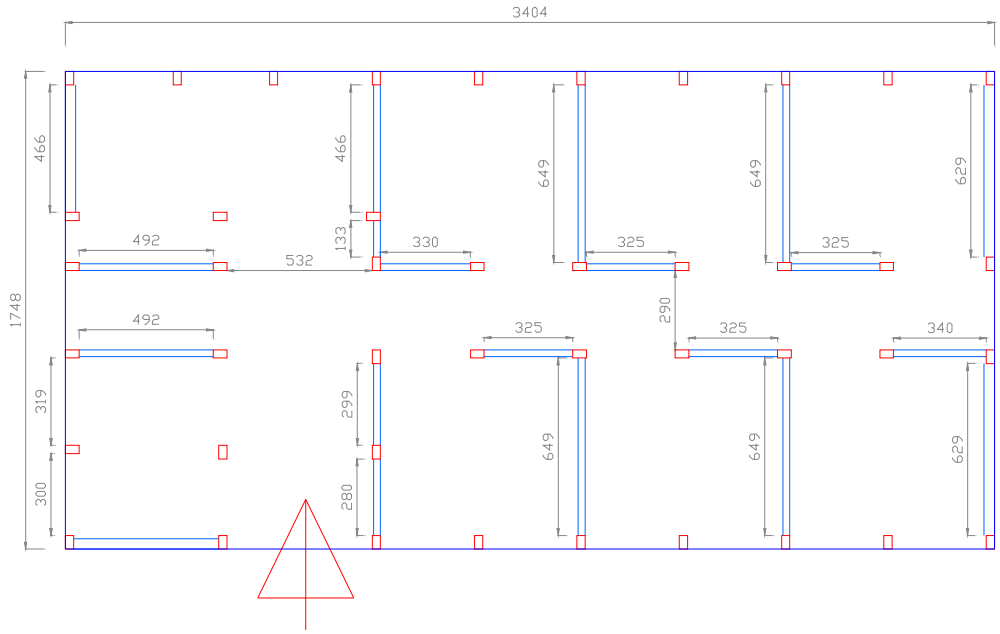

Figure 5.68 Typical school plan without shear walls. All the walls shown in the drawing refer to those occupying a full span. Walls with openings are excluded. All the columns have dimensions of 0.3m x 0.5m. The arrow indicates the entrance to the building. Dimensions are in cm.

One of the most common structural problems observed in these buildings was the presence of captive columns, which made the structures vulnerable to shear failures. In almost all the schools, openings for small windows in the furnace room and restrooms were placed adjacent to columns. The exterior rectangular columns were oriented with the strong axis resisting moments in the short direction of the building layout in Figure 5.68. Therefore, windows on the exterior walls in the long direction of the building exposed columns to shear forces acting perpendicular to their weak axis for bending (Figure 5.71). It was observed also that crushing of the masonry walls in the upper corners created captive columns (Figure 5.72).

In the school buildings that were visited the detailing of structural members was inadequate with respect to requirements of modern seismic codes. Lack of confinement in plastic hinge regions of the columns was observed to be one of the most significant causes of damage. Even though the spacing of the stirrups was reduced in the end regions of some columns, the amount of transverse reinforcement provided was not sufficient to prevent shear failures, particularly in the case of captive columns (Figure 5.73). Another detailing deficiency commonly observed was the inadequate anchorage of the free ends of the stirrup reinforcement.

Figure 5.69 School buildings with typical floor plan. Column dimensions are the same regardless of the number of floors.

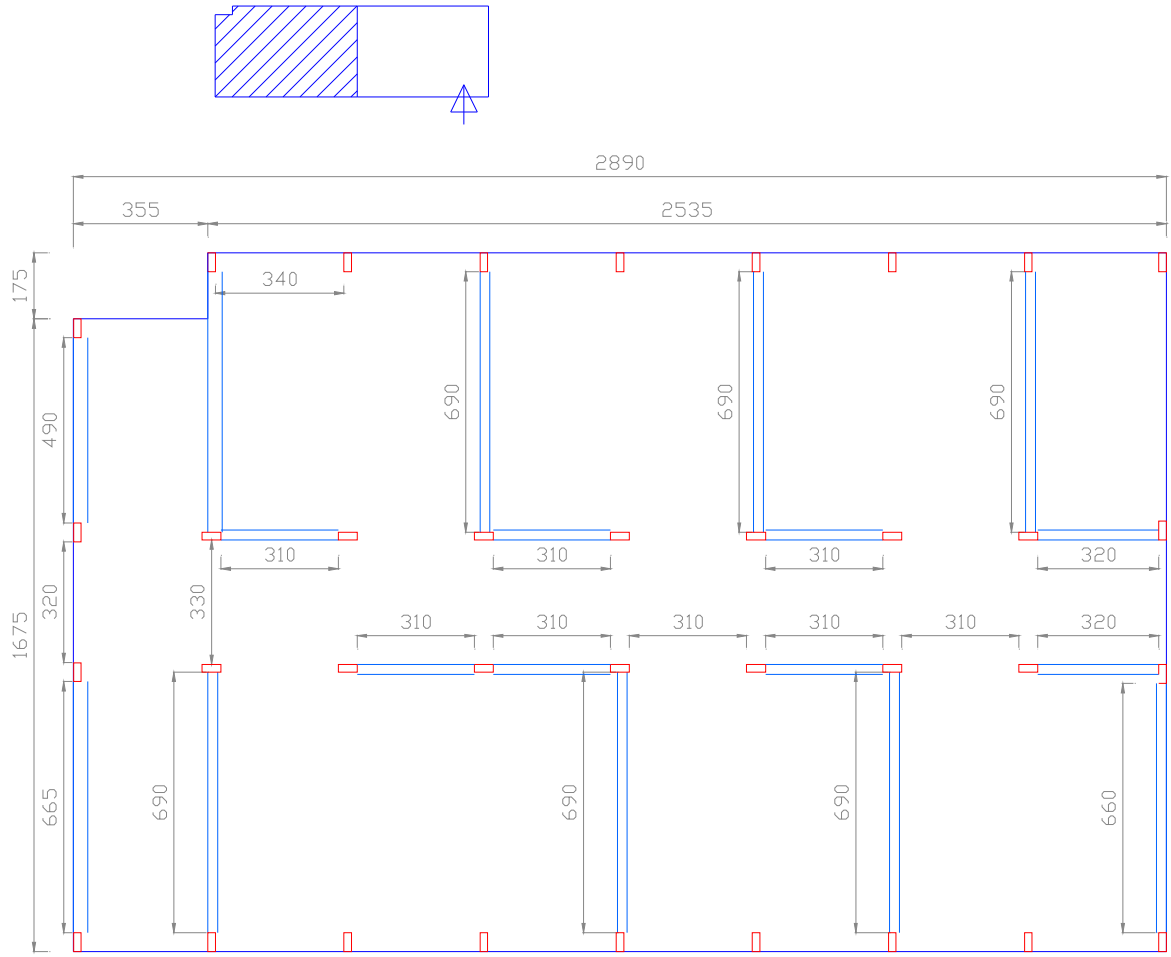

Figure 5.70 The floor plan for C-12-02. The structural system is a moment-resisting frame. The columns are 0.2m x 0.5m. The school building comprises two independent structures separated by an insufficient expansion joint. Only the shaded part in the upper figure was surveyed. The arrow indicates the entrance to the building. The dimensions are in cm.

Figure 5.71 Shear failure of captive columns created by the small windows of the furnace room in building C-14-03.

Figure 5.72 Shear failure of captive columns as a result of crushing of upper corner of masonry walls in building C-14-01.

Figure 5.73 Typical confinement detail of a column in building C-13-09. The shear failure in the columns initiated the collapse of the first floor. The spacing of the transverse reinforcement is 10 cm at the top 30-cm portion of the columns. The ends of the stirrups were not anchored properly.

5.4.3.2. School and Dormitory Buildings with Dual Systems

The schools with dual systems surveyed can be categorized into four groups.

Buildings C-13-04A and C-13-04B

These buildings were part of the same school complex comprising five different structures separated by expansion joints. Buildings C-13-04A and C-13-04B had a similar lateral load resisting system, shown in Figure 5.74. The only difference between the buildings was the location of masonry walls. The total shear wall area of the structure in the longitudinal and transverse directions was 1.4 and 2.0 percent of the floor area, respectively.

There were no indications of structural damage in the buildings, and the masonry walls were only lightly damaged.

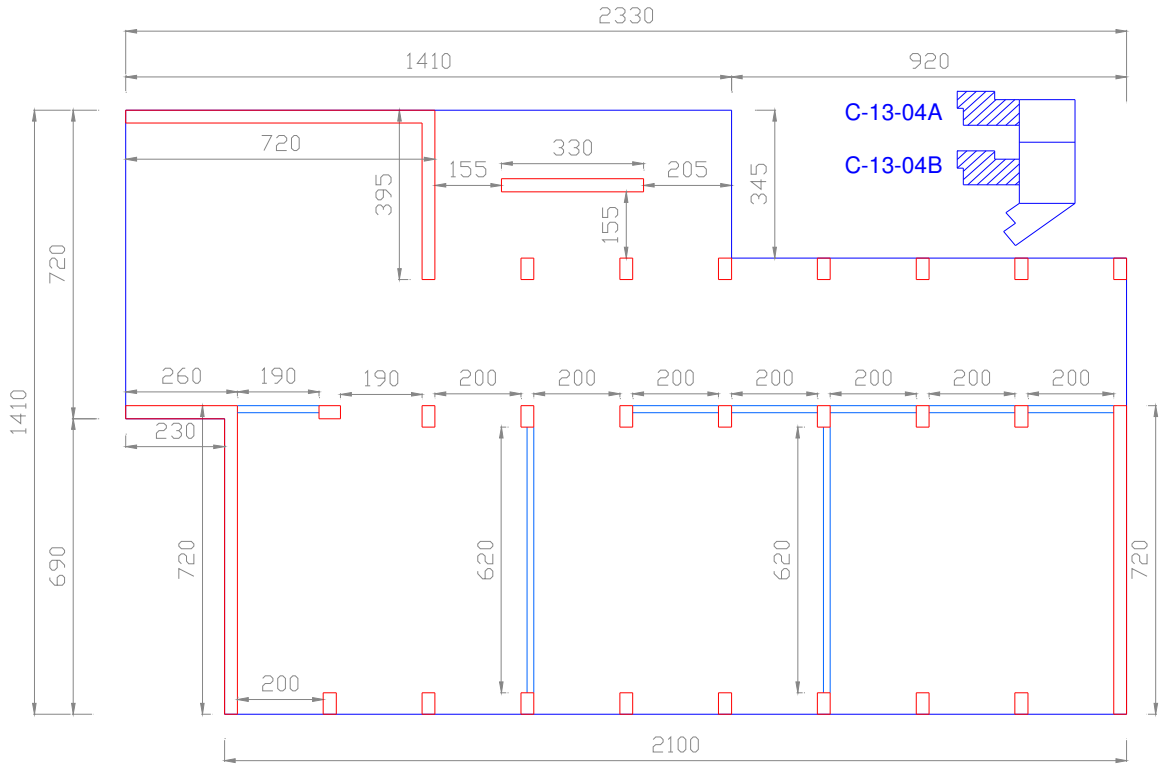

Figure 5.74 Structural floor plan for building C-13-04A. All the columns have dimensions of 0.3m x 0.5m. The thickness of the reinforced concrete and masonry walls were 0.3m and 0.16m, respectively. Dimensions are in cm.

Buildings C-13-03, C-14-08, C-14-09 and C-15-03

Each one of these buildings is one structure of a three-structure complex that conforms to the plans for a typical high school building commonly used by the Ministry of Education of Turkey. Each of the buildings is a four-story structure. Although the buildings C-14-09 of C-15-03 are smaller than the other two, the structural plans of all four are similar. The main difference is that the smaller buildings have two fewer bays in the longer direction. The total column area was 1.5 percent of the floor area for all the buildings. The ratio of shear wall area to area of the floor was not uniform. Building C-14-08, which had the smallest ratio of shear wall to floor area, had a wall area of 0.7 percent and 0.4 percent of the total floor area in the two principal directions (Figure 5.75). The highest ratio of wall to floor area was found in building C-13-03 (Figure 5.76).

The most severe damage in this group was observed in C-14-09. A cold joint in one of the shear walls in the structure initiated a horizontal crack along the joint during the earthquake. Although the rest of the structural members did not show any sign of damage, the building was classified to be severely damaged because of the damaged shear wall. The masonry walls of the building did not suffer any severe damage.

In building C-14-08, damage to the structural system is confined to significant crushing of concrete in the shear walls as shown in section 5.4.2.2. There was no damage observed in the columns and a few beams had severe flexural cracks. The structural system of this building was rated as severely damaged. The masonry walls were separated from the structural frame because of crushing of the bricks at the edge of the walls. There was no partial or full collapse of the masonry walls.

Buildings C-13-03 and C-15-03 with higher shear wall ratios than the other two (ratio of wall to floor area) had only moderate damage to their structural systems and the masonry walls.

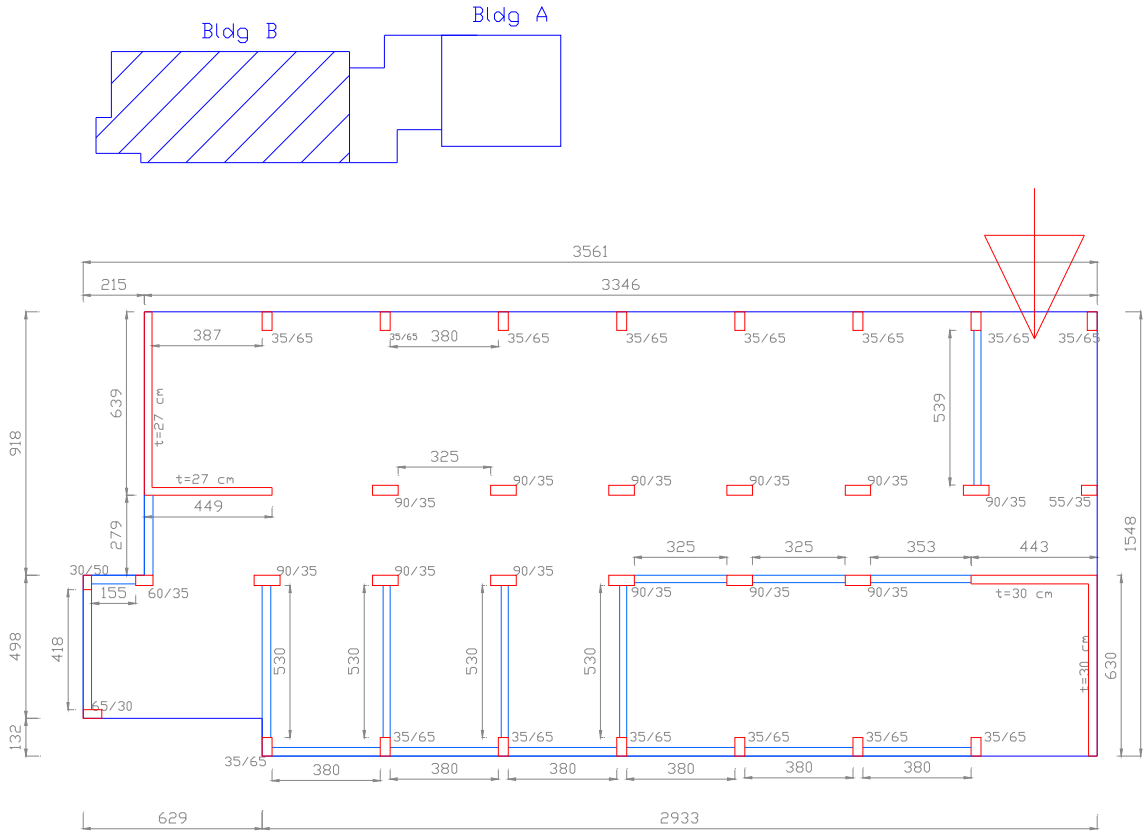

Figure 5.75 Structural floor plan for building C-14-08. The thickness of interior and exterior masonry walls were 0.25m and 0.3 m, respectively. The arrow shows the entrance to the building. Dimensions are in cm.

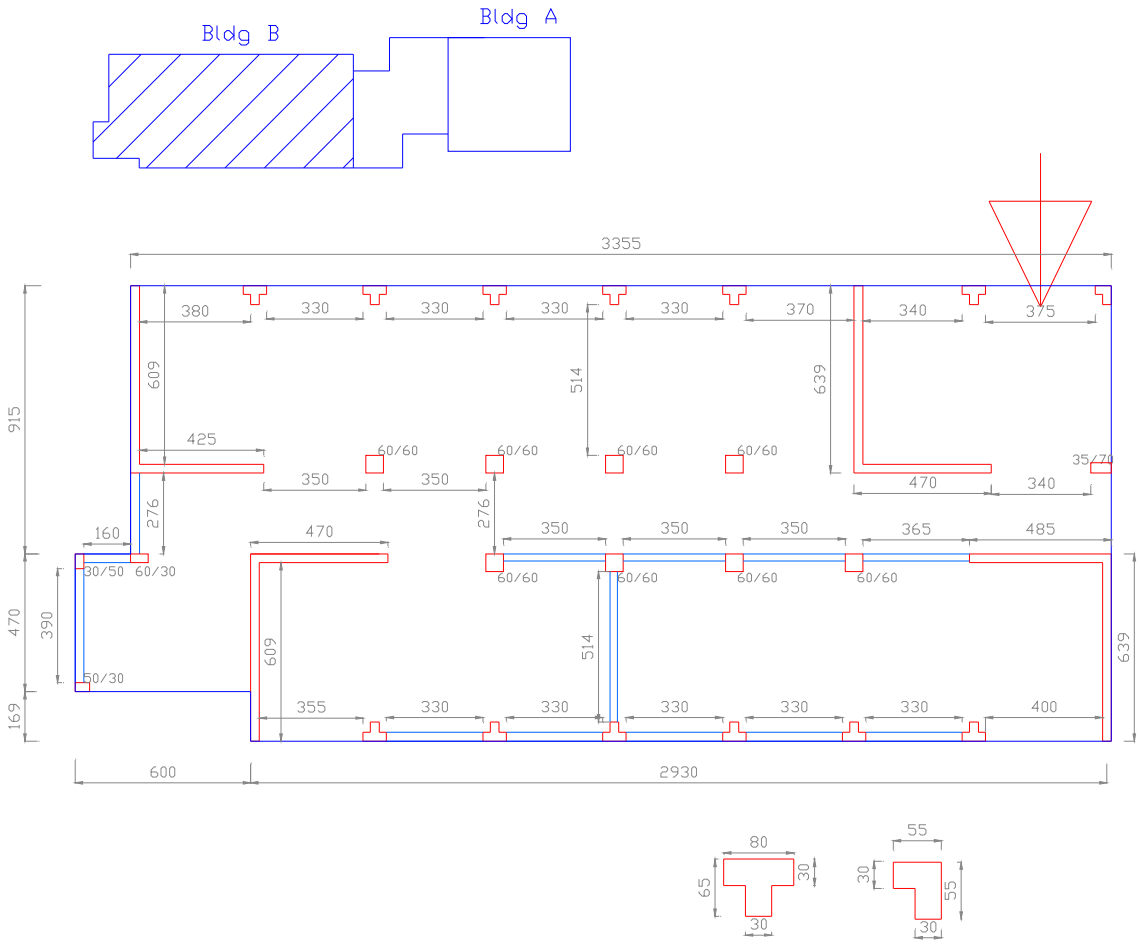

Figure 5.76 Structural floor plan for building C13-03. The thickness of the shear walls was 0.3m. The masonry wall thickness was 0.25m for the interior walls and 0.3m for the exterior walls. The arrow shows the entrance to the building. Dimensions are in cm.

Building C-17-03

Building C-17-03 had another structure adjacent to its west end. Although the buildings were separated by an expansion joint, the gap provided between the two was very small. Building C-17-03 had 4 stories. The total column area was 1.1 percent of the floor area. The area of shear walls was 0.8 and 1.0 percent of the floor area in the longitudinal and transverse directions respectively. The structural floor plan of the building is shown in Figure 5.77.

Damage to the structural system and the masonry walls were both rated as moderate. There were no inclined cracks observed in the columns or shear walls. There was some local damage to members in the form of spalling of concrete cover as a result of construction defects.

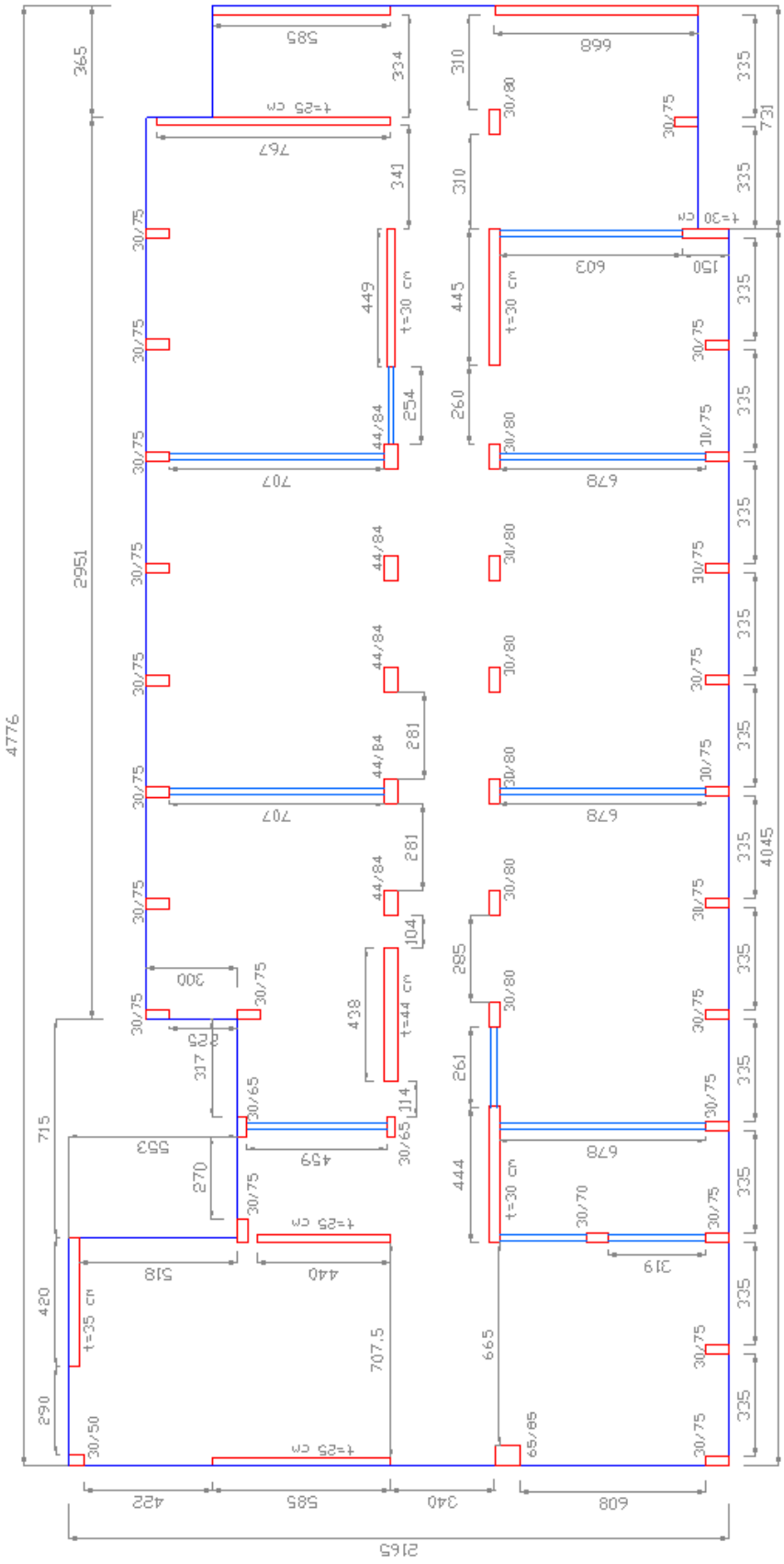

Figure 5.77 Structural floor plan for building C-17-03. Masonry wall thickness was 0.19m. Dimensions are in cm.

Dormitory Buildings (D-16-02, D-17-01, D-17-02 and D-17-04)

These buildings did not have any other structures adjacent to them. They had identical floor plans shown in Figure 5.78, and all of them were four-story structures. The structural system of these schools had a column area of 0.7 percent of the floor area, and wall areas of 1.0 percent and 1.5 percent of the floor area in the two principal directions.

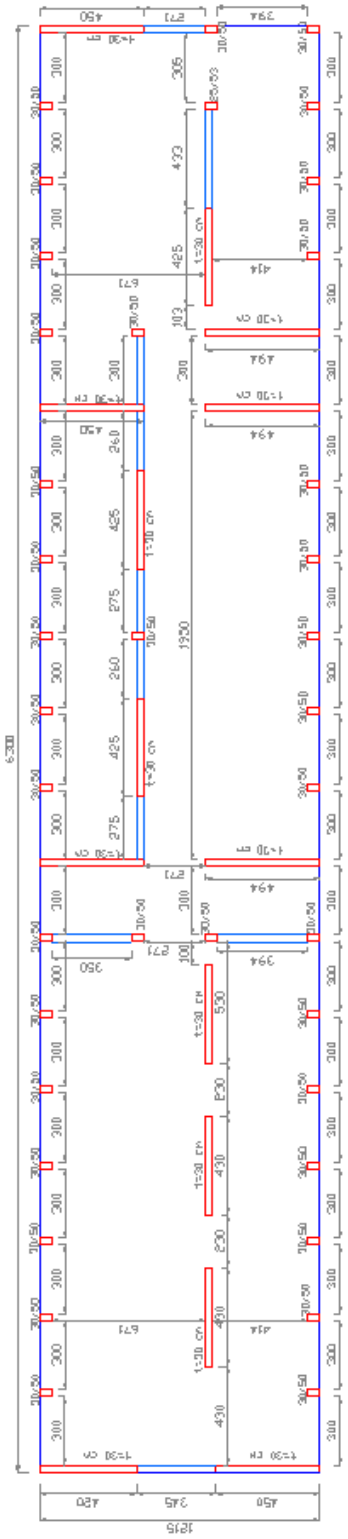

Figure 5.78 Structural floor plan for dormitory buildings. The masonry wall thickness was 0.3m. Dimensions are in cm.

Of the four dormitory buildings that were surveyed, the structural systems of two of them, D-17-01 and D-17-02, were rated as severely damaged because of the inclined cracks on the captive columns. There were also inclined hairline cracks on the shear walls. Some of the beams had flexural and shear cracks, and damage was commonly observed in beams that framed into other beams as opposed to columns.

Because buildings D16-02 and D-17-04 had inclined hairline cracks on shear walls and shear and flexure cracks on beams the damage to them was rated as moderate.

The most striking damage in these buildings was the collapse of the free standing masonry walls separating the sleeping units in the upper levels. These walls were not included in the damage rating because they were unattached to the structural system. However, they presented a serious hazard to the students living in these dormitories because in some cases the walls collapsed on the beds (Figure 5.79). Fortunately the collapse of the walls did not result in any fatalities because almost all the beds so affected were happened to be unoccupied.

Figure 5.79 Collapse of the free standing masonry walls onto the beds in the dormitory buildings.

5.4.3.3. Comparison of the Performance of the Frame and Dual Systems

For the purpose of comparing the performance of both groups of school buildings, the damage assessments were categorized using the procedure proposed by Hassan and Sozen (1997). The wall and column indexes in this procedure are defined and calculated as given in Section 5.3.3.2. The wall index is calculated for both main horizontal axes of the buildings, and the smaller of the two is taken as the wall index for the given building.

The wall and column indexes calculated for the school and dormitory buildings in Bingöl are given in Table 5.9. The correlation between the damage category of the buildings and the wall and column indexes are presented in Figure 5.80. As the figure shows, the damage level tended to decrease as the wall and column indexes increased.

Damage observations in the buildings indicate that the performance of buildings with dual systems was satisfactory. Even though some of the dual system buildings were rated as severely damaged because of the damage caused by structural defects such as captive columns and cold joints, observed damage to the masonry walls indicate that the reinforced concrete walls were effective in maintaining the lateral drift below a reasonable limit. Buildings with moment-resisting frame systems did not perform as well during the earthquake. Although the quality of construction is quite uniform for all the buildings, frame systems were more vulnerable to damage associated with deficiencies in construction practice. The flexibility of moment frame buildings resulted in larger drift demands than those in buildings with dual systems, which caused severe damage and in many cases the collapse of the structure. The damage level of infill masonry walls in moment frame buildings that were severely damaged supports the conclusion that the drift demand was excessive. The shear damage to columns was very severe in buildings with moment resisting frames.

Based on the damage assessment of these buildings, a boundary for the minimum column and wall indices for satisfactory performance is shown in Figure 5.80.

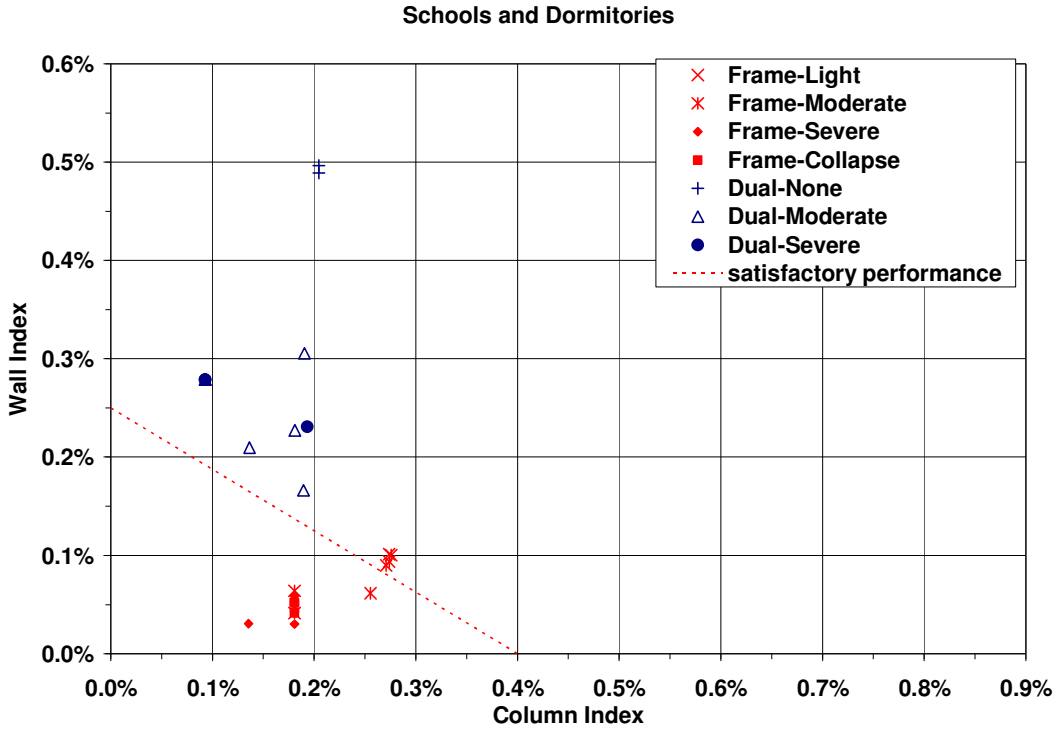

Figure 5.80 Correlation between the structural performance and the wall and column indexes defined by Hassan and Sozen (1997).

Table 5.8 List of the school and dormitory buildings visited

School ID	Name	Location	GPS N	GPS E	Type	Position
C-13-01	75. Yıl İlköğretim Okulu	Bingöl	38 53.665	40 29.565	Frame	Independent bldg
C-13-02	Anadolu Öğretmen Lisesi	Bingöl	38 53.745	40 30.749	Frame	Dependent bldg
C-13-03	Rekabet Kurumu Lisesi (Building B)	Bingöl	38 54.001	40 29.660	Dual	Dependent bldg
C-13-04A	Mustafa Kemal Paşa İlköğretim Okulu Building A1	Bingöl	38 54.242	40 29.512	Dual	Dependent bldg
C-13-04B	Mustafa Kemal Paşa İlköğretim Okulu Building A2	Bingöl	38 54.242	40 29.512	Dual	Dependent bldg
C-13-05	Şehit Mustafa Gündoğdu İlköğretim Okulu	Bingöl	38 54.105	40 30.247	Frame	Independent bldg
C-13-06	Kazım Karabekir İlköğretim Okulu	Bingöl	38 53 866	40 30.663	Frame	Independent bldg
C-13-07	Vali Kurtuluş Şişmantürk İlköğretim Okulu	Bingöl	38 53.789	40 31.091	Frame	Independent bldg
C-13-08	Kaleönü İlköğretim Okulu	Bingöl	38 54.486	40 32.994	Frame	Independent bldg
C-13-09	Sarıçiçek Köyü İlköğretim Okulu	Sarıçiçek	38 53.556	40 36.300	Frame	Independent bldg
C-13-10	Çeltiksuyu İlköğretim Okulu	Çeltiksuyu	38 51.587	40 34.855	Frame	Independent bldg
C-14-01	Karaelmas İlköğretim Okulu	Bingöl	38 52.905	40 30.179	Frame	Independent bldg
C-14-02	Fatih İlköğretim Okulu	Bingöl	38 52.776	40 29.664	Masonry	Independent bldg
C-14-03	Mehmet Akif Ersoy İlköğretim Okulu	Bingöl	38 52.964	40 29.837	Frame	Independent bldg
C-14-04	Atatürk Lisesi	Bingöl	38 52.934	40 29.758	Frame	Independent bldg
C-14-05	Vali Güner Orbay İlköğretim Okulu (Main Building)	Bingöl	38 53.054	40 29.352	Frame	Independent bldg
C-14-06	Vali Güner Orbay İlköğretim Okulu (2nd Building)	Bingöl	38 53.054	40 29.352	Frame	Independent bldg
C-14-07	Atatürk İlköğretim Okulu	Bingöl	38 53.236	40 29.507	Frame	Independent bldg
C-14-08	Bingöl Lisesi (Building B)	Bingöl	38 53.139	40 30.317	Dual	Dependent bldg
C-14-09	Bingöl İmam Hatip Lisesi (Building B)	Bingöl	38 52.917	40 29.763	Dual	Dependent bldg
C-15-01	Sarayiçi İlköğretim Okulu	Bingöl	38 53.159	40 30.894	Frame	Independent bldg
C-15-02	Murat İlköğretim Okulu	Bingöl	38 52.681	40 29.337	Frame	Independent bldg
C-15-03	Bingöl 100.Yıl İlköğretim Okulu (Building B)	Bingöl	38 53.133	40 29.593	Dual	Dependent bldg
D-16-01	Ekinyolu Köyü İlköğretim Okulu	Bingöl	38 54.374	40 34.564	Frame	Independent bldg
D-16-02	Ilıcalar Yatılı İlköğretim Bölge Okulu Dormitory Bldg	Ilicalar	38 59.581	40 41.250	Dual	Independent bldg
D-17-01	Merkez Cumhuriyet Kız Yatılı İlköğretim Bölge Okulu Boys' Dormitory Building	Bingöl	38 54.411	40 28.941	Dual	Independent bldg
D-17-02	Merkez Cumhuriyet Kız Yatılı İlköğretim Bölge Okulu Girls' Dormitory Building	Bingöl	38 54.419	40 29.021	Dual	Independent bldg
D-17-03	Merkez Cumhuriyet Kız Yatılı İlköğretim Bölge Okulu School Building	Bingöl	38 54.430	40 28.999	Dual	Independent bldg
D-17-04	Sancak Yatılı İlköğretim Bölge Okulu Dormitory Building	Sancak	39 05.235	40 23.452	Dual	Independent bldg

Table 5.9 Damage state and structural information of the school buildings

	Building Number	Damage to RC	Damage To Masonry	Number of Stories	Floor Area (m2)	RC Wall Area EW (m2)	Masonry Wall Area EW (m2)	RC Wall Area NS (m2)	Masonry Wall Area NS (m2)	Column Area (m2)	CI	Minimum Wl
Moment Resisting Frame (Schools)	C-13-07	Light	Moderate	2	589	0.00	16.84	0.00	11.92	6.45	0.27	0.10
	C-13-02	Moderate	Moderate	2	528	0.00	19.49	0.00	6.50	5.40	0.26	0.06
	C-13-05	Moderate	Light	2	585	0.00	18.69	0.00	11.71	6.45	0.28	0.10
	C-13-06	Moderate	Light	2	589	0.00	15.74	0.00	11.02	6.45	0.27	0.09
	C-14-06	Moderate	Moderate	2	595	0.00	15.99	0.00	10.69	6.45	0.27	0.09
	C-14-04	Moderate	Moderate	3	595	0.00	12.49	0.00	11.41	6.45	0.18	0.06
	C-14-05	Moderate	Moderate	3	595	0.00	7.39	0.00	17.13	6.45	0.18	0.04
	C-13-01	Severe	Severe	3	595	0.00	15.99	0.00	10.57	6.45	0.18	0.06
	C-14-01	Severe	Severe	3	595	0.00	15.74	0.00	9.41	6.45	0.18	0.05
	C-14-03	Severe	Severe	3	595	0.00	5.38	0.00	12.74	6.45	0.18	0.03
	C-14-07	Severe	Moderate	3	595	0.00	15.99	0.00	8.95	6.45	0.18	0.05
	C-15-01	Severe	Severe	4	595	0.00	14.91	0.00	7.31	6.45	0.14	0.03
	C-15-02	Severe	Severe	3	595	0.00	14.36	0.00	10.57	6.45	0.18	0.06
	D-16-01	Severe	Severe	3	595	0.00	14.82	0.00	7.67	6.45	0.18	0.04
	C-13-08	Collapsed	Collapsed	3	595	0.00	18.34	0.00	7.39	6.45	0.18	0.04
	C-13-09	Collapsed	Collapsed	3	595	0.00	15.99	0.00	9.25	6.45	0.18	0.05
	C-13-10	Collapsed	Collapsed	3	595	0.00	15.99	0.00	9.25	6.45	0.18	0.05
Dual System (schools)	C-13-04A	None	Moderate	3	281	3.93	1.90	5.51	1.98	3.45	0.20	0.49
	C-13-04B	None	Moderate	3	281	3.93	2.53	5.51	3.01	3.45	0.20	0.50
	C-13-03	Moderate	Moderate	4	524	7.49	3.28	5.55	8.49	7.99	0.19	0.31
	C-14-08	Moderate	Severe	4	523	3.62	9.00	2.54	9.35	7.94	0.19	0.17
	C-15-03	Moderate	Moderate	4	396	3.15	4.45	4.46	3.67	5.74	0.18	0.23
	D-17-03	Moderate	Moderate	4	895	7.41	0.98	8.81	9.72	9.78	0.14	0.21
	C-14-09	Severe	Moderate	4	381	3.22	2.97	3.57	5.10	5.89	0.19	0.23
Dual System (Dorms)	D-16-02	Moderate	Moderate	4	765	8.00	5.41	11.11	4.08	5.68	0.09	0.28
	D-17-04	Moderate	Moderate	4	765	8.00	5.41	11.11	4.08	5.68	0.09	0.28
	D-17-01	Severe	Moderate	4	765	8.00	5.41	11.11	4.08	5.68	0.09	0.28
	D-17-02	Severe	Moderate	4	765	8.00	5.41	11.11	4.08	5.68	0.09	0.28

5.5 NONENGINEERED AND SPECIAL STRUCTURES

5.5.1 Special Structures/Monuments Nonengineered and Special Structures

While inspecting school, private, and public buildings, a series of observations was made on the earthquake performance of nearby mosques in the city of Bingöl (Figure 5.81 shows the locations of the mosques mentioned below). The biggest mosque in the city is the Ulu Cami (Grand Mosque). Situated next to the town square, the main structure and minarets of this mid-1980s mosque are constructed of reinforced concrete. The mosque sustained no damage (Figure 5.82). However, within a few blocks and due northwest of it, the main reinforced concrete structure of the Hacı Hıdır Mosque and unreinforced light-weight masonry block minaret sustained heavy damage and had to be demolished (Figure 5.83). Experience indicates that masonry structures, whether walls, infills or minarets, gain in strength and integrity if reinforced with ring or collar beams at various intervals over the height. In the absence of such features [traditionally termed 'hatıl' in Turkish usage] masonry structures perform poorly when subjected to heavy shaking in earthquakes.

In the district of Yenimahalle, the Yenimahalle Mosque lost both of its minarets. As can be seen from the debris in Figure 5.84, unreinforced masonry blocks were used in the construction of the minarets. Besides fallen debris from the collapsed minarets, the main building sustained some damage. It is worth noting that across the Yenimahalle Mosque a 5-story reinforced concrete building had a total collapse of its 2nd story (Figure 5.85). The second mosque that was to be demolished in town was the Yeni/Hacılar Mosque near the Mehmet Akif Ersoy Primary School and the İmam Hatip High School (Figure 5.86). Even though the presumably lightly reinforced concrete minaret sustained only minor spalling, the reinforced concrete and masonry combination main structure sustained enough damage to be slated for demolition. A similarly built minaret was found in the mosque complex next to Sarayiçi Primary School (Figure 5.87). While the main building sustained minimal damage, the minaret lost its tip and part of the rail guard. Two other minarets of similar construction were seen in the vicinity of the ground motion recording station. Neither of these minarets (Figures 5.88 and 5.89) had signs of damage. As with all other buildings, the quality of workmanship and attention to detail materially affect the seismic performance of special structures including places of worship like mosques.

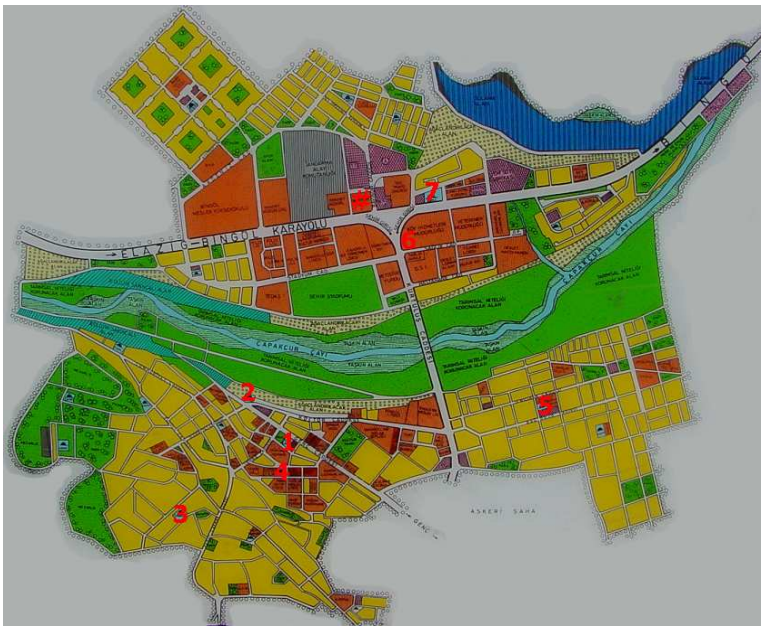

Figure 5.81 Figure 5.81. Map of the city of Bingöl. # indicates the location of the recording station; 1. Ulu Cami (Grand Mosque); 2. Hacı Hıdır Mosque; 3. Yenimahalle Mosque; 4. Yeni/Hacılar Mosque; 5. Mosque next to Sarayiçi Primary School; 6. and 7. Mosques on the highway near the recording station.

Figure 5.82 Ulu Cami (Grand mosque)

Figure 5.83 Hacı Hıdır mosque.

Figure 5.84 Yenimahalle mosque.

Figure 5.85 View of Yenimahalle mosque with the private residential building that lost its 2nd story.

Figure 5.86 Yeni/Hacılar mosque with spalling in its minaret. The structure is being demolished.

Figure 5.87 Mosque next to Sarayiçi primary school. Minaret lost its tip and part of its rail guard.

Figure 5.88 Mosque across the recording station site. Minaret is similar to those in Figures 5.86 and 5.87.

Figure 5.89 Mosque on the main highway close to recording station. Minaret is similar to those in Figures 5.86 and 5.87

5.5.2 Performance of Rural Housing

Within the vicinity of the Bingöl downtown area, the majority of the buildings are engineered, reinforced concrete frame type structures with a small percentage of masonry type buildings. Most of the masonry structures in the downtown area are also engineered. In the rural surroundings of Bingöl city, the opposite is valid and a majority of the houses are masonry type nonengineered structures. The houses generally have one story and the common construction material is stone (Figure 5.90). Some of these buildings have basements that are used for food storage or animal shelter. Some of the rural masonry buildings demonstrate hybrid construction materials with crude timber frames and hollow or mud brick infill. In some cases the infill comprises kiln fired bricks (Figure 5.91 and Figure 5.92).

Figure 5.90 Common masonry construction in rural areas

The categorization of nonengineered structures is not easy due to the large variation in construction techniques and workmanship. However, the majority of the houses in rural areas are constructed using large stones either in rectangular shapes or boulder like irregular forms. Those stones are commonly placed together using weak mortar along their contact surfaces with the other stones. On a smaller number of occasions, the walls are made out of solid fire bricks with wooden struts in the diagonal and vertical directions showing indications of engineering ingenuity (Figure 5.91). Such masonry construction usually performed better during the earthquake due to their lightweight construction and shear resistance shown by the diagonal struts. A portion of the nonengineered rural building stock composed of stone wall layers which are divided by the use of collar or ring beams in the form of band-like horizontal wooden layers (Figure 5.92). This type of construction has performed better than the stone-only type of construction with some instances of partial failure (Figure 5.93) because of the box-like action and integrity imparted by the ring beams.

Figure 5.91 Hybrid masonry construction in rural areas (bricks and diagonal wooden struts)

Figure 5.92 Hybrid masonry construction in rural areas (bricks and collar beams in the form of all-round horizontal wooden layers)

Figure 5.93 Partial collapse of hybrid masonry walls (bricks and horizontal wooden layers)

Most of the rural stone-masonry type building collapses are initiated by collapse of the wall midsection towards the top, due to lateral instability (Figures 5.94 and 5.95). Only a few instances of total house collapses are documented. The majority of the nonengineered structures, being mainly single storey dwellings, satisfied life-safety criteria.

Figure 5.94 Stone-masonry type wall collapse initiation

Figure 5.95 Stone-masonry type wall collapse

CHAPTER AUTHORS

Coordinators

J. A. Ramirez, Purdue University
A. Yakut, Middle East Technical University

Contributors

U. Akyüz, Middle East Technical University
T. Gür, Purdue University
A. Irfanoglu, WJE Assoc., Inc.
A. Matamoros, University of Kansas
G. Özcebe, Middle East Technical University
M. A. Sozen, Purdue University
A. Türer, Middle East Technical University
S. T. Wasti, Middle East Technical University

6

CONCLUDING REMARKS

Turkey has suffered several major earthquakes in different regions over the last decade with much loss of life and property. As mentioned in the Preface, a general awareness of the effects of earthquakes on buildings has taken root. The earthquake threat has come to be recognized by the population as one urgently needing preparedness. This positive attitude needs to influence engineering practice to ensure that buildings constructed in the future fare better in earthquakes than those they have replaced. While it is difficult to bring about high standards of seismic resistance in single-story family dwellings in Turkey some of which are not even engineered, serious attempts can be made on the basis of lessons already learned to introduce minimum levels of seismic safety into semi-urban or urban medium-rise reinforced concrete buildings of, say, up to seven stories. Whether used for residential, commercial or public purposes, such structures have long enjoyed popularity in Turkey as streamlined, modern buildings and builders find them profitable to construct and sell.

The May 1, 2003 Bingöl earthquake was a colossal tragedy that, unfortunately, confirmed many of the lessons learned from previous events. The observations documented in this report point out that for medium-rise construction, building plans continue to remain irregular and that the quality of concrete used is poor on the whole. Defects in the detailing of both longitudinal and transverse reinforcement are very common. The reconnaissance studies made in the aftermath of Bingöl earthquake exemplified the tragic consequences of such errors one more time.

It is relevant to note that Turkey has a modern seismic code and a modern reinforced concrete code of practice. Furthermore, engineers are, on the whole, well educated and competent. However, there is a striking gap between the requirements of these codes and actual construction practice - both in the rural and the urban areas. The disconnect between the code requirements and the apparent quality of reinforced concrete buildings finds its roots in the lack of enforcement of the codes in effect. Laws not enforced will not be obeyed. In Bingöl the disconnect between code requirements and implementation resulted in a very high toll in terms of human lives and number of people left homeless.

The most tragic collapse occurred at Çeltiksuyu Primary Boarding School. Since the earthquake occurred at 3:27 a.m. local time, the majority of the students were asleep in the dormitory in which 84 (out of 195) students and 1 teacher lost their lives. The most disturbing aspect of the tragedy was that the children died because of obvious and preventable mistakes in the construction of the dormitory.

The deficiencies causing the collapse of the dormitory can and need to be corrected with informed planning and better technical supervision of construction. There is much food for thought in the present report for every civil engineer to digest. Unfortunately, because each improvement in strength and quality brings increased costs in its wake, builders unwisely tend to ignore elementary precautions. Therefore new proposals that will be made towards safe buildings should consider the current habits in construction practice as an important one among the essential parameters of the problem. Planning and proportioning of the structure should make it insensitive to the instinctive prerogatives of the builders.

In Bingöl, the performance of buildings with structural walls (with or without frames working in parallel) was observed to be quite satisfactory from the viewpoint of safety. Buildings with higher ratios of structural wall to floor area had less damage, because the stiffness of the lateral load resisting

system reduced the drift demand and the damage to structural and nonstructural elements. The performance of structural walls was found to be insensitive to inadequate detailing practices, inaccurate placement of reinforcement, and substandard materials.

These observations give us sufficient confidence to promote the use of structural systems which are less dependent on detailing in order to provide adequate safety against collapse. For this purpose we strongly recommend the compulsory use of structural walls especially in the construction of school buildings. These walls should be placed along both principal directions of the building plan and over the total height of the building. The total cross-sectional area of the structural walls in each direction should not be less than 1 percent of the total ground floor area for all buildings up to four stories. This ratio should be increased by 0.25 percent for each additional story over four. These walls shall be located as symmetrically in plan as possible, preferably spread out towards the outer extremes of the building.

The clash between architectural and structural demands deserves close scrutiny. Building code requirements need to ensure that structural performance is not compromised as it was in many of the school buildings in Bingöl. The good and the bad instances of the Bingöl experience confirmed categorically that low-rise school buildings need to be proportioned to limit drift and that the use of adequate amounts of structural wall is the optimum solution for safety.

It is partly because of the plentiful lessons provided by the present report that it is planned to issue an abridged version in Turkish to drive home the thrust of the findings herein to local technical and nontechnical readers alike.

Contributors

G. Özcebe, Middle East Technical University
J. A. Ramirez, Purdue University
Mete A. Sozen, Purdue University
S. T. Wasti, Middle East Technical University

REFERENCES

Ahmed F. Hassan and Mete A. Sozen, (1997). "Seismic Vulnerability Assessment of Low-Rise Buildings in Regions with Infrequent Earthquakes," ACI Structural Journal, V. 94, No.1, January-February.

Ambraseys, N.N. and J.A. Jackson (1998). Faulting associated with historical and recent earthquakes in the Eastern Mediterranean region, *Geophysics J. Int.* **33**, 390-406.

Ambraseys, N.N. (1985). Engineering seismology, *Earthquake Engineering and Structural Dynamics*, **17**, 1-105.

Boore D.M., V.M. Grazier, A.F. Shakal and J.C. Tinsley (2003). Unusual ground motion amplification at the Coyote Lake Dam, California, submitted for possible publication to the *Bulletin of the Seismological Society of America*.

Boore D.M. (2001). Effect of baseline corrections on displacements and response spectra for several recordings of the 1999 Chi-Chi, Taiwan earthquake, *Bulletin of the Seismological Society of America*, **91**, 1199-1211.

Converse, A.M. and A.G. Brady (1992). BAP — Basic strong-motion accelerogram processing software; Version 1.0, *U.S. Geol. Surv. Open-File Rept. 92-296A*, 174p.

Emre, O., Herece, E., Doğan, A., Parlak, O., Ozaksoy, V., Çıplak, R ve Özalp, S., (2003), "1 Mayıs 2003 Bingöl Depremi", http://www.mta.gov.tr/Bingöl/Bingöl.asp 17pp. (unpublished report in Turkish).

Iwan, W.D., M.A. Moser and C.-Y. Peng, (1985). Some observations on strong-motion earthquake measurement using a digital accelerograph, *Bulletin of the Seismological Society of America*, **75**, 1225-1246.

Koçyiğit A. and N. Kaymakçı (2003). The report of May 1, 2003 Sudüğünü (Sancak-Bingöl) earthquake, *Tectonics and Earthquake Research Laboratory Rept. 14*, Department of Geological Engineering, Middle East Technical University, Ankara Turkey (in Turkish).

Seymen, I. and A. Aydın (1972). The Bingöl earthquake fault and its relationship with the north Anatolian fault, *MTA J.*, **79**, 1-8 (in Turkish).

Şaroğlu, F., Emre, O. ve Boray, A., (1987), "Türkiye'nin aktif faylari ve depremsellikleri.", MTA Rapor No:8174. 394 pp (unpublished report in Turkish).

Şaroğlu, F., Emre, O. ve Kuşçu, I., (1992), "Türkiye'nin diri fay haritası", MTA Yayını (in Turkish).

Travasarou, T., D.B. Jonathan and N.A. Abrahamson (2003), Empirical attenuation relationship for Arias Intensity, *Earthquake Engineering and Structural Dynamics*, 32, 1133-1155.

Trifunac, M.D. and A.G. Brady (1975). A study on the duration of strong earthquake ground motion, Bulletin of the Seismological Society of America, **65**, 581-626.

Turkish Ministry of Public Works and Settlement, General Directorate of Disaster Affairs, Ankara, Turkey (http://www.deprem.gov.tr)

United States Geological Survey, USGS, Reston, Virginia, US. (http://www.usgs.gov)

ESRI, ARCGIS 8.1, Geographic Information Systems Software. USA. (www.esri.com)